UNIVERSITÀ
DEGLI STUDI
FIRENZE

DOTTORATO DI RICERCA IN SCIENZE CHIMICHE

CICLO XXX

COORDINATORE Prof. PIERO BAGLIONI

MASS SPECTROMETRY AS A TOOL TO STUDY METAL-CONTAINING COMPOUND/PROTEIN INTERACTIONS FOR ANTICANCER METALLODRUG DISCOVERY

Settore Scientifico Disciplinare CHIM/03

Dottorando
Dott.ssa Elena Michelucci

Tutore
Prof. Luigi Messori

Coordinatore
Prof. Piero Baglioni

Anni 2014/2017

TABLE OF CONTENTS

LIST OF ACRONIMS AND ABBREVIATIONS

AA	ammonium acetate
Ambic	ammonium bicarbonate
Atox1	human antioxidant protein 1
Aubipy^{aa}	[Au(bipy^{dmb}-H)(NH(CO)CH$_3$)][PF$_6$]
Aubipy^{c}	[Au(bipy^{dmb}-H)(OH)][PF$_6$]
Au$_2$bipy^{c}	[Au$_2$(bipy^{dmb}-H)$_2$(μ-O)][PF$_6$]$_2$
Au(cyclam)	[Au(1,4,8,11-tetraazacyclotetradecane)]$^{3+}$
[Au(dppe)$_2$]Cl	bis[1,2-bis(diphenylphosphino)ethane]gold(I) chloride
Auoxo$_6$	[Au$_2$(bipy^{2Me})$_2$(μ-O)$_2$][PF$_6$]
auranofin	[(2,3,4,6-tetra-*O*-acetyl-1-(thio-κS)-β-D-glucopyranosato) (triethyl-phosphine)gold(I)]
bipy	2,2'-bipyridine
bipy^{dmb}	6-(1,1-dimethylbenzyl)-2,2'-bipyridine
bipy^{2Me}	6,6'-dimethyl-2,2'-bipyridine
carboplatin	*cis*-diammine-1,1-cyclobutanedicarboxylate-platinum(II)
CDDP	*cis*-[diamminedichloroplatinum(II)], cisplatin
CE	capillary electrophoresis
CID	collision induced dissociation
*cis*PtBr$_2$	*cis*-PtBr$_2$(NH$_3$)$_2$
CRC	colorectal cancer
cyclam	1,4,8,11-tetraazacyclotetradecane
Cyt *c*	horse heart cytochrome *c*
dien	diethylendiamine
DMSO	dimethyl sulfoxide
DTT	dithiothreitol
en	ethylenediamine
ESI	electrospray ionization
ESI-MS	electrospray ionization mass spectrometry
ETD	electron transfer dissociation
FASP	filter aided sample preparation
FDA	food and drug administration
Ft	ferritin
FT	Fourier transform
FT-ICR	Fourier transform ion cyclotron resonance
GSH	glutathione
HSA	human serum albumin

Hewl	hen egg white lysozyme
IAA	iodoacetamide
ICP	inductively coupled plasma
ICP-AES	inductively coupled plasma atomic emission spectrometry
IEF	isoelectric focusing
Im	imidazole
IMS	ion mobility spectrometry
ImH	imidazolium
IR	infrared
IT	ion trap mass analyzer
KP1019	indazolium *trans*-[tetrachlorobis(1H-indazole)ruthenate(III)] [IndH][trans-$RuCl_4(Ind)_2$]
LC	liquid chromatography
LC-ESI-MS/MS	liquid chromatography-electrospray ionization-tandem mass spectrometry
MALDI	matrix assisted laser desorption ionization
MALDI-TOF	matrix assisted laser desorption ionization-time of flight
MS	mass spectrometry
MS/MS	tandem mass spectrometry
MTs	metallothioneins
MudPIT	multidimensional protein identification technology
MW	molecular weight
NAMI-A	new anti-tumor metastasis inhibitor A [ImH] *trans*-[tetrachloro(dimethylsulfoxide)(Im)ruthenate(III)] [ImH][*trans*-$RuCl_4$(DMSO)(Im)]
NHCs	N-heterocyclic carbenes
NMR	nuclear magnetic resonance
Oxaliplatin	*trans*-L-1,2-diaminocyclohexane oxalatoplatinum(II)
RCSB PDB	research collaboratory for structural bioinformatics protein data bank
phen	1,10-phenanthroline
pta	1,3,5-triaza-7-phosphadamantane
PtI_2(DACH)	[(1R,2R)-cyclohexane-1,2- diamine]diiodideplatinum(II)
Q-TOF	quadrupole-time of flight
RAPTA	ruthenium η^6-arene 1,3,5-triaza-7-phosphadamantane
RAPTA-C	[Ru(η^6-*p*-cymene)Cl_2(pta)]
RNase A	bovine pancreas ribonuclease A
RP	reverse phase
rt	room temperature

SCX	strong cation exchange
SNAP	smart numerical annotation procedure
SOD	bovine erythrocyte superoxide dismutase
TBP	tributylphosphine
terpy	2,6-bis(2-pyridyl)-pyridine, terpyridine
TFA	trifluoroacetic acid
TLC	thin layer chromatography
TOF	time of flight
TrxR	thioredoxin reductase
Ub	red blood cell ubiquitin
UV/Vis	ultraviolet/visible
XRD	X-ray crystallography diffraction
2DGE	two-dimensional gel electrophoresis

SUMMARY

In this PhD thesis, mass spectrometry-based approaches were used to characterize, at molecular level, the adducts formed between some metallodrugs (or novel, promising metal compounds) and several proteins. Valuable information were gained about the chemical nature, the binding stoichiometry and the binding site location of the adducts formed. The obtained results can be profitably exploited for a more rational design of novel anticancer metallodrugs through a "mechanism oriented" approach.

The whole work was organized into seven distinct chapters, as detailed below.

In chapter 1 we reported a general review on the use of metals as anticancer agents, from the past years to present days, focusing the attention on platinum, ruthenium and gold compounds. The importance of studying metal-based anticancer drug/protein interactions was discussed and the key role of MS in this field was highlighted.

In chapter 2, first of all we described the past studies performed in our laboratories, which constitute the research background of this project. Then, we explained the aims of this PhD thesis, pursued through two main search directions:
i) the survey on the chemical nature and the binding stoichiometry of the adducts formed between small size proteins and: a) new analogues of cisplatin and oxaliplatin anticancer drugs (chapter 3); b) novel Au(III) complexes (chapter 4);
ii) the development and introduction in our laboratories of an efficient and generally applicable method for metallodrugs binding site location on proteins, regardless of the MW and nature of the protein and the type of metal complex under investigation, in order to get closer to the study of real, interesting biological systems (chapters 5 and 6).

In chapter 3, the chemical and biological profiles of the novel complexes *cis*$PtBr_2$ and PtI_2(DACH) were studied in comparison to those of their precursors, respectively cisplatin and oxaliplatin.
In chapter 4, analogues studies were performed on Au(III) complexes bearing chelating nitrogen/carbon donors or quinoline derivatives as N-/O-donors.
A detailed discussion was carried out on the ESI-MS results obtained by studying the interactions of these metal compounds with the model proteins HEWL, RNase A, Cyt *c* and Atox1. The importance of the information obtained about the chemical nature and the binding stoichiometry of the metallo fragments, as well as on the oxidation state of the metal center, was discussed.

In chapter 5, we reported the design and the application of a general and systematic protocol to test, *a priori*, the stability of metallodrug-protein adducts under the typical conditions of the FASP/bottom-up mass spectrometry approach, being this latter the methodology we chose for the binding site location studies described in chapter 6. The protocol was specifically applied to two representative model systems, the more investigated Cyt *c*-CDDP adducts and the less studied Cyt *c*-RAPTA-C ones. The different obtained results highlighted the advisability to perform a test-protocol like this when starting any bottom-up MS investigation on protein-metallodrug systems, especially with novel, or scarcely studied, metal complexes.

In chapter 6, we applied, for the first time in our laboratories, the FASP/bottom-up MS approach for cisplatin binding site location on the model protein Cyt *c* and the actual target protein HSA.
For the CDDP-Cyt *c* system we obtained results in good agreement with those already present in the literature. The FASP/bottom-up approach proved its capability to highlight the selective binding of CDDP to Cyt *c*, and it also demonstrated its extensibility, in a systematic way, to other simple, model systems endowed of the needed stability. Moreover, we discussed in detail all the critical issues related to the lack of specific softwares for metalloproteomics data analysis.
The application of the FASP/bottom-up MS approach to the more complex system CDDP-HSA produced results which do not find a match with those reported in the literature, already poorly concordant with each other. The possible causes of this discrepancy were discussed. Finally, we declared the advisability of a more detailed investigation on the CDDP-HSA system before attempting to extend the methodology, in a systematic way, to other proteins of large size.

In chapter 7 we presented the general conclusions and we proposed possible future research topics to be developed.

1. INTRODUCTION

1.1 Anticancer metallodrugs

1.1.1 Metal complexes with pharmacological properties

The pharmaceutical use of metal complexes has an excellent potential. A broad array of medicinal applications of metal complexes has been investigated, and several recent reviews summarize advances in these fields [1-3]. Now the list of therapeutically prescribed metal containing compounds includes platinum (anticancer), silver (antimicrobial), gold (antiarthritic), bismuth (antiulcer), antimony (antiprotozoal), vanadium (antidiabetic) and iron (antimalarial). Metal ions are electron deficient, whereas most biological molecules (DNA, proteins) are electron rich; consequently, there is a general tendency for metal ions to bind to and interact with many important biological targets. These considerations alone have fueled much of the past and current interest in developing novel means to use metals or metal containing agents to modulate biological systems.

In general, a metal complex that is administered, is likely to be a "prodrug" that undergoes an *in vivo* transformation before reaching its target site. Most importantly, the biological properties of metal complexes depend not only on the metal nature and its oxidation state but also on its ligands, which can render either the whole complex inert to ligand substitution reactions or can activate other coordination positions stereospecifically. Besides the metal itself, the ligands can also be the centers of redox, hydrolytic or other reactions.

Medicinal inorganic chemistry is a relatively young, interdisciplinary research field and the rational design of metal-based drugs is a relatively new concept too. Developing metal complexes as drugs, however, is not an easy task. Accumulation of metal ions in the body can lead to very deleterious effects. Thus, biodistribution and clearance of metal complex, as well as its pharmacological specificity, have to be carefully considered. Favorable physiological responses of the candidate drugs need to be demonstrated by *in vitro* studies with targeted biomolecules and tissues, as well as *in vivo* investigation with xenografts and animal models, before they may enter clinical trials. A mechanistic understanding on how metal complexes produce their biological activities is crucial to their clinical success, as well as to the rational design of new compounds with lower toxicity and improved potency.

1.1.2 Metal-based anticancer drugs

The modern era of metal-based anticancer drugs began with the serendipitous discovery of cisplatin by Rosenberg and co-workers in the late 1960s. Stimulated by

the success of cisplatin, cisplatin analogues, as well as other coordination compounds based on ruthenium, gold, titanium, copper, rhodium, vanadium and cobalt, were tested for their anticancer activities and several promising candidates are currently in (pre)clinical evaluation [4-10].
Of particular interest is the elucidation of the mechanism of action of the various non-platinum metal complexes and the investigation of their final targets. Indeed, while several data are now available regarding the mechanism of Pt(II) compounds, limited work has been done on the mechanism of action of non-platinum metal complexes which exhibit encouraging cytotoxicity and antitumor activity profiles.
Among non-platinum antitumor metal complexes there are two groups of compounds which deserve special attention: these are the ruthenium and gold complexes. For example, contrary to cisplatin, the Ru(III) complex called NAMI-A has a unique feature, namely a higher activity against metastases than against primary tumors [11]. Moreover, at variance with platinum complexes, it is noteworthy to mention that DNA seems not to be the primary cellular target mediating the antitumor activity for most non-platinum metal-based drugs [11,12].

1.1.3 Platinum-based anticancer drugs

The interest in platinum-based antitumor drugs has its origin in the 1960s, when Rosenberg observed the inhibition of *E. coli* cell division induced by Pt complexes [13].
Since then, thousands of platinum compounds have been prepared and evaluated as potential chemotherapeutic agents, although few have entered clinical use (fig. 1.1).

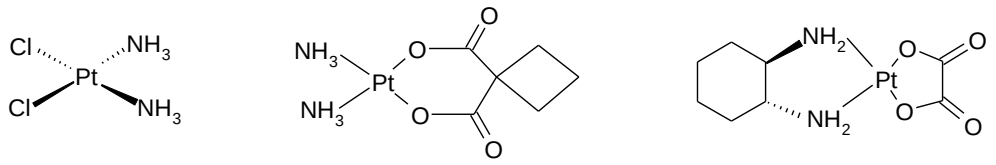

cisplatin carboplatin oxaliplatin

Fig 1.1 Chemical formulae of the worldwide approved platinum anticancer drugs cisplatin, carboplatin and oxaliplatin.

Cisplatin (fig. 1.1), a square planar Pt(II) complex (d^8, diamagnetic, dsp^2 hybridization), is highly effective against a number of cancer types, especially testicular cancer, for which it has a greater than 90 % cure rate [14].
Despite its clinical success, there are several disadvantages associated with cisplatin, such as low water solubility [15], significant toxicity, which limits patient doses [15],

severe side effects such nausea, nephrotoxicity, neurotoxicity [16] and intrinsic or acquired resistance in some cancer types [17,18].

Cisplatin is generally believed to exert its anticancer effect by interacting with DNA and inducing programmed cell death (apoptosis) [17,19,20]. Following intravenous administration, cisplatin encounters a relatively high chloride concentration in blood flow (approximately 100 mM) that limits replacement of its chloride ligands by water molecules, thus preventing aquation process [14]. However, cisplatin is vulnerable to attack by proteins found in the blood plasma, particularly by those that contain thiol groups, such as human serum albumin [21,22]. In fact, studies have shown that one day after cisplatin administration, 65-98 % of Pt in the blood plasma is protein bound [23]. This protein binding has been blamed for the deactivation of the drug and for some of the severe side effects of cisplatin treatment. The intact cisplatin can enter tumor cells mainly by passive diffusion through the cell membrane, although facilitated or activated transport mechanisms may contribute to the cellular uptake as well [17,18]. The intracellular chloride concentration is relatively low (approximately 4-20 mM); hence one of the chloride ligand of the intact complex is rapidly replaced by water, forming the reactive, positively charged species $[(NH_3)_2PtCl(H_2O)]^+$ (scheme 1.1) that cannot readily leave the cell [24]. Cisplatin, as well as the most part of metallodrugs, acts here as a "prodrug", in other words an activation step is required before it can react with its biomolecular targets and cause its specific biological effects.

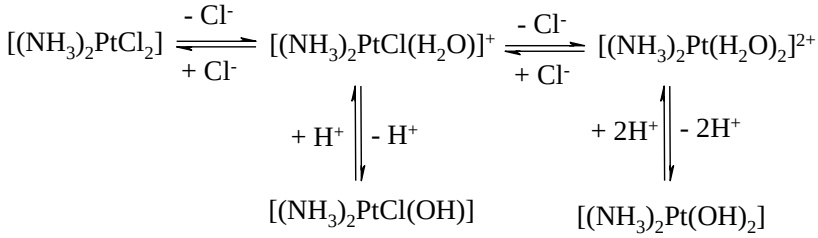

Scheme 1.1 Hydrolysis reactions of CDDP.

This monoaquated platinum species is predominant in cytoplasm [25] and reacts with one of the DNA bases, usually guanine, forming monofunctional DNA adducts. Ring closure to form a bifunctional adduct with the nucleic acid may occur, either directly from the monofunctional adduct or may involve aquation of the second chloride ligand followed by rapid closure [26,27]. The major site of platination in DNA derives from 1,2-intrastrand crosslinks between two neighboring guanines but 1,3-intrastrand crosslinks are also possible (fig. 1.2) [28].

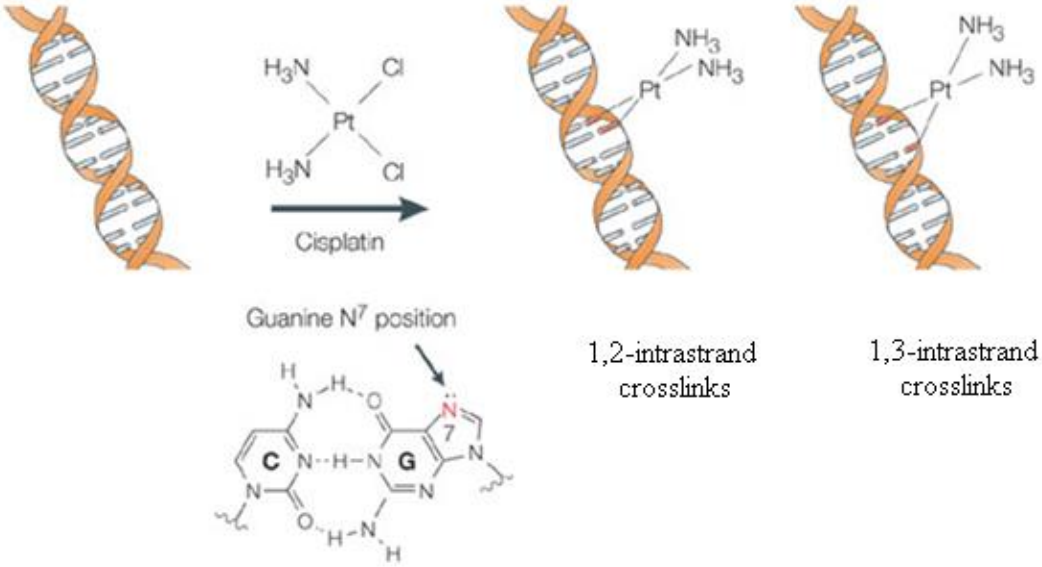

Fig 1.2 Cisplatin undergoes aquation to form $[Pt(NH_3)_2Cl(OH_2)]^+$ and $[Pt(NH_3)_2(OH_2)_2]^{2+}$ once inside the cell. The platinum atom of cisplatin binds covalently to the N^7 position of guanines to form 1,2- or 1,3-intrastrand crosslinks, and interstrand crosslinks (figure taken from "D. Wang, S. J. Lippard, *Nat. Rev. Drug Discov*., **2005**, *4*, 307-320").

The formation of covalent crosslinks between cisplatin and the DNA double helix causes a significant distortion of the helical structure and results in inhibition of DNA replication/transcription thus leading to cytotoxicity [17,29,30].
However, the effectiveness of CDDP treatment is greatly limited by the phenomenon of tumor resistance. Several tumors are intrinsically resistant to cisplatin while others acquire resistance after exposure to the drug over time. The cellular mechanism of CDDP resistance has been identified as decreased intracellular accumulation (the mechanism is not clear but the cell has probably some control over the entering of cisplatin, thus suggesting that this drug does not enter the cell by passive diffusion alone but that some active transport system may be involved) [31], strong binding to inactivating sulphur–containing molecules inside the cell (MTs and GSH) [32] and increased repair of platinated DNA by enzymes [33].
Researchers have focused attention on designing new platinum compounds with improved pharmacological properties and a broader range of antitumor activity. In general, for a platinum drug to gain clinical approval, it must possess at least one distinct clinical advantage over cisplatin. Such advantage may include: activity against cancers with intrinsic or acquired resistance to CDDP, reduced toxic side effects or the ability to be orally administered. Several platinum complexes are currently in clinical

trials but these new complexes have not yet demonstrated significant advantages over cisplatin [34].
Carboplatin and oxaliplatin (fig. 1.1) are considered the main exponents, respectively, of the second- and third-generation platinum anticancer drugs.
In carboplatin [35] the two chloride ligands are replaced with the bulkier cyclobutanedicarboxylate bidentate ligand. The spectrum of the biological action of carboplatin substantially reproduces that of cisplatin, implying an identical mechanism of action [28,35,36], but carboplatin manifests a more favorable toxicological profile than cisplatin itself. The reasons of this lie in the fact that the aquation process of carboplatin is far slower than in the case of CDDP: studies on the interaction of carboplatin with small molecules or peptides containing sulphur indicated that this reaction proceeds *via* ring-opening of the cyclobutanedicarboxylate ligand, thus lowering the rate of the aquation and thereby the reactivity of the compound [37].
Oxaliplatin [35,37] is the only platinum compound to have displayed activity against colorectal cancer so far [38,39]. The chemical structure of oxaliplatin differs from those of cisplatin and carboplatin by the attachment of a cyclohexane ring to the nitrogen atoms. It is a compound with relatively good water solubility; it achieved good efficacy in experimental tumor models and displayed low haematological toxicity and minimal or no nephrotoxicity in preclinical studies [39]. Oxaliplatin shows comparable chemical behavior and has a similar mechanism of action as compared to the previous platinum derivatives, but its hydrolysis process (displacement of the oxalate group) is slower than for cisplatin [40].
Other noteworthy Pt-compounds are [35]: *trans*-platinum, polynuclear platinum and platinum(IV) complexes. In particular, the latter have good prospect for oral administration so that the quality of life of cancer patients could be improved avoiding the upsetting effects of intravenous administration of Pt-drugs. It is generally believed that platinum(IV) complexes are reduced to platinum(II) by extracellular and intracellular agent prior to reaction with DNA, thus acting as a "pro-drug" through a redox activation process.

1.1.4 Ruthenium anticancer agents

Ruthenium complexes have attracted interest for their potential use as anticancer agents in the past 30 years [41,42]. In detail, ruthenium compounds show low systemic toxicity and appear to enter the tumor cells, to bind effectively DNA and proteins and to manifest, in some cases, selective antimetastatic properties.
There are three main properties that make ruthenium compounds well suited for medical applications [43]: i) the range of accessible oxidation states, ii) the ability to mimic iron in binding to many biological molecules, iii) the rate of ligand exchange.
For anticancer ruthenium complexes, at variance with platinum drugs, two different accessible oxidation states are possible under physiological conditions: Ru(II) (d^6,

diamagnetic, d^2sp^3 hybridization) and Ru(III) (d^5, paramagnetic, d^2sp^3 hybridization). Therefore, the ruthenium complexes are redox-active agents that can undergo electron-transfer reactions with biological reactants. For example, the drug can be administered as relatively inert Ru(III) complex, which is activated by reduction in diseased tissues. In fact, in many cases, the altered metabolism associated with cancer, results in a lower oxygen concentration in these tissues, compared to healthy ones, and this promotes a reductive environment.

The ability of ruthenium compounds to mimic iron in binding to certain biological molecules, including serum proteins (*e.g.*, transferrin and albumin), is believed to contribute to the general low toxicity of ruthenium drugs. Moreover, the high iron requirement of tumor cells results in the expression of a large number of receptors for the iron transport protein transferrin which is believed to result in the accumulation of Ru(III) complexes in tumors. Transferrin is thought to act like a ‘‘Trojan Horse’’, transporting the Ru-complex instead of or in addition to the required iron into the cell [6].

Many Ru(II) and Ru(III) complexes have been evaluated for clinical applications due to their kinetics of ligand exchange, similar to those of Pt(II) compounds. Ligand exchange is an important characteristic for biological activity as very few metal drugs reach the biological target without being modified.

Finally, Ru(II) and Ru(III) complexes, at variance with square planar Pt(II) compounds, are characterized by an octahedral geometry and this may suggest different manners of action.

The first ruthenium agent to enter clinical trials in 1999 was NAMI-A [44] (fig 1.3).

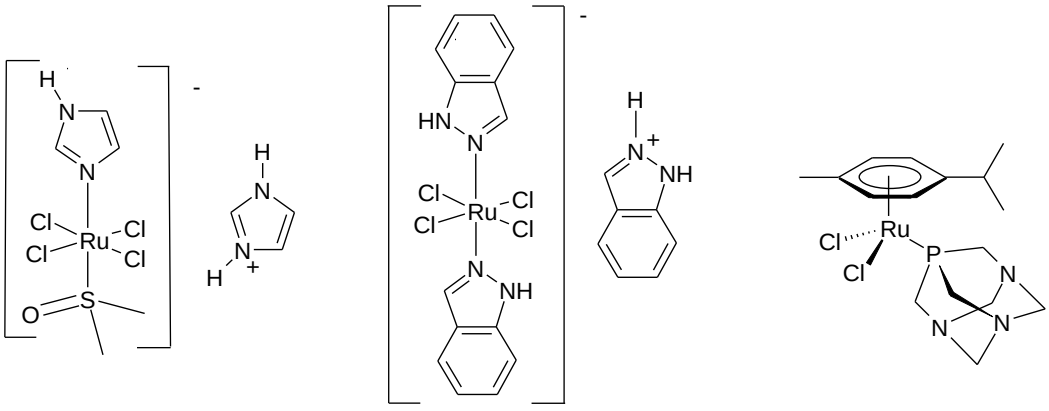

NAMI-A KP1019 RAPTA-C

Fig 1.3 Chemical formulae of ruthenium compounds NAMI-A, KP1019 and RAPTA-C.

NAMI-A (-A suffix indicates that this is the first of a potential series) binds DNA and produces effects similar to those of cisplatin but, unlike cisplatin, only at relatively high concentrations. Interestingly, NAMI-A turned out to be a potent agent against solid tumor metastases. This is potentially very important because, although great progresses have been made in treating primary cancers (including surgery, chemotherapy and radiotherapy), secondary metastases still represent a major clinical challenge. The antimetastatic effect of NAMI-A is likely due to either interference with specific proteins involved in signal transduction pathway or altered cell adhesion processes [45,46]. NAMI-A binds also transferrin, an event which is supposed to target the compound to cancer cells.

The second Ru(III) compound currently in clinical trials is KP1019 [6] (fig. 1.3). This compound was developed by Keppler and co-workers and, despite its structural similarity to NAMI-A, is active against primary tumors. The mode of action of KP1019 probably involves accumulation in transferrin receptor-(over)expressing tumor cells via the transferrin receptor, subsequent reduction to Ru(II) species, reaction with DNA (with a preference shown for G and A residues) and induction of apoptosis via the intrinsic mitochondrial pathway. KP1019 binding with human serum albumin in the blood stream has also been proved and is believed to provide a ‘‘reservoir’’ for the drug.

More recently, another class of ruthenium anticancer agents, named RAPTA, has been developed by Dyson and co-workers [45]. The RAPTA family is characterized by the presence of a Ru center (R), a η^6-arene tridentate ligand (A) and a 1,3,5-triaza-7-phosphadamantane monodentate ligand (PTA). The RAPTA compounds have piano-stool geometry and the remaining two coordination sites can be occupied by two chlorides or other ligands. The compounds of general formula [Ru(η^6-arene)Cl_2(pta)], the prototype being [Ru(η^6-*p*-cymene)Cl_2(pta)] (RAPTA-C) (fig. 1.3), were developed in order to create pH-dependent DNA-damaging agents but they resulted to be only poorly toxic towards cancer cells *in vitro* [11]. Like NAMI-A, these agents are inactive against primary tumors but they show activity against metastases *in vivo* [11]. As NAMI-A, the indications are that proteins, rather than DNA, are the biomolecular targets for action of the drug.

1.1.5 Gold complexes as antitumor agents

Gold compounds have a long and important tradition in medicine and they were widely used in early times of modern pharmacology for the treatment of several diseases, especially as anti-infective and antitubercular agents [47]. Nowadays, gold compounds find rather limited medical application and are presently used only for the treatment of severe rheumatoid arthritis [48]. This is probably the result of relevant systemic

toxicity (*e.g.*, nephrotoxicity) and of the poor chemical stability of some of the tested compounds.

Remarkably, during the last two decades, a large number of Au(I) and Au(III) compounds have been reported to show relevant antiproliferative properties *in vitro* against selected human tumor cell lines, qualifying themselves as excellent candidates for further pharmacological evaluation [49–52].

Gold can exist in a number of oxidation states, but apart from Au(0) in the colloidal and elemental forms, only Au(I) and Au(III) give rise to compounds reasonably stable in aqueous/biological environments. In any case, both Au(I) and Au(III) are thermodynamically unstable with respect to Au(0) and are, thus, readily reduced to elemental gold by mild reducing agents. Au(I) is more stable than Au(III); accordingly, Au(III) complexes are generally strong oxidizing agents and potentially toxic in biological systems, where their reduction can be driven by biologically occurring reducing agents such as thiols. Au(I) has a d^{10} closed-shell configuration that gives rise to three main coordination geometries: linear two-coordination (by far the most common, sp hybridization), trigonal three-coordination (sp^2 hybridization) and tetrahedral four-coordination (sp^3 hybridization). Instead, Au(III) compounds typically adopt a tetra-coordinate square planar geometry (d^8, diamagnetic, dsp^2 hybridization) as Pt(II). While Au(I) is a "soft" cation, and shows preference for "soft" ligands (*e.g.*, S, Se, cyanide, etc.), Au(III) is a "borderline" cation showing a preference for soft ligands but also for nitrogen donors [53].

Gold(I) anticancer compounds are divided into two classes (fig. 1.4):

(i) Au(I) phosphine compounds, such as the linear two-coordinated auranofin and the tetrahedral four-coordinated $[Au(dppe)_2]Cl$;

(ii) Au(I) NHCs complexes.

There are evidences that both classes of compounds act by mechanisms involving mitochondrial cell death pathways [54].

The aqueous solution chemistry of auranofin has been intensively investigated [55,56] and indicates that thiolate ligands are usually more labile than phosphine ligands and undergo rapid aquation. The resulting cationic species usually show a strong reactivity with biomolecules containing thiol groups, thus limiting its antitumor activity *in vivo*. Auranofin has been shown to induce apoptosis *via* selective inhibition of the mitochondrial isoform of thioredoxin reductase, an enzyme involved in the thiol redox balance in cell and up-regulated in malignant diseases. This inhibition is attributable to the binding of Au(I) to the redox-active selenocysteine residue of TrxR: the selenocysteine group, in the reduced form, displays a high reactivity toward "soft" metal ions [54].

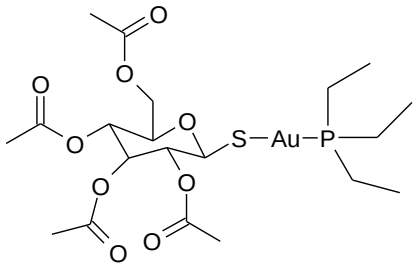

auranofin

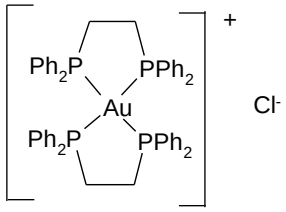

$[Au(dppe)_2]^+Cl^-$

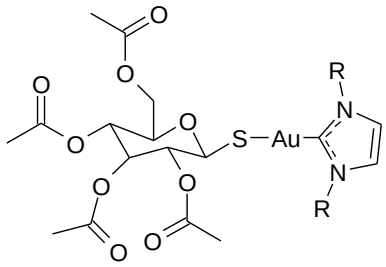

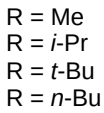

Examples of Au(I)-NHC complexes

Fig 1.4 Chemical formulae of auranofin, $[Au(dppe)_2]Cl$ and some examples of Au(I)-NHC complexes.

In order to reduce the high thiol reactivity of linear two-coordinated Au(I) compounds, investigations were carried out on Au(I) complexes with chelate diphosphines: for example, $[Au(dppe)_2]Cl$ showed to exhibit significant antitumor activity against a range of model tumors in mice [57]. However, due to the severe hepatotoxicity observed in dogs [54], this compound was abandoned. The antitumor activity of tetrahedral Au(I) phosphine complexes may stem from the lipophilic, cationic properties of these compounds, as for other delocalized lipophilic cations that accumulate in mitochondria [54].

Many studies have shown that NHCs ligands have similar properties to phosphines in the way they interact with metals, including gold. These similarities led the researchers to investigate on Au–NHC complexes as potential new antitumour agents. For this class of compounds, a mechanism of action targeting mitochondria and involving TrxR inactivation is supposed, too [54].

Since Au(III) complexes are isoelectronic and isostructural with Pt(II) compounds (d^8, diamagnetic, dsp^2 hybridization, tetra-coordinate square planar geometry), soon they seemed to be excellent and innovative candidates for anticancer testing. However, at variance with Pt(II) compounds, Au(III) complexes were readily found to manifest a rather poor stability profile being kinetically more labile than the corresponding Pt(II) compounds, light-sensitive and easily reducible to metallic gold. As a results of these difficulties and, also, of detection of important *in vivo* toxicity, Au(III) compounds were quickly abandoned. Nonetheless, during the 90's, there was a strong return of interest toward gold(III)-based compounds as anticancer agents, especially when a few novel Au(III) complexes exhibiting improved stability, lower toxicity and favourable *in vitro* and *in vivo* pharmacological properties [49], were prepared.

A vast array of Au(III) complexes showing rather variegated structural chemistry has been considered as potential anticancer drugs [58]. From a structural point of view, the gold(III) compounds of interest may be grouped into the four following classes [59] (fig. 1.5):

(i) classical mononuclear gold(III) complexes. These compounds are square planar gold(III) compounds accompanied with nitrogen or halide ligands: $[AuCl_4]^-$, $[Au(dien)Cl]Cl_2$, $[Au(en)_2]Cl_3$, $[Au(cyclam)](ClO_4)_2Cl$, $[Au(terpy)Cl]Cl_2$ and $[Au(phen)Cl_2]Cl$. Nitrogen ligands are less labile than chloride ligands, while chloride ligands undergo far more facile aquation reactions. In turn, nitrogen ligands induce significant stabilization of the oxidation state +3;

(ii) gold(III) porphyrins. The porphyrin ligand greatly stabilizes the Au(III) center and drastically reduces its redox reactivity and oxidizing character. Reduction of gold(III) to gold(I) or elemental gold is very rare;

(iii) organogold(III) compounds. These complexes have at least one direct carbon–gold(III) bond which stabilizes oxidation state of gold. Organogold(III) compounds are stable under physiological conditions and have a limited tendency to be reduced to gold(I). They are significantly cytotoxic to human tumor cell lines;

(iv) dinuclear gold(III) complexes. These complexes are very stable under physiological-like conditions and have significant antiproliferative effects toward different human tumor cell lines. All these compounds contain a common structural motif, consisting of an Au_2O_2 "diamond core" linked to two bipyridine ligands in a roughly planar arrangement. Importantly, the introduction of different alkyl or aryl substituents on the 6 (and 6') position(s) of the bipyridine ligand leads to small structural changes that greatly affect the reactivity of the metal centers.

Advanced pharmacological testing performed with various gold (III) compounds suggests a mechanism that is distinct from classical platinum(II) compounds. Even though some evidence for direct DNA damage has been obtained in a few cases, effects on nucleic acids appear to be very modest for Au(III) complexes, so that it is unlikely that DNA is their primary target [60]. Instead, as in the case of auranofin, a

mechanism of action causing direct mitochondrial damage through selective modification of the active selenol site in TrxR is supposed [54].

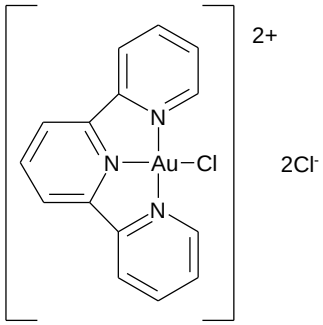

(i)
$[Au(terpy)Cl]Cl_2$

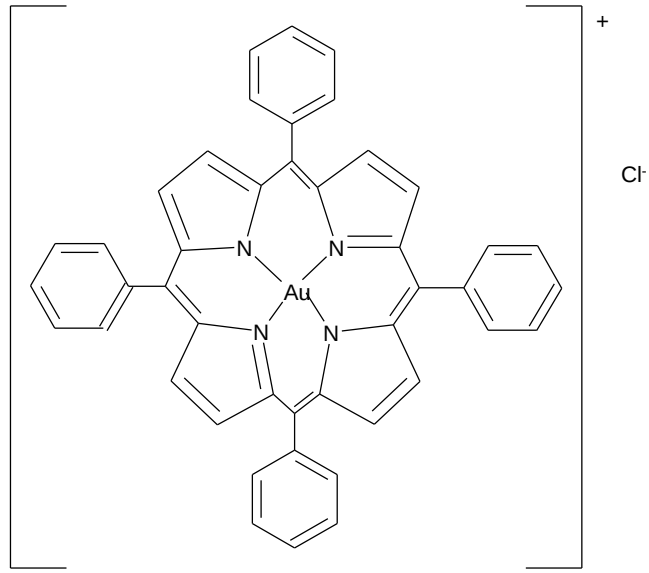

(ii)
meso-tetraphenylporphyrin gold chloride

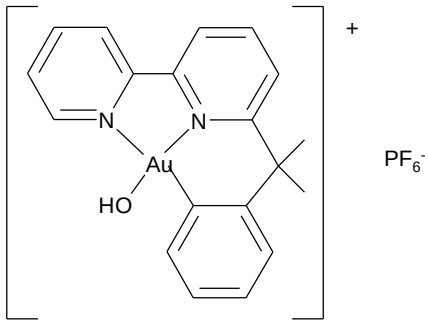

(iii)
Aubipy[c]

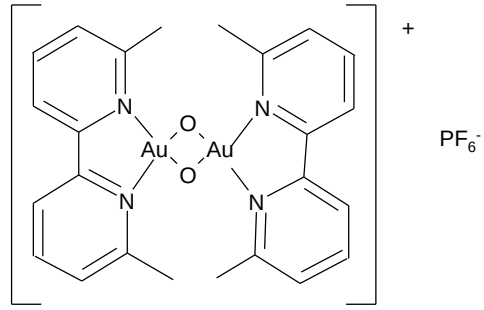

(iv)
$Auoxo_6$

Fig 1.5 Representative Au(III) compounds belonging to classes (i)-(iv).

1.1.6 The importance of studying metal-based anticancer drug/protein interactions

During the last four decades, the interest of the scientific community working on anticancer metal compounds has mostly been focused on their interactions with DNA,

the commonly accepted primary target for platinum compounds, that were described and analyzed in hundreds of papers [20].
In contrast, the reactions of platinum and non-platinum anticancer metallodrugs with proteins have initially received very poor attention but this topic is now attracting more and more interest. It is in fact increasingly evident that the interactions of anticancer metallodrugs with proteins play crucial roles not only in their uptake and biodistribution processes, but also in determining their overall toxicity profile, as for example in the case of Pt-drugs and the two major serum proteins albumin and transferrin [61-65]. Moreover, the inactivation of metallodrugs, and the resistance phenomena to metallodrugs, can be related to metal complex interaction with proteins, as in the case of cisplatin and metallothioneins, low molecular weight cysteine-rich proteins mainly involved in soft metal ion detoxification process [66]. Even more interesting, anticancer metallodrug-protein interaction has demonstrated to be likely involved in some crucial aspects of the mechanism of action of specific antitumor agents, as already mentioned in paragraphs 1.1.4 and 1.1.5, respectively, for Ru and Au compounds.
Thus, further work is absolutely needed to better understand the reactions of metallodrugs with proteins at the molecular level, in order to identify common trend in these reactions, characterize the structure and reactivity of the resulting "adducts" (in which the metallic fragment is coordinatively bound to protein) and identify the most important intracellular protein targets for the various classes of anticancer metallodrugs. In fact, a mechanistic understanding of how metal complexes produce their biological activities is crucial to their clinical success, as well as to the rational design of new and more efficient drugs through a "mechanism oriented" approach.

1.2 Mass spectrometry as a tool to study anticancer metallodrug-protein interactions

1.2.1 An overview

A combination of various techniques and approaches has been used for studying the biological effects of selected anticancer metallodrugs or novel transition metal complexes synthesized for application in therapy: chromatographic techniques (TLC or LC), mass spectrometry, nuclear magnetic resonance, microscopy, computational methods, capillary electrophoresis, isothermal titration calorimetry and differential scanning calorimetry, IR or UV/Vis spectroscopy, circular dichroism [67-69].
Despite of the abundance of available techniques, the gold standard for structural information on metallodrug-protein adducts at atomic resolution remains X-ray crystallography diffraction. The main challenge in XRD is sample preparation. Optimization of protein crystallization can be a lengthy process, if indeed it is

achievable at all [70]. Moreover, this technique provides only a static vision of metal complex-protein adducts in the solid state.
To date NMR is the method of choice for data collection at molecular level in the liquid phase; however, it is time consuming, protein size limited and may only work effectively under solution or substrate concentration conditions that may be unfavorable for the formation of stable protein adducts and which do not mimic physiological conditions. Moreover, as for XRD, strict requirements on sample purity are mandatory.
Mass spectrometry has been recognized as having great potential for the analysis of biomolecule/ligand adducts, due to its high sensitivity, specificity, high-throughput capability. The biological targets studied may include not only proteins but also enzymes and DNA [71] and the classes of ligands analyzed encompass not only anticancer metallodrugs but also peptides, proteins, nucleic acids, metal ions, drugs in general [72-75]. Through MS experiments valuable and independent structural information can be obtained in order to enrich and complete the data coming from the other analytical techniques. An example of the combined use of MS and X-ray crystallography can be found in a recent paper of Merlino and coworkers [76].

1.2.2 Mass spectrometry ionization techniques for studying the interactions of metallodrugs with proteins

In MS, the most common ionization techniques for studying the interactions of metal complexes with proteins are inductively-coupled plasma, electrospray ionization and matrix assisted laser desorption ionization.
ICP-MS relies on the atomization and ionization of the sample in the plasma, thus generating mainly singly-charged positive metal ions which can be detected in the MS analyzer. Consequently, ICP-MS tends to be employed for the determination of total metal contents in biological samples but does not give structural information [77].
Instead, ESI [78] and MALDI [79,80] techniques have enabled scientists to observe ion species of intact proteins and intact metallodrug-protein adducts. These two ionization methods have widely been used and are essential in the structural study of biological molecules. The two techniques are so important that the inventors, John B. Fenn and Koichi Tanaka, shared a portion of the Nobel Prize in chemistry in 2002.
ESI source was developed by Fenn and coworkers in 1984 [81] and is schematically represented in fig. 1.6

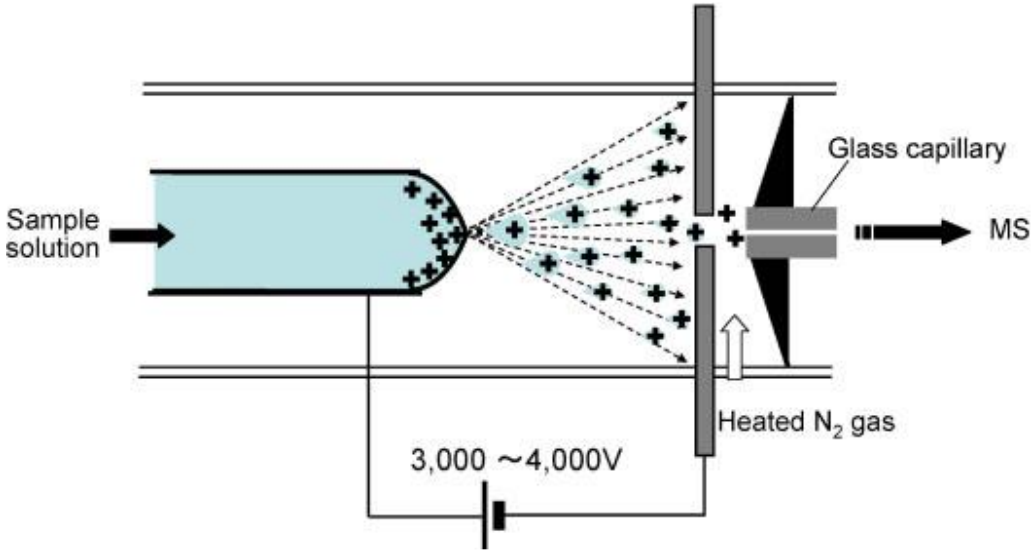

Fig. 1.6 A schematic illustration of ESI source developed by Fenn *et al.* in 1984 (figure taken from "S. Akashi, *Med. Res. Rev*., **2006**, *26*, 339–368").

This source generated ions in the gas phases at atmospheric pressure by spraying a sample solution from a metal needle where high voltage, such as + 3-4 kV, was applied. In addition, heated nitrogen gas helped to dry the sample droplets formed in the spraying process. A glass capillary was used as an orifice for transporting the ions from the ionization source at atmospheric pressure to the mass spectrometer under high vacuum. Several improvements have been accomplished based on the original ESI ion source, and now ESI mass spectra of various biological molecules can easily be obtained using commercially available instruments. ESI can generate ions with multiple charges, such as $[M + nH]^{n+}$ (when positive voltage is applied to the needle) or $[M - nH]^{n-}$ (when negative voltage is applied to the needle). The molecular weight of the biomolecule under examination can be then automatically calculated by using a deconvolution software.

Today, ESI-MS represents a very powerful method for molecular characterization of metal complex-biomolecule adducts. A series of pioneering studies carried out by Dan Gibson and coworkers during the 1990s and the early 2000s highlighted the advantages of this method and defined the experimental conditions for its application to investigate metallodrug-protein [82-84] or nucleobase [84] systems: information on the chemical nature of the adducts formed, the binding stoichiometry and the binding site location were obtained. ESI-MS can also provide information on binding specificity from competition experiments [85] and dissociation constants (K_d value) of protein-ligand complexes from titration experiments [86].

Laser desorption is another ionization method that can generate molecular ion of biological macromolecules. During the 1980s, several groups tried to ionize non-volatile molecules using lasers. In 1985, Hillenkamp and Karas [87] showed that aromatic matrix could be used to facilitate the volatilization of small molecules, but they did not succeed in ionization of biological macromolecules at that time. In 1987, Tanaka *et al.* [79] reported that large biomolecules could be ionized by a laser desorption method using a 337-nm low-energy (nitrogen) laser and a matrix of glycerol containing colloidal particles. They succeeded in ionization of intact proteins, and singly and doubly charged ions were detected. This was a breakthrough for the laser desorption method in its application to biological macromolecules. This technique has been mainly improved by Hillenkamp *et al.* as MALDI [80]. A schematic representation of MALDI is reported in fig. 1.7.

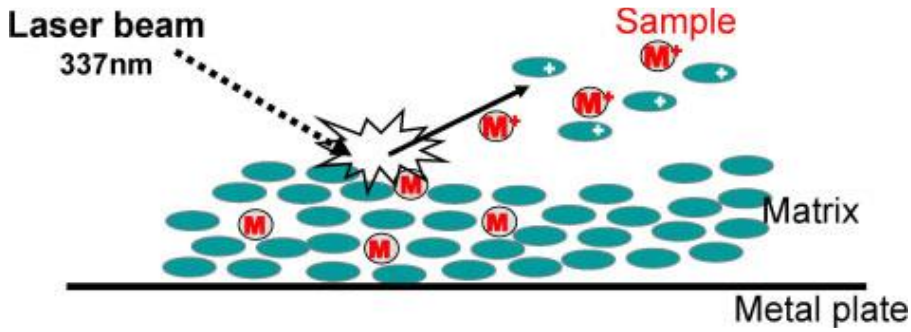

Fig. 1.7 A schematic representation of MALDI process (figure taken from "S. Akashi, *Med. Res. Rev*., **2006**, *26*, 339–368").

In MALDI, the sample is co-crystallized on a target plate with a matrix compound, such as sinapinic acid, in about a 1:1,000 molar ratio. Laser desorption occurs when the sample is irradiated with a focused laser beam in the ion source of the mass spectrometer. Most of the energy from the 337 nm pulsed laser beam is first adsorbed by the matrix and then used for vaporization and ionization of both the matrix and analyte molecules. The exact mechanism of MALDI, however, is not completely understood.

Since MALDI is robust and very tolerant of impurities in comparison to ESI, it is applicable to a large variety of compounds. However, there are only a limited number of reports on the detection of intact non-covalent complexes by MALDI-MS [88–94], because the dried sample mixed with the organic matrix is not ideal for the observation of non-covalent complexes that function under physiological conditions in solution phase. In addition, it is difficult to differentiate the ions of specific non-covalent

complexes from those of non-specific associations. Consequently, application of MALDI-MS to the detection of intact ions of non-covalent complexes is now far from being routine, and the literature on the ESI method for non-covalent complex analysis is now rapidly expanding [72]. Regarding specifically the strength of the coordinative bond between metallodrugs and protein, we have to say that it manifests an appreciable grade of stability under ESI conditions. Instead MALDI, though considered a soft ionization technique as ESI, can induce a certain degree of cleavage in metallodrug-protein adducts, both at protein-metal and metal-ligand bond level [95,96]. However, a general behavior rule is not easily predictable and the stability of the metal-protein adducts to the ionization conditions must be evaluated/ascertained time by time, being it related to the nature of the metal, the type of complex and the protein chosen.

1.2.3 High resolution mass analyzers for the study of metallodrug-protein adducts

High resolution mass analyzers, such as the quadrupole-time of flight [97], the Fourier transform-based Orbitrap [98] and the FT-ion cyclotron resonance [99], represent the state-of-the-art instruments. The advent of this kind of analyzers, endowed with isotopic resolution and high mass accuracy (< 5 ppm), has made possible to characterize proteins and metallodrug-protein adducts without proteolytic digestion, but simply by the direct fragmentation of the whole molecule in the mass spectrometer and the accurate acquisition of the masses of the fragments and the intact protein (or adduct) [100-102]. This procedure is referred to as top-down approach.

1.2.4 Mass spectrometry and metalloproteomics

Metallomics encompasses metalloproteomics as well as metallometabolomics. It is an emerging field addressing the role, uptake, transport and storage of trace metals essential for protein functions, but can also focus on metallometabolites, which may appear in the environment or which circulate in organisms as metal carriers. In this frame, extrapolating, the study of the fate of metallodrugs inside the human body can be ascribed to metallomics field and, more specifically, to metalloproteomics if the interaction of the metal complexes concern proteins.

The use of advanced protein separation techniques (*e.g.*, LC, CE, 2DGE), coupled to very sensitive metal detection methods, hold promise for successful analysis of complex mixtures of metallated proteins and for identification of those proteins that act as primary metallodrug receptors and/or metallodrug target. Thus, these latter techniques open the way to the investigation of far more complicated systems, such as metallodrug-treated cell populations and/or cell homogenates, that reflect more closely the reality of metallic species in the cell world.

ICP-MS, opportunely interfaced with a specific separation system, is a high specificity, high sensitivity technique. However, the derived data provide only information about the presence or absence of a specific metal element inside the biological sample, but it

will not allow any in-depth identification or characterization of the analyzed molecules [77].

The bottom-up MS approach, that is, metallodrug-protein adducts characterization by the combination of proteolytic digestion, LC separation and mass measurement, has successfully been applied on single protein, mixture of standard proteins and real samples (human blood serum, rat kidney cytosolic extracts, *E. coli* cells), in order to identify Pt- and Ru-bound proteins and the nature and position of the metallo fragments formed. In these experiments the classical bottom-up approach:

i) was applied as such [103];

ii) was preceded by laser ablation inductively coupled plasma mass spectrometry (LA-ICP-MS) on 1D or 2D gels in order to identify the bands/spots containing Pt [104,105];

iii) exploited a multidimentional protein identification technology (MudPIT) that combines SCX and RP chromatography [106-108];

iv) was applied only to the Pt-containing fractions obtained by a peptide or protein pre-fractionation step in OFFGEL-IEF [109,110];

v) exploited the ion mobility separation technique [111].

Mass spectrometry reveals to be a powerful technique for the analysis of complex mixtures in the molecular profiling approach, too. This approach gives an overview on alterations in protein expression between different cell states as, for example, the protein profile regulation in colon carcinoma cell lines treated with different metallodrugs (label-free quantitative proteomic approach) [112].

Finally, the recent advancements in data handling software, MS instrumentation and histological sample preparation make possible to analyze proteins and metallodrug-protein adducts directly on fresh tissue samples (mass spectrometry imaging) [113,114], for a better understanding of the *in vivo* drug distribution and drug-biomolecule interactions.

1.3 References

[1] P. J. Sadler, H. Li, H. Sun, *Coord. Chem. Rev*., **1999**, *185-186*, 689-709.

[2] A. Y. Louie, T. J. Meade, *Chem. Rev*., **1999**, *99*, 2711-2734.

[3] W. A. Volkert, T. J. Hoffman, *Chem. Rev*., **1999**, *99*, 2269-2292.

[4] M. J. Clarke, F. Zhu, D. R. Frasca, *Chem. Rev*., **1999**, *99*, 2511-2533.

[5] A. M. Evangelou, *Crit. Rev. Oncol. Hematol*., **2002**, *42*, 249-265.

[6] C. G. Hartinger, S. Zorbas-Seifried, M. A. Jakupec, B. Kynast, H. Zorbas, B. K. Keppler, *J. Inorg. Biochem*., **2006**, *100*, 891-904.

[7] N. Katsaros, A. Anagnostopoulou, *Crit. Rev. Oncol. Hematol*., **2002**, *42*, 297-308.

[8] I. Kostova, *Anticancer Agents Med. Chem*., **2006**, *6*, 19-32.

[9] I. Kostova, *Anticancer Agents Med. Chem*., **2009**, *9*, 827-842.

[10] I. Ott, R. Gust, *Arch. Pharm. Chem. Life Sci*., **2007**, *340*, 117-126.
[11] P. J. Dyson, G. Sava, *Dalton Trans*., **2006**, 1929-1933.
[12] C. Gabbiani, A. Casini, L. Messori, *Gold Bull*., **2007**, *40*, 73-81.
[13] B. Rosenberg, L. Van Camp, T. Krigas, *Nature*, **1965**, *205*, 698-699.
[14] P. Pil, S. J. Lippard, in *Encyclopedia of Cancer*, **1997**, vol. 1, J. R. Bertino (Ed.), Academic Press, San Diego, 392.
[15] B. A. Chabner, C. J. Allegra, G. A. Curt, P. Calabresi in *Goodman and Gilman's: The Pharmacological Basis of Therapeutics*, **1996**, G. J. Hardman, E. L. Limbird, G. A. Gilman (Eds.); McGraw-Hill, New York, 1233-1287.
[16] P. J. Loehrer, L. H. Einhorn, *Ann. Intern. Med*., **1984**, *100*, 704-713.
[17] E. R. Jamieson, S. J. Lippard, *Chem. Rev*., **1999**, *99*, 2467-2498.
[18] L. R. Kelland, *Drugs*, **2000**, *59 (suppl. 4)*, 1-8.
[19] B. Lippert, *Cisplatin: Chemistry and Biochemistry of a Leading Anticancer Drug*, **1999**, Wiley, New York.
[20] D. Wang, S. J. Lippard, *Nat. Rev. Drug Discov*., **2005**, *4* ,307-320.
[21] E. L. M. Lempers, J. Reedijk, *Adv. Inorg. Chem.*, **1991**, *37*, 175-217.
[22] Z. J. Guo, P. J. Sadler, *Adv. Inorg. Chem*., **2000**, *49*, 183-306.
[23] F. Kraft in *Metal Complexes in Cancer Chemotherapy*, *1993*, B. K. Keppler (Ed)., VCH, Weinheim, Germany, 391.
[24] S. E. Miller, D. A. House, *Inorg. Chim. Acta*, **1989**, *166*, 189-197.
[25] M. C. Lim, R. B. Martin, *J. Inorg. Nucl. Chem*., **1976**, *38*, 1911-1914.
[26] D. P. Bancroft, C. A. Lepre, S. J. Lippard, *J. Am. Chem. Soc*., **1990**, *112*, 6860-6871.
[27] K. J. Barnham, S. J. Berners-Price, T. A. Frenkiel, U. Frey, P. J. Sadler, *Angew. Chem. Int. Edit*., **1995**, *34*, 1874-1877.
[28] D. Wang, S. J. Lippard, *Nat. Rev. Drug Discov*., **2005**, *4*, 307-320.
[29] P. J. Whitehead, S. J. Lippard in *Metal Ions in Biological Systems*, **1996**, vol. 32, A. Sigel, H. Sigel (Ed.), Marcel Dekker, Inc., New York.
[30] K.-B. Lee, D. Wang, S. J. Lippard, P. A. Sharp, *Proc. Natl. Acad. Sci*., **2002**, *99*, 4239-4244.
[31] W. R. Waud, *Cancer Res*., **1987**, *47*, 6549-6555.
[32] C. Meijer, N. H. Mulder, G. A. P. Hospers, D. R. A. Uges, E. G. E. De Vries, *Br. J. Cancer*, **1990**, *62*, 72-77.
[33] A. Eastman, N. Schulte, *Biochem.*, **1988**, *27*, 4730-4734.
[34] R. B. Weiss, M. C. Christian, *Drugs*, **1993**, *46*, 360-377.
[35] M. S. Robillard, J. Reedijk, Platinum-based anticancer drugs. In: *Encyclopedia of Inorganic Chemistry*, 2nd ed., R. B. King (Ed.), John Wiley & Sons, Ltd.: Chichester, UK, **2005**, 4488-4498.
[36] V. Brabec, *V. Progr. Nucl. Acid Res. Mol. Biol*., **2002**, *71*, 1-68.

[37] M. A. Jakupec, M. Galanski, B. K. Keppler, *Rev. Physiol. Biochem. Pharmacol*., **2003**, *146*, 1-53.
[38] D. Lebwohl, R. Canetta, *Eur. J. Cancer***, 1998**, *34*, 1522-1534.
[39] F. Lévi, G. Metzger, C. Massari, G. Milano, *Clin. Pharmacokinet*., **2000**, *38*, 1-21.
[40] D. M. Kweekel, H. Gelderblom, H.-J. Guchelaar, *Cancer Treatment Rev*., **2005**, *31*, 90-105.
[41] R.E. Aird, J. Cummings, A. A. Ritchie, M. Muir, R. E. Morris, H. Chen, P. J. Sadler, D. I. Jodrell, *Br. J. Cancer*, **2002**, *86*, 1652-1657.
[42] H. Depenbrock, S. Schmelcher, R. Peter, B. K. Keppler, G. Weirich, T. Block, J. Rastetter, A.-R. Hanauske, *Eur. J. Cancer*, **1997**, *33*, 2404-2410.
[43] C. S. Allardyce, P. J. Dyson, *Platinum Metal Rev*., **2001**, *45 (2)*, 62-69.
[44] G. Sava, E. Alessio, A. Bergamo, G. Mestroni, *Top. Biol. Inorg. Chem.*, **1999**, *1*, 143-169.
[45] W. H. Ang, P. J. Dyson, *Eur. J. Inorg. Chem*., **2006**, 4003-4018.
[46] G. Pintus, B. Tadolini, A. M. Posadino, B. Sanna, M. Debidda, F. Bennardini, G. Sava, C. Ventura, *Eur. J. Biochem*., **2002**, *269*, 5861-5870.
[47] S. P. Fricker, *Transit. Metal. Chem*., **1996**, *21*, 377–383.
[48] L. Messori, G. Marcon, *Met. Ions. Biol. Syst*., **2004**, *41*, 279–304.
[49] S. Nobili, E. Mini, I. Landini, C. Gabbiani, A. Casini, L. Messori, *Med. Res. Rev.*, **2010**, *30*, 550–580.
[50] A. Casini, L. Messori, *Curr. Top. Med. Chem*., 2**011**, *11*, 2647–2660.
[51] E. M. Nagy, L. Ronconi, C. Nardon, D. Fregona, *Mini-Rev. Med. Chem*., **2012**, *12*, 1216–1229.
[52] S. J. Berners-Price, A. Filipovska, *Metallomics*, **2011**, *3*, 863–873.
[53] M. A. Cinellu, I. Ott, A. Casini, in *Bioorganometallic Chemistry: Application in Drug Discovery, Biocatalysis and Imaging*, **2015**, G. Jaouen, M. Salmain (Eds), Wiley-VCH, Weinheim, 117-139.
[54] P. J. Barnard, S. J. Berners-Price, *Coord. Chem. Rev*., **2007**, *251*, 1889-1902.
[55] C. F. Shaw III, *Comments Inorg. Chem*., **1989**, *8*, 233-267.
[56] C. F. Shaw III, *Chem. Rev.*, **1999**, *99*, 2589-2600.
[57] S. J. Burners-Price, C. K. Mirabelli, R. K. Johnson, M. R. Mattern, F. L. McCabe, L. F. Faucette, C.-M. Sung, S.-M. Mong, P. J. Sadler, S. T. Crooke, *Cancer Res.*, **1986**, *46*, 5486-5493.
[58] A. Casini, C. Hartinger, C. Gabbiani, E. Mini, P. J. Dyson, B. K. Keppler, L. Messori, *J. Inorg. Biochem*., **2008**, *102*, 564-575.
[59] N. Arsenijević, V. Volarević, M. Milovanović, Ž. D. Bugarčić in *Encyclopedia of Metalloproteins*, R. H. Kretsinger, V. N. Uversky, E. A. Permyakov (Eds.), Springer, Heidelberg, **2013** , 922-927.
[60] M. Coronnello, G. Marcon, S. Carotti, S., B. Caciagli, E. Mini, T. Mazzei, P. Orioli, L. Messori, *Oncol. Res*., **2000**, *12*, 361–370.

[61] A. I. Ivanov, J. Christodoulou, J. A. Parkinson, K. J. Barnham, A. Tucker, J. Woodrow‖, P. J. Sadler, *J. Biol. Chem*., **1998**, *273*, 14721-14730.
[62] W. C. Cole, W. Wolfe, *Chem.-Biol. Interations*, **1980**, *30*, 223-235.
[63] I. Khalaila, C. S. Allardyce, C. S. Verma, P. J. Dyson, *Chem. Bio. Chem*., **2005**, *6*, 1788-1795.
[64] C. S. Allardyce, P. J. Dyson, J. Coffey, N. Johnson, *Rapid Commun. Mass Spectrom*., **2002**, *16*, 933-935.
[65] Y. Y. Zhao, R. Mandal, X. F. Li, *Rapid Commun. Mass Spectrom*., **2005**, *19*, 1956-1962.
[66] D. Hagrman, J. Goodisman, J. C. Dabrowiak, A.-K. Souid, *Drug Metab. Dispos*., **2003**, *31*, 916-923.
[67] D. Esteban-Fernández, E. Moreno-Gordaliza, B. Canãs, M. A. Palacios, M. M. Gómez-Gómez, *Metallomics*, **2010**, *2*, 19-38.
[68] F. Kratz, in *Metal Complexes in Cancer Chemotherapy*, **1993**, B. K. Keppler (Ed.), VCH: Weinheim, Germany, 391.
[69] K. J. Pacholarz, R. A. Garlish, R. J. Taylor, P. E. Barran, *Chem. Soc. Rev.*, **2012**, *41*, 4335-4355.
[70] A. M. Hassell, G. An, R. K. Bledsoe, J. M. Bynum, H. L. Carter, S. J. J. Deng, R. T. Gampe, T. E. Grisard, K. P. Madauss, R. T. Nolte, W. J. Rocque, L. P. Wang, K. L. Weaver, S. P. Williams, G. B. Wisely, R. Xu, L. M. Shewchuk, *Acta Crystallogr*., *Sect. D: Biol. Crystallogr*., **2007**, *63*, 72–79.
[71] C. G. Hartinger, M. Groessl, S. M. Meier, A. Casini, P. J. Dyson, *Chem. Soc. Rev.*, **2013**, *42*, 6186-6199.
[72] J. A. Loo, *Mass Spectrom. Rev.*, **1997**, *16*, 1–23.
[73] S. Akashi, *Med. Res. Rev*., **2006**, *26*, 339–368.
[74] Y. J. Kim, Z. H. Li, D. H. Kim, J. H. Hahn, *Bioorg. Med. Chem. Lett*., **1996**, *6*, 1449–1452.
[75] J. Zaia, L. C. Jiang, M. S. Han, J. R. Tabb, Z. C. Wu, D. Fabris, C. Fenselau, *Biochemistry*, **1996**, *35*, 2830–2835.
[76] A. Merlino, T. Marzo, L. Messori, *Chem. Eur. J*., **2017**, *23*, 6942-6947.
[77] K. Wrobel, K. Wrobel, J. A. Caruso, in *Applications of Physical Methods to Inorganic and Bioinorganic Chemistry*, **2007**, R. A. Scott, C. M. Lukehart (Eds.), John Wiley & Sons, Chichester, 205–225.
[78] J. B. Fenn, M. Mann, C. K. Meng, S. F. Wong, C. M. Whitehouse, *Science*, **1989**, *246*, 64-71.
[79] K. Tanaka, H. Waki, Y. Ido, S. Akita, Y. Yoshida, T. Yohida, *Rapid Commun. Mass Spectrom.*, **1988**, *2*, 151–153.
[80] M. Karas, F. Hillenkamp, *Anal. Chem*., **1988**, *60*, 2299–2301.
[81] M. Yamashita, J. B. Fenn, *J. Phys. Chem*., **1984**, *88*, 4451–4459.
[82] D. Gibson, C. E. Costello, *Eur. Mass Spectrom*., **1999**, *5*, 501-510.

[83] T. Peleg-Schulman, D. Gibson, *J. Am. Chem. Soc*., **2001**, *123*, 3171-3172.
[84] T. Peleg-Schulman, Y. Najajreh, D. Gibson, *J. Inorg. Biochem*., **2002**, *91*, 306-311.
[85] A. Casini, C. Gabbiani, E. Michelucci, G. Pieraccini, G. Moneti, P. J. Dyson, L. Messori, *J. Biol. Inorg. Chem.*, **2009**, *14*, 761-770.
[86] M. C. Jecklin, S. Schauer, C. E. Dumelin, R. Zenobi, *J. Mol. Recognit*., **2009**, *22*, 319-329.
[87] M. Karas, D. Bachmann, F. Hillenkamp, *Anal. Chem.*, **1985**, *57*, 2935–2939.
[88] F. Hillenkamp, in *Matrix-assisted laser desorption/ionization of non-covalent complexes. New Methods for the study of biomolecular complexes, NATO ASI series C: Mathematical and Physical Sciences 510*, **1998,** Dordrecht, The Netherlands Kluwer Academic Publishers, 181–191.
[89] J. G. Kiselar, K. M. Downard. *J. Am. Soc. Mass Spectrom.*, **2000**, *11*, 746–750.
[90] K. Strupat, D. Saga, J. Peter-Katalinic, H. Bonisch, G. Schafer, *Analyst*, **2000**, *125*, 563–567.
[91] A. S. Woods, M. A. Huestis, *J. Am. Soc. Mass Spectrom*., **2001**, *12*, 88–96.
[92] S. D. Friess, J. M. Daniel, R. Hartmann, R. Zenobi, *Int. J. Mass Spectrom*., **2002**, *219*, 269–281.
[93] M. Zehl, G. Allmaier, *Anal. Chem*., **2005**, *77*, 103–110.
[94] B. Tissot, F. Gonnet, A. Iborra, C. Berthou, N. Thielens, G. J. Arlaud, R. Daniel, *Biochemistry*, **2005**, *44*, 2602–2609.
[95] C. G. Hartinger, W. H. Ang, A. Casini, L. Messori, B. K. Keppler, P. J. Dyson, *J. Anal. At. Spectrom*., **2007**, *22*, 960–967.
[96] F. Gonnet, F. Kocher, J. C. Blais, G. Bolbach, J. C. Tabet, J. C. Chottard, *J. Mass Spectrom.*, **1996**, *31*, 802–809.
[97] G. L. Glish, D. E. Goeringer, *Anal. Chem*., **1984**, *56*, 2291-2295.
[98] A. Makarov, *Anal. Chem*., **2000**, *72*, 1156-1162.
[99] M. B. Comisarow, A. G. Marshall, *Chem. Phys. Lett.*, **1974**, *25*, 282-283.
[100] C. G. Hartinger, Y. O. Tsybin, J. Fuchser, P. J. Dyson, *Inorg. Chem*., **2008**, *47*, 17-19.
[101] E. Moreno-Gordaliza, B. Canãs, M. A. Palacios, M. M. Gómez-Gómez, *Anal. Chem.* **2009**, *81*, 3507–3516.
[102] H. Li, T.-Y. Lin, S. L. Van Orden, Y. Zhao, M. P. Barrow, A. M. Pizarro, Y. Qi, P. J. Sadler, P. B. O'Connor, *Anal. Chem*., **2011**, *83*, 9507–9515.
[103] E. Moreno-Gordaliza, B. Cañas, M. A. Palacios, M. M. Gómez-Gómez, *Talanta*, **2012**, *88*, 599–608.
[104] C. S. Allardyce, P. J. Dyson, F. R. Abou-Shakra, H. Birtwistle, J. Coffey, *Chem. Comm*., **2001**, 2708-2709.

[105] E. Moreno-Gordaliza, D. Esteban-Fernández, C. Giesen, K. Lehmann, A. Lázaro, A. Tejedor, C. Scheler, B. Cañas, N. Jakubowski, M. W. Linscheidb, M. M. Gómez-Gómez, *J. Anal. At. Spectrom*., **2012**, 27, 1474-1483.
[106] J. Will, A. Kyas, W. S. Sheldrick, D. Wolters, *J. Biol, Inorg. Chem*., **2007**, *12*, 883–894.
[107] J. Will, W. S. Sheldrick, D. Wolters, *J. Biol, Inorg. Chem*., **2008**, *13*, 421–434.
[108] J. Will, D. A. Wolters, W. S. Sheldrick, *ChemMedChem,* **2008**, *3*, 1696–1707.
[109] I. Moraleja, E. Moreno-Gordaliza, M. L. Mena, M. M. Gómez-Gómez, *Talanta*, **2014**, *120*, 433–442.
[110] I. Moraleja, E. Moreno-Gordaliza, D. Esteban-Fernández, M. L. Mena, M. W. Linscheid, M. M. Gómez-Gómez, *Anal. Bioanal. Chem*., **2015**, *9*, 2393–2403.
[111] J. P. Williams, H. I. A. Phillips, I. Campuzano, P. J. Sadler, *J. Am. Soc. Mass Spectrom.*, **2010**, *21*, 1097-1106.
[112] D. Kreutz, A. Bileck, K. Plessl, D. Wolrab, M. Groessl, B. K. Keppler, S. M. Meier, C. Gerner, *Chem. Eur. J*., **2017**, *23*, 1881-1890.
[113] A. Bouslimani, N. Bec, M. Glueckmann, C. Hirtz, C. Larroque, *Rapid Commun. Mass Spectrom*., **2010**, *24*, 415–421.
[114] K. Wu, F. Jia, W. Zheng, Q. Luo, Y. Zhao, F. Wang, *J. Biol. Inorg. Chem*., **2017**, *22*, 653-661.

2. OUTLINE AND AIMS OF THE RESEARCH PROJECT

2.1 Research background

The study of the interaction between anticancer metallodrugs (or novel, promising metal compounds) and biomolecules (DNA, proteins) has been the object of investigation for many years in our laboratories, with the purpose to contribute to a deeper understanding of such interactions and to provide the basis for a rational design of new metallodrugs, less toxic and more selective for cancer therapy. In particular, valuable structural and functional information on the adducts formed among proteins and anticancer metallodrugs/metal compounds were mainly obtained through XRD and MS experiments.

XRD studies involved the use of Pt(II)-, Au(I)-, Au(III)-compounds and proteins of very different MW, ranging from the small, model proteins Cyt *c*, RNase A, Hewl, SOD, to the bigger, transport serum proteins Ft and HSA [1-11]. A complete description of the results obtained in these experiments is beyond the scope of this paragraph and it will be selectively and comparatively faced out in chapter 6.

In the past years, a wide variety of MS studies were carried out in our laboratories on metallated protein adducts and a representative selection is listed below.

The most investigated metallodrugs included: Pt(II)-compounds, as cisplatin, carboplatin and oxaliplatin [12,13]; Ru(III)- and Ru(II)-compounds, as, respectively, NAMI-A [14] and RAPTA family [15]; Au(I) complexes, as Auranofin [16]. Often, these metallodrugs were studied in comparison with their new and promising analogues. Thus, cisplatin and carboplatin analogues, as well as novel promising Ru(II), Au(I) and Au(III) compounds, were investigated: Pt(II) iminoethers [17]; Pt(II) complexes were ammonia ligands were replaced by the bidentate ethylenediamine ligand [13]; diiodidediamine platinum(II) complexes [18,19]; Pt(II) compounds bearing sulfur, phosphorus or oxygen mono/bidentate ligands [20-22]; the trans-(dimethylamino)(methylamino)dichloridoplatinum(II) complex [23]; the Ru(II) complex *fac*-[$Ru(CO)_3Cl_2(N^1$-1,3-thiazole)] [24]; two analogues of RAPTA compounds [25]; Au(I)/Au(III) complexes bearing saccharinate ligands [26]; mononuclear Au(III) and dinuclear oxo-bridged Au(III) derivatives both bearing heteroaromatic ligands [27-29].

At variance with XRD experiments reported in references 1-11, the proteins we used in the above mentioned MS studies were mainly model proteins: Ub, Cyt *c*, RNase A, Hewl, SOD monomer. These proteins are of moderate to small size, with MW ranging from 8 to 16 kDa; they are all commercially available and relatively cheap, water soluble and manifest a high stability in solution under physiological-like conditions. In

addition, these proteins are easily detectable by MS in positive ion mode. An essential step in this research area is in fact represented by the firm characterization and modelization of the interactions taking place between representative metallodrugs and protein side-chains. It is reasonable to assume that, in spite of the intrinsic structural diversity of the various proteins, some common patterns may hold in metal-protein interactions related to the specific nature of the metal center and of protein side-chains. To this purpose, studies of simple model proteins have turned out to be valuable since the choice of relatively simple systems reduces the variables to be taken into account and focuses on analogies and differences between the various compounds in the presence of different proteins.

It is not the intent of this paragraph to list all the specific results obtained in the above mentioned MS experiments but, rather, to point out the general information that could be obtained from the study of this kind of simplified systems: not only the exact binding stoichiometry was detected but, thanks to the use of the Orbitrap analyzer, the nature of the metallo fragment bound to the protein was unambiguously revealed (see, as exemplificative case, reference [30]).

When the biomolecule's size increases, as in the case of systems constituted by real target proteins, the achievement of a such deep level of molecular information becomes more and more difficult. Some experiments, performed in our laboratories with the MALDI-TOF and ESI-LTQ-Orbitrap mass spectrometers, confirmed this limit. In particular, a MALDI-TOF analysis conducted on the cytosolic TrxR1 enzyme (MW ≅ 55 kDa per monomer) incubated with different gold compounds was only able to suggest, due to the inadequate instrumental resolution at those MW, the binding of an imprecise number of gold-containing fragments (5-10 equivalents) [31]. Thus, in order to gain further insight on the occurring gold-enzyme interactions, and identify those residues that undergo metallation, a tryptic digestion of the adducts was performed. Moreover, some attempts were made with medium to large size protein metal adducts analyzed in the ESI-Orbitrap mass spectrometer: disappointing results were obtained since this high resolution mass analyzer explicates its optimal performances with maximum molecular weights of about 20-30 kDa.

The solution to this problem can be found by using different MS analyzers endowed with higher resolving powers as, for example, the Q-TOF or better the FT-ICR. Alternatively, the above mentioned enzymatic digestion strategy can be exploited. This latter approach, besides providing information about the nature of the metallo fragments and the binding stoichiometry, is mainly used to reveal the metal binding site location on protein, as shown by us in the case of the carboplatin/Cyt *c* and *cis*-diphosphane platinum(II) dichlorides/Cyt *c* systems: a limited proteolysis with AspN enzyme (due to the Cyt *c* sequence, only two fragments were generated) was performed in order to elucidate the binding site position of platinum on that protein [13,22].

Finally, we have to say that, excluding these three shy approaches attempted on TrxR1 and Cyt *c*, our research group have never faced out yet the topic of metallodrug binding site location on proteins in a general and systematic way.

2.2 Aims of the research project

Within this frame, the aim of this research project was the widening of the knowledge related to the characterization, at molecular level, of the adducts formed between various kind of metallodrugs (or novel, promising metal compounds) and a number of proteins, by using mass spectrometry.
This aim was pursued through two main search directions:
i) the study on the chemical nature and the binding stoichiometry of the adducts formed between small size proteins and: a) new analogues of cisplatin and oxaliplatin anticancer drugs (chapter 3); b) novel Au(III) complexes (chapter 4);
ii) the development and introduction in our laboratories of an efficient and generally applicable method for metallodrugs binding site location on proteins, regardless of the MW and nature of the protein and the type of metal complex under investigation, in order to get closer to the study of real, interesting biological systems (chapters 5 and 6).

2.3 References

[1] A. Casini, G. Mastrobuoni, C. Temperini, C. Gabbiani, S. Francese, G. Moneti, C. T. Supuran, A. Scozzafava, L. Messori, *Chem. Commun.*, **2007**, 156–158.
[2] L. Messori, T. Marzo, A. Merlino, *Chem. Commun*., **2014**, *50*, 8360–8362.
[3] D. Marasco, L. Messori, T. Marzo, A. Merlino, *Dalton Trans*., **2015**, *44*, 10392–10398.
[4] M. Serratrice, L. Maiore, A. Zucca, S. Stoccoro, I. Landini, E. Mini, L. Massai, G. Ferraro, A. Merlino, L. Messori, M. A. Cinellu, *Dalton Trans*., **2016**, *45*, 579–590.
[5] L. Messori, F. Scaletti, L. Massai, M. A. Cinellu, C. Gabbiani, A. Vergara, A. Merlino, *Chem. Commun*., **2013**, *49*, 10100–10102.
[6] I. Russo Krauss, L. Messori, M. A. Cinellu, D. Marasco, R. Sirignano, A. Merlino, *Dalton Trans*., **2014**, *43*, 17483–17488.
[7] G. Ferraro, L. Massai, L. Messori, M. A. Cinellu, A. Merlino, *Biometals*, **2015**, *28*, 745–754.
[8] G. Ferraro, L. Massai, L. Messori, A. Merlino, *Chem. Commun.*, **2015**, *51*, 9436–9439.

[9] N. Pontillo, F. Pane, L. Messori, A. Amoresano, A. Merlino, *Chem. Commun*., **2016**, *52*, 4136–4139.
[10] V. Calderone, A. Casini, S. Mangani, L. Messori, P. L. Orioli, *Angew. Chem. Int. Ed.*, **2006**, *45*, 1267-1269.
[11] G. Ferraro, L. Messori, A. Merlino, *Chem. Commun*., **2015**, *51*, 2559-2561.
[12] A. Casini, C. Gabbiani, G. Mastrobuoni, L. Messori, G. Moneti, G. Pieraccini, *ChemMedChem*, **2006**, *1*, 413-417.
[13] C. Gabbiani, A. Casini, G. Mastrobuoni, N. Kirshenbaum, O. Moshel, G. Pieraccini, G. Moneti, L. Messori, D. Gibson, *J. Biol. Inorg. Chem*., **2008**, *13*, 755-764.
[14] A. Casini, G. Mastrobuoni, M. Terenghi, C. Gabbiani, E. Monzani, G. Moneti, L. Casella, L. Messori, *J. Biol. Inorg. Chem*., **2007**, *12*, 1107-1117.
[15] A. Casini, G. Mastrobuoni, W. H. Ang, C. Gabbiani, G. Pieraccini, G. Moneti, P. J. Dyson, L. Messori, *ChemMedChem*, **2007**, *2*, 631-635.
[16] C. Gabbiani, L. Massai, F. Scaletti, E. Michelucci, L. Maiore, M. A. Cinellu, L. Messori, *J. Biol. Inorg. Chem*., **2012**, *17*, 1293-1302.
[17] A. Casini, C. Gabbiani, G. Mastrobuoni, R. Z. Pellicani, F. P. Intini, F. Arnesano, G. Natile, G. Moneti, S. Francese, L. Messori, *Biochemistry*, **2007**, *46*, 12220-12230.
[18] L. Messori, A. Casini, C. Gabbiani, E. Michelucci, L. Cubo, C. Rios-Luci, J. M. Padrón, C. Navarro-Ranninger, A. G. Quiroga, *ACS Med. Chem. Lett*., **2010**, *1*, 381-385.
[19] L. Messori, L. Cubo, C. Gabbiani, A. Álvarez-Valdés, E. Michelucci, G. Pieraccini, C. Rios-Luci, L. G. León, J. M. Padrón, C. Navarro-Ranninger, A. Casini, A. G. Quiroga, *Inorg. Chem*., **2012**, *51*, 1717-1726.
[20] C. Mügge, C. Rothenburger, A. Beyer, H. Görls, C. Gabbiani, A. Casini, E. Michelucci, I. Landini, S. Nobili, E. Mini, L. Messori, W. Weigand, *Dalton Trans*., **2011**, *40*, 2006-2016.
[21] C. Mügge, R. Liu, H. Görls, C. Gabbiani, E. Michelucci, N. Rüdiger, J. H. Clement, L. Messori, W. Weigand, *Dalton Trans*., **2014**, *43*, 3072-3086.
[22] C. Mügge, E. Michelucci, F. Boscaro, C. Gabbiani, L. Messori, W. Weigand, *Metallomics*, **2011**, *3*, 987-990.
[23] L. Messori, T. Marzo, E. Michelucci, I. Russo Kraus, C. Navarro-Ranninger, A. G. Quiroga, A. Merlino, *Inorg. Chem*., **2014**, *53*, 7806-7808.
[24] D. Valensin, P. Anzini, E. Gaggelli, N. Gaggelli, G. Tamasi, R. Cini, C. Gabbiani, E. Michelucci, L. Messori, H. Kozlowski, G. Valensin, *Inorg. Chem*. **2010**, *49*, 4720-4722.
[25] T. Marzo, A. Savić, L. Massai, E. Michelucci, T. J. Sabo, S Grguric-Šipka, L. Messori, *Biometals*, **2015**, *28*, 425-430.
[26] L. Maiore, M. A. Cinellu, E. Michelucci, G. Moneti, S. Nobili, I. Landini, E. Mini, A. Guerri, C. Gabbiani, L. Messori, *J. Inorg. Biochem*., **2011**, *105*, 348-355.

[27] M. A. Cinellu, L. Maiore, M. Manassero, A. Casini, M. Arca, H.-H. Fiebig, G. Kelter, E. Michelucci, G. Pieraccini, C. Gabbiani, L. Messori, *ACS Med. Chem. Lett*., **2010**, *1*, 336-339.
[28] C. Gabbiani, L. Massai, F. Scaletti, E. Michelucci, L. Maiore, M. A. Cinellu, L. Messori, *J. Biol. Inorg. Chem*., **2012**, *17*, 1293-1302.
[29] C. Gabbiani, F. Scaletti, L. Massai, E. Michelucci, M. A. Cinellu, L. Messori, *Chem. Commun.*, **2012**, *48*, 11623-11625.
[30] A. Casini, C. Gabbiani, E. Michelucci, G. Pieraccini, G. Moneti, P. J. Dyson, L. Messori, *J. Biol. Inorg. Chem.*, **2009**, *14*, 761-770.
[31] C. Gabbiani, G. Mastrobuoni, F. Sorrentino, B. Dani, M. P. Rigobello, A. Bindoli, M. A. Cinellu, G. Pieraccini, L. Messori, A. Casini, *Med. Chem. Comm*., **2011**, *2*, 50-54.

3. DIRECT INFUSION ESI-ORBITRAP ANALYSES TO STUDY THE INTERACTION OF MODEL PROTEINS WITH CISPLATIN AND OXALIPLATIN ANALOGUES

The results presented in this chapter have been published in the following two papers:
- "Cisplatin and its dibromido analogues: a comparison of chemical and biological profiles". T. Marzo, G. Bartoli, C. Gabbiani, G. Pescitelli, M. Severi, S. Pillozzi, E. Michelucci, B. Fiorini, A. Arcangeli, A. G. Quiroga, L. Messori, *Biometals*, **2016**, *29*, 535-542.
- "PtI_2(DACH), the iodido analogue of oxaliplatin as a candidate for colorectal cancer treatment: chemical and biological features". D. Cirri, S. Pillozzi, C. Gabbiani, J. Tricomi, G. Bartoli, M. Stefanini, E. Michelucci, A. Arcangeli, L. Messori, T. Marzo, *Dalton Trans.*, **2017**, *46*, 3311-3317.

3.1. Introduction

Cisplatin is a leading and established anticancer compound in widespread clinical use. It is very effective against a few cancer types, such as testicular and ovarian cancer, but, despite its clinical success, there are several disadvantages associated with this metallodrug, including low water solubility [1], significant toxicity, which limits patient doses [1], severe side effects such nausea, nephrotoxicity, neurotoxicity [2] and intrinsic or acquired resistance in some cancer types [3,4]. Moreover, cisplatin is scarcely active against other important and more frequent solid tumors, like colorectal, ovarian and lung cancer [5-7].
In particular, CRC is today the fourth most common cause of death due to cancer worldwide. Adjuvant chemotherapy for CRC mainly relies on fluoropyrimidine compounds combined with oxaliplatin. Oxaliplatin (Eloxatin™) is a third-generation platinum compound approved by United States FDA in 2002 for the treatment of advanced colorectal cancer. Despite its success, frequent intrinsic or acquired pharmacological resistance [8], as well as important side effects, such as acute and chronic neurotoxicity [9], are still limiting factors to its clinical use.
With the aim to overcome the main drawbacks of cisplatin and oxaliplatin, in the last few decades many analogues of these clinically established metallodrugs have been synthesized and tested.
While thousands of analogues of cisplatin have been prepared and tested so far, quite surprisingly the immediate parent platinum compounds that are obtained through simple replacement of the two chlorides with different halides as metal ligands (in

particular the diiodide and dibromide derivatives) were poorly investigated. Most likely, this situation arises from the early misconception and/or generalization that chloride replacement with other halides may result into substantial loss of the anticancer activity for cisplatin [10-12]. These arguments led us to explore this kind of modification in a more systematic way and analyze its chemical and biological consequences.

Recently, we demonstrated that the diiodide analogue of cisplatin manifests truly interesting biological properties and warrants a more extensive pharmacological evaluation [13]. This encouraging result prompted us to synthetize even the dibromide analogue of cisplatin (*cis*$PtBr_2$; fig. 3.1).

Similarly, we have prepared the oxaliplatin analogue where the bidentate oxalate ligand was replaced by two iodide ligands (PtI_2(DACH); fig. 3.1). Notably, this oxaliplatin derivative was reported and structurally characterized in 2011 by R. Pažout and coworkers [14], but no biological studies were then attempted. The reason that makes PtI_2(DACH) of particular interest for inorganic medicinal chemists is essentially twofold.

(i) We believe that the replacement of the bidentate oxalate ligand with two iodides may affect mainly the activation process of the Pt center, both kinetically and thermodynamically, influencing accordingly its overall biological profile.

(ii) In addition, insertion of two iodide ligands in the place of oxalate is expected to increase considerably the lipophilic character of the resulting drug, hopefully enhancing cellular uptake and bioavailability.

3.2 Materials and MS method

The dibromide analogue of cisplatin and the diiodide analogue of oxaliplatin were synthesized in accordance with the procedure described in the two published papers reported at pg. 35.

The selected model proteins for this study were Hewl and RNase A (fig. 3.2). Hewl has an average MW of 14305.1 Da (129 amino acids) in its oxidized form and is a particularly suitable protein for ESI-MS investigation, as already explained in paragraph 2.1. Moreover, this protein is well-known among crystallographers as a protein very prone to crystallization, thus turning out very appropriate for possible XRD comparative studies of its metallodrug adducts. Similar features can be ascribed to RNase A, a protein with an average MW of 13682.2 Da (124 amino acids) in its oxidized form.

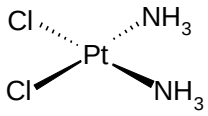

cisplatin

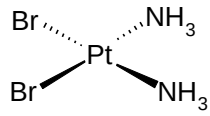

cis$PtBr_2$

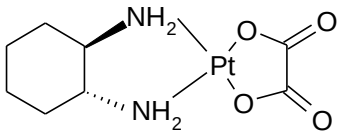

oxaliplatin

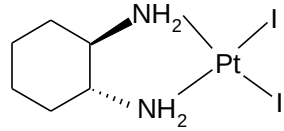

PtI_2(DACH)

Fig 3.1 Chemical formulae of cisplatin and its dibromide analogue (*cis*$PtBr_2$), and oxaliplatin and its diiodide analogue (PtI_2(DACH)).

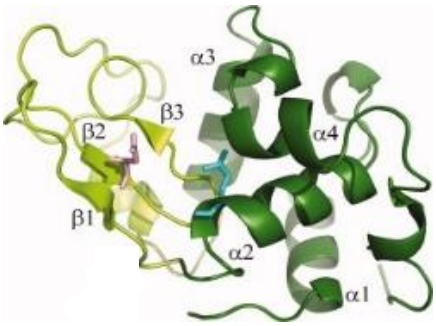

Hewl

RNase

Fig. 3.2 Crystal structures of Hewl (PDB 4LZT) and RNase A (PDB 1FS3).

The metal complex-protein adduct formation was accomplished by incubating the proteins with a three times molar excess of the selected metal compound at different incubation times at 37 °C in 20 mM ammonium acetate buffer (pH 6.8).
The incubated samples did not require purification or separation steps: a simple dilution with water was performed before direct infusion of the adduct solution in ESI-Orbitrap mass spectrometer. Mass spectrometry ionization process is usually sensitive to the presence of buffers/salts in the samples but, in this case, buffer removing was not necessary thanks to the choice of an MS compatible one. Moreover, adducts were not purified from metal complex excess since our previous experience (not reported here) and a specific study conducted on this topic (see paragraph 5.3.4), have demonstrated that it does not promote false positive adduct formation in ESI source and Orbitrap mass spectrometer. Finally, our methodological approach is fast and robust not only during sample preparation, but also in terms of instrumental analysis: even in the absence of a chromatographic separation among the various adducts formed, very clear and informative mass spectra were acquired thanks to the Orbitrap high resolution mass analyzer.
We have also to underline that sample acidification (an usual step in MS protein analysis) was not mandatory for the MS analysis of this kind of metal-protein adducts: the choice of suitable and well MS-responsive model proteins allowed us to avoid acid addition to the samples, thus preventing the possible metallo fragment-protein bond impairment (see paragraph 5.3.1)
For more details on "Materials and methods" see the two published papers reported at pg. 35.

3.3 Results and discussion

A detailed discussion of all the results obtained in the two published papers reported at pg. 35 is not the aim of this chapter. Instead, we want to focus our attention on the information obtained through the ESI-MS experiments (the chemical nature and the binding stoichiometry of the metal-protein adduct formed, as declared in paragraph ″2.2 Aims of the research project″) in relationship with those acquired with the other investigation techniques used in these two articles.
When tested in ESI-MS with the Hewl model protein, *cis*$PtBr_2$ showed a Pt coordination that involves the preferential detachment of halide ligands and the full retention of ammonia ligands (fig. 3.3).

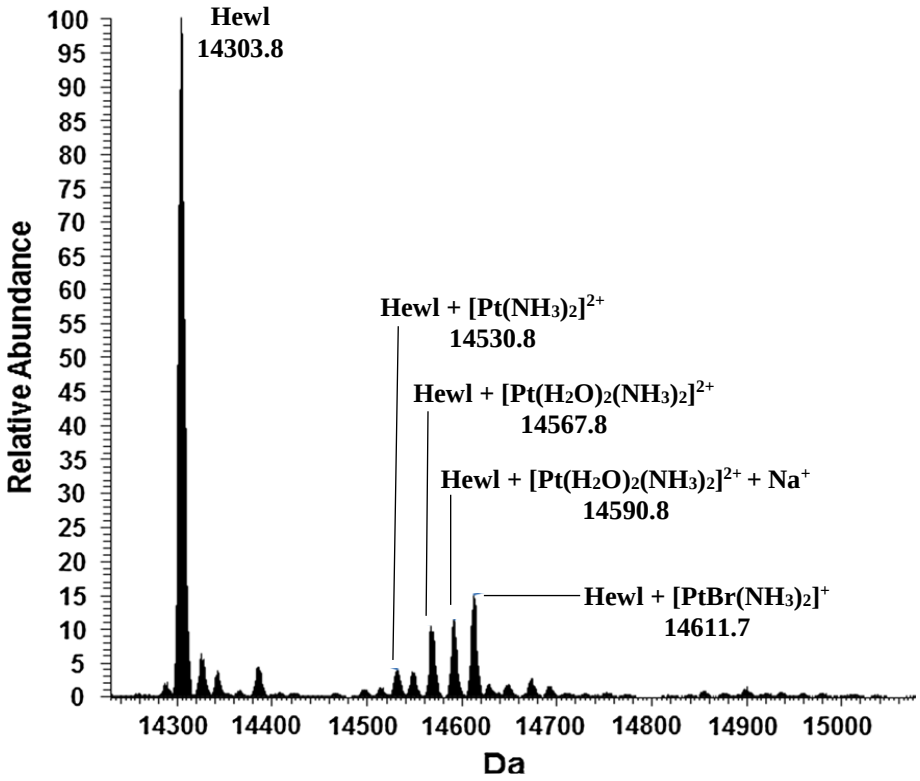

Fig. 3.3 Deconvoluted ESI-Orbitrap mass spectrum of Hewl incubated with *cis*$PtBr_2$ (metal:protein ratio = 3:1) recorded after 72 h incubation at 37 °C in 20 mM AA buffer at pH 6.8.

This kind of protein metalation strictly resembles that produced by cisplatin, this latter resulting in an adduct characterized by selective Pt coordination to His15 following the release of the two chloride ligands [15]. Analogously, the study of the in-solution behavior (spectrophotometric investigation) and the interaction with calf thymus DNA (examined by circular dichroism) showed similarities among the two compounds. Cellular studies demonstrated generally comparable cytotoxic effects and the slightly greater effects of *cis*$PtBr_2$ on FLG 29.1 cell line (human acute myeloid leukaemia) may be, at least partially, ascribed to its higher lipophilicity compared to cisplatin, which could ensue into an increased cellular uptake. Also, even the possible small differences in the kinetic of halides release may be invoked to play some role in the slight but meaningful differences in the pharmacological effect between cisplatin and its dibromide analogue.

Regarding PtI_2(DACH), a survey was conducted in order to study it in comparison to oxaliplatin. PtI_2(DACH) was incubated with Hewl and RNase A and, in both cases, no

metallodrug–protein adduct was detected in ESI-MS, indicating that PtI_2(DACH), in contrast to oxaliplatin [16,17], is not able to bind these model proteins. An explanation for this unexpected behaviour is not straightforward. We previously reported [16,17] that coordination of oxaliplatin to Hewl and RNase A could imply a multi-step reaction at the level of aspartate residues. First, non-covalent coordination of oxaliplatin to the protein occurs; then detachment of one oxygen atom of oxalate from Pt coordination (a ring-opening step leading to monodentate oxalate) is observed with concomitant Pt coordination of the carboxylate group from an aspartate residue. Finally, the oxalate ligand is fully released. We might hypothesize that this multi-step mechanism is inhibited when the oxalate ligand is replaced by two iodides due to the lack of "recognition" of intact PtI_2(DACH) by these model proteins. This hypothesis is supported by the results coming from the solution behavior studies that indicated a faster release of the two iodide ligands of PtI_2(DACH) in comparison with the oxalate in oxaliplatin.

ESI-MS studies in negative ion mode were also performed to analyze the interactions between oxaliplatin, or PtI_2(DACH), and standard DNA oligonucleotides. In analogy with its parent drug oxaliplatin [18], PtI_2(DACH) interacts extensively with a standard oligonucleotide bearing the GG motif (ODN2, average MW = 3596.4 Da) through a classical reaction pattern involving preferential release of iodide ligands (fig. 3.4).

Regardless of the differences and analogies of behavior highlighted by ESI-MS experiments, oxaliplatin and PtI_2(DACH) induced roughly comparable cytotoxicity in three representative CRC cell lines. This implies that the replacement of oxalate with two iodide does not impair the cellular effects of oxaliplatin, that may be thus attributed mainly to the $[Pt(DACH)]^{2+}$ chemical moiety.

Finally, we strongly believe that the information obtained in this chapter through ESI-MS experiments are similar to the single tiles of an immense puzzle that, together with the information derived from other analytical techniques, provide a better picture of the mechanism of action, at the molecular level, for Pt-metallodrugs.

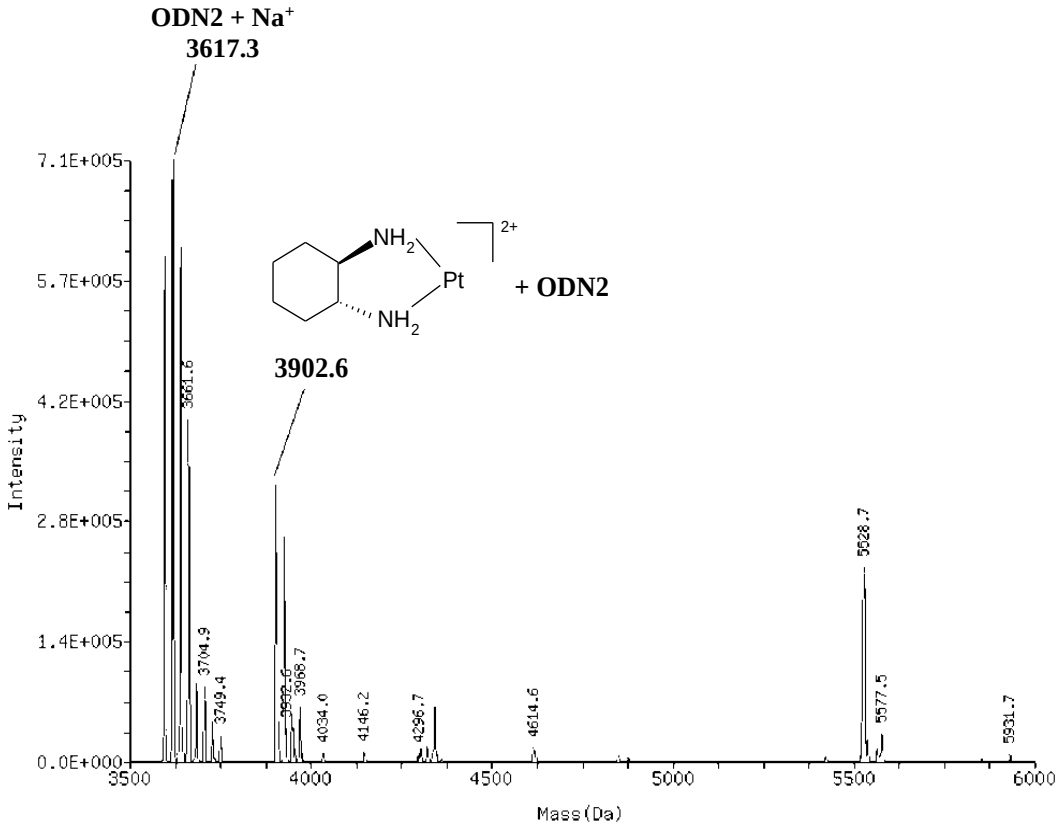

Fig. 3.4 Deconvoluted ESI-Orbitrap mass spectrum of PtI_2(DACH) incubated with ODN2 in water for 72 h at 37 °C; metal to oligonucleotide ratio 1:1.

3.4 References

[1] B. A. Chabner, C. J. Allegra, G. A. Curt, P. Calabresi in *Goodman and Gilman's: The Pharmacological Basis of Therapeutics*, **1996**, G. J. Hardman, E. L. Limbird, G. A. Gilman (Eds.); McGraw-Hill, New York, 1233-1287.
[2] P. J. Loehrer, L. H. Einhorn, *Ann. Intern. Med*., **1984**, *100*, 704-713.
[3] E. R. Jamieson, S. J. Lippard, *Chem. Rev*., **1999**, *99*, 2467-2498.
[4] L. R. Kelland, *Drugs*, **2000**, *59 (suppl. 4)*, 1-8.
[5] P. A. De Simone, E. Davilla, P. R. Jochimsen, A. A. Bartolucci, *Cancer Treat. Rep*., **1986**, *70*, 1229–1230.
[6] S. J. Wang, G. S. Wu, *J. Biol. Chem*., **2014**, *289*, 17163–17173.
[7] R. Rosell, R. V. N. Lord, M. Taron, N. Reguart, *Lung Cancer*, **2002**, *38*, 217–227.

[8] J. L. Misset, H. Bleiberg, W. Sutherland, M. Bekradda, E. Cvitkovic, *Crit. Rev. Oncol./Hematol*., **2000**, *35*, 75-93.
[9] G. D. Leonard, M. A. Wright, M. G. Quinn, S. Fioravanti, N. Harold, B. Schuler, R. R. Thomas, J. L. Grem, *BMC Cancer*, **2005**, *5*, 116.
[10] J. J. Wilson, S. J. Lippard, *Chem. Rev*., **2014**, *114*, 4470–4495.
[11] T. M. Johnstone, G. Y. Park, S. J. Lippard, *Anticancer Res*., **2014**, *34*, 471–476.
[12] M. J. Cleare, J. D. Hoeschele, *Bioinorg. Chem*., **1973**, *2*, 187–210.
[13] T. Marzo, S. Pillozzi, O. Hrabina, J. Kasparkova, V. Brabec, A. Arcangeli, G. Bartoli, M. Severi, A. Lunghi, F. Totti, C. Gabbiani, A. G. Quiroga, L. Messori, *Dalton Trans*., **2015**, *44*, 14896–14905.
[14] R. Pažout, J. Houskova, M. Dušek, J. Maixner, P. Kačer, *Struct. Chem*., **2011**, *22*, 1325-1330.
[15] A. Casini, G. Mastrobuoni, C. Temperini, C. Gabbiani, S. Francese, G. Moneti, C. Supuran, A. Scozzafava, L. Messori, *Chem. Commun*., **2007**, *2*, 156–158.
[16] L. Messori, T. Marzo, A. Merlino, *Chem. Commun*., **2014**, *50*, 8360-8362.
[17] L. Messori, T. Marzo, A. Merlino, *J. Inorg. Biochem*., **2015**, *153*, 136-142.
[18] S. Mowaka, M. Ziehe, D. Mohamed, U. Hochkirch, J. Thomale, M. W. Linscheid, *J. Mass Spectrom*., **2012**, *47*, 1282-1293.

4. DIRECT INFUSION ESI-ORBITRAP AND MALDI-TOF ANALYSES TO STUDY THE INTERACTION OF MODEL PROTEINS WITH GOLD(III) COMPLEXES

The results presented in this chapter have been published in the following three papers:
- "Gold (III) complexes with hydroxyquinoline, aminoquinoline and quinoline ligands: synthesis, cytotoxicity, DNA and protein binding studies". C. Martín-Santos, E. Michelucci, T. Marzo, L. Messori, P. Szumlas, P. J. Bednarski, R. Mas-Ballesté, C. Navarro-Ranninger, S. Cabrera, J. Alemán, *J. Inorg. Biochem*, **2015**, *153*, 339-345.
- "Organogold(III) compounds as experimental anticancer agents: chemical and biological profiles". L. Massai, D. Cirri, E. Michelucci, G. Bartoli, A. Guerri, M. A. Cinellu, F. Cocco, C. Gabbiani, L. Messori, *Biometals*, **2016**, *29*, 863-872.
- "Interactions of the organogold(III) compound Aubipy^c with the copper chaperone Atox1: a joint mass spectrometry and circular dichroism investigation". T. Marzo, F. Scaletti, E. Michelucci, C. Gabbiani, G. Pescitelli, L. Messori, L. Massai, *Biometals*, **2015**, *28*, 1079-1085.

4.1 Introduction

Among non-platinum anticancer drugs, in recent years gold(I) and gold(III) complexes have attracted much attention because of their strong cytotoxicity *in vitro* and their different mode of action in comparison to cisplatin [1–12]. Indeed, although platinum(II) and gold(III) complexes are isoelectronic (d^8 configuration) and isostructural (square planar geometry), they were found to show different biological profiles and mechanisms of action [13]. As already reported in chapter 1, DNA is commonly believed to be the primary target for platinum(II) complexes, while inhibition of a few crucial proteins seems to be the main mechanism of action for cytotoxic gold complexes. In addition, ligand exchange is faster in gold(III) complexes compared to platinum(II) ones. In this sense, the chelation of the metallic center with multidentate ligands turned out to enhance the stability of the complex, but an excessive stabilization of the gold center may be detrimental to the biological activity (*e.g.*, Au(cyclam)) [14]. The selection of ligands is also crucial to modulate the oxidizing character of the gold(III) center and decrease its pronounced tendency to be reduced to gold(I).
Chelating nitrogen donors, such as phen, bipy, terpy and en, were proposed to control these two features [15,16]. Moreover, the presence of a direct C–Au bond further

stabilizes the gold(III) center against reduction, as in the case of Aubipy^c (**1**) [16]. Examples of Au(III) complexes bearing these chelating ligands are reported in fig. 4.1.

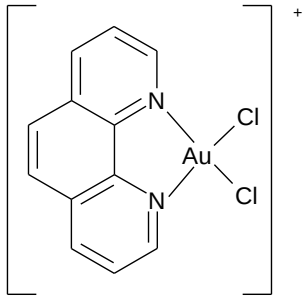

[Au(phen)Cl_2]Cl

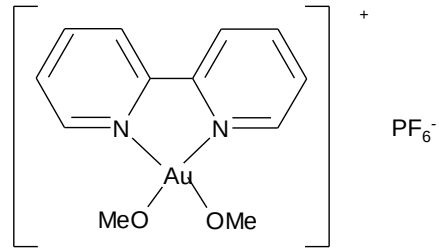

[Au(bipy)$(OMe)_2$][PF_6]

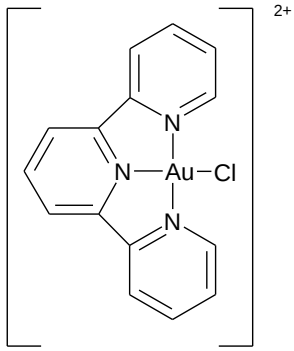

[Au(terpy)Cl]Cl_2

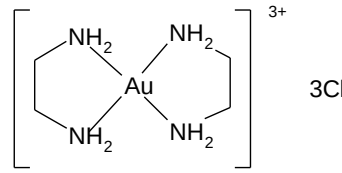

[Au$(en)_2$]Cl_3

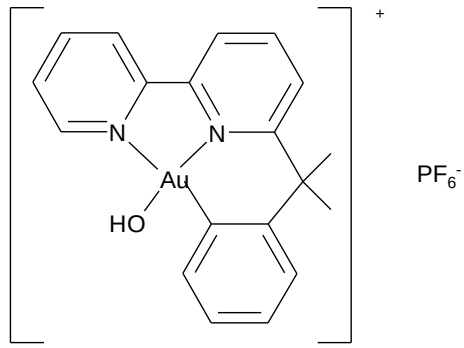

1

Aubipy^c

Fig 4.1 Chemical formulae of representative Au(III) complexes bearing chelating nitrogen donors.

We decided to focus our attention on Aubipy^{c}, that is stable under pseudo-physiological conditions but sufficiently cytotoxic towards different ovarian cancer cell lines either sensitive and resistant to cisplatin [17]. In previous studies we tested the compound against a panel of 12 cancer cell lines and it was found to produce moderate antiproliferative effects [18]. Further studies on the interaction of Aubipy^{c} with model proteins revealed that small amounts of metal–protein adducts are formed with Cyt *c* and Hewl; notably, in these adducts the gold(III) center and the C,N,N pincer ligand are conserved [19].
Recently, Aubipy^{c} was reported to form stable adducts, containing gold in the oxidation state +1, with the metallochaperone Atox1 protein, as evidenced by electrospray ionization high-resolution mass spectrometry [20].
Having said this, we decided to elucidate, in deeper detail, the nature of the gold binding site in the Aubipy^{c}-Atox1 adduct by MS analyses based on tryptic digestion and metal competition experiments. Moreover, we extended our investigations to a comparative study involving Aubipy^{c} and its dimer Au_2bipy^{c}, on one hand, and the new compound Aubipy^{aa}, on the other (fig. 4.2).

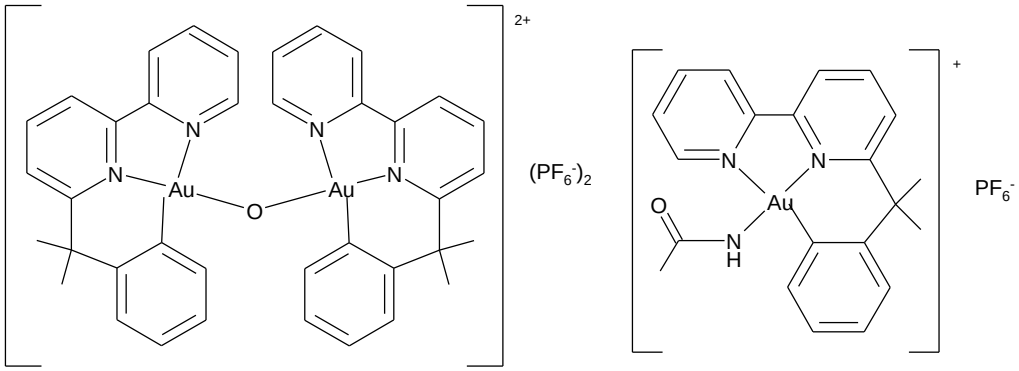

2
Au_2bipy^{c}

3
Aubipy^{aa}

Fig 4.2 Chemical formulae of Au_2bipy^{c} (**2**) and Aubipy^{aa} (**3**).

Finally, our interest was attracted by new gold(III) complexes containing quinoline (**4**), aminoquinoline (**5**) and hydroxyquinolines (**6a, 6b**) as ligands (fig 4.3). This interest originated from the fact that, in the context of polyaromatic ligands, hydroxyquinolines are reported to be promising therapeutic agents for Alzheimer's dementia [21–24] and are known to exhibit a variety of biological activities [25–29]. Regarding the anticancer activity of the hydroxyquinolines, a number of interesting features were highlighted. They are classified as proteasome inhibitors through complexation with

copper ions [30–33]; they induce apoptosis in human cancer cell lines by targeting zinc to lysosomes [34]; they are NF-kappa β inhibitors [35,36], or stimulate macrophages to release tumor necrosis factor alpha [37], among other anticancer activities. All these applications are related to the use of hydroxyquinolines as scavengers of metals involved in the pathogenesis of various diseases. Recently, new platinum complexes containing hydroxyquinolines in their structure were synthesized and their *in vitro* antitumor activity and interactions with DNA were demonstrated [38]. Therefore, we considered worthy of interest the synthesis of new gold(III) complexes analogous to these platinum ones in order to study their chemical and biological profile.

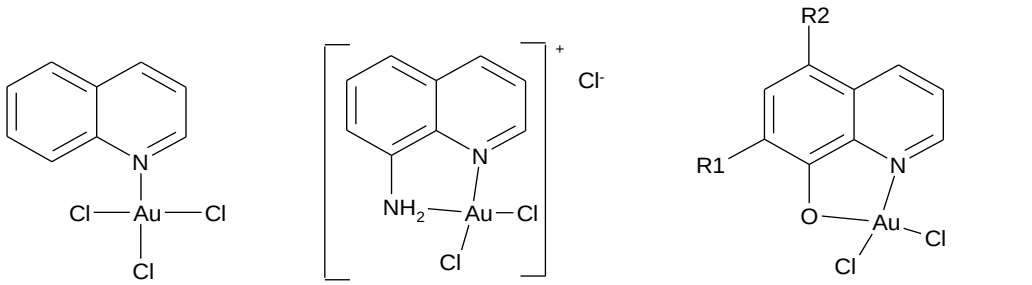

4
[$AuCl_3$(quinoline)]

5
[$AuCl_2$(8-NH_2-quinoline)]Cl

6a (R1 = H, R2 = H
[$AuCl_2$(8-O-quinoline)]

6b (R1 = H, R2 = Cl)
[$AuCl_2$(5-Cl-8-O-quinoline)]

Fig 4.3 Gold(III) complexes containing quinoline (**4**), aminoquinoline (**5**) and hydroxyquinolines (**6a** and **6b**) as ligands.

4.2 Materials and MS methods

The gold(III) complexes **1-6** were synthesized and characterized as described in the three published papers reported at pg. 43.
The selected model proteins for MS studies were not only the already mentioned (see paragraph 3.2) Hewl and RNase A, but also the Cyt *c* and the Atox1 (fig. 4.4).

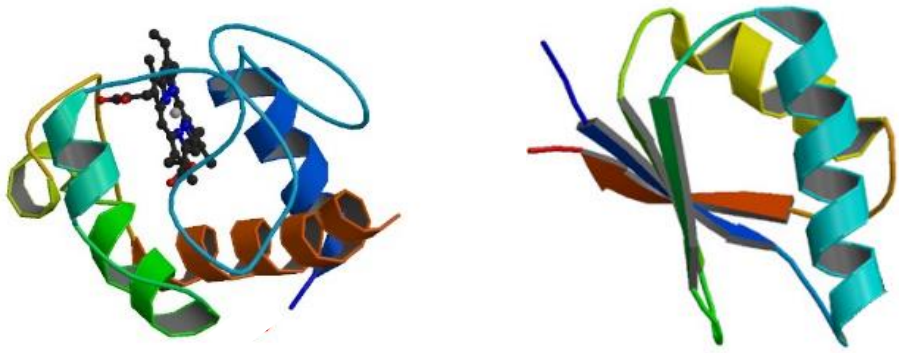

Cyt *c* Atox1

Fig. 4.4 Crystal structures of Cyt *c* (RCSB PDB 1HRC) and Atox1 (RCSB PDB 5F0W).

Cyt *c* has an average MW of 12360.1 Da (104 amino acids) and is a particularly suitable protein for ESI-MS investigation, as already explain in paragraph 2.1. Moreover, it has been shown to play a role in apoptosis of cancer cells [39] and so could represent a protein target for anti-cancer metallodrugs.
Atox1, an intracellular metallochaperone protein with an average MW of 7401.6 Da (68 amino acids), was cloned from human cDNA expressed in *E. Coli*. This protein is crucially involved in copper trafficking and contains the CXXC motif for copper(I) binding in the vicinity of the N-terminus: the Cu(I) center is bound to the two cysteines Cys12 and Cys15. The CXXC motif is well prone to accommodate, beyond copper, a variety of ‘‘soft’’ metal ions and metallodrugs. Accordingly, it was suggested and experimentally proved that the copper trafficking system may play a key role in the cellular uptake and processing of platinum-based anticancer drugs with relevant pharmacological consequences, making thus Atox1 something more than a simple model protein for MS studies with metallodrugs. A few studies documented that cisplatin reacts with Atox1 forming stable derivatives [40-43]. Structures of cisplatin derivatives of Atox1 were then solved through X-ray diffraction [44] or NMR measurements [45], showing a direct interaction of the platinum(II) center with the CXXC motif. In turn, a study by Pernilla Wittung-Stafshede *et al.* investigated the reaction of cisplatin with Atox1 through a variety of biophysical methods and demonstrated that copper(I) and platinum(II) ions may bind simultaneously to this protein to nearby, yet independent and not mutually exclusive, anchoring sites [46,47]. Finally, we have recently demonstrated tight binding to Atox1 of a variety of gold compounds of medicinal interest, among them being Aubipy^{c} [20].

The metal complex-protein adduct formation was performed as already described in paragraph 3.2, except in the case of Atox1-metal compound incubations, where rt and protein to metal ratios 1:1 or 1:5 were used; a particular attention was paid in order to preserve Cys12 and Cys15 in their reduced form (addition of the reducing agent dithiothreitol (DTT) and presence of N_2 inert atmosphere to avoid O_2 effects).
As already discussed in the case of Pt compounds (see paragraph 3.2), the incubated samples did not require any purification, acidification or separation steps before ESI-Orbitrap analysis. Only in the case of Atox1 and Atox1 adducts, the samples were diluted with 1% HCOOH, instead of water, before MS analysis, in order to improve their ESI detection in positive ion mode. In fact, while the other proteins used so far have a basic pI (over 9.5), human Atox1 has a pI = 6.71.
The digestion of Atox1 and Atox1-Aubipy^c adducts was performed on immobilized trypsin tips. This kind of tryptic digestion is faster than the classic in solution one, thus limiting the possible oxidation of the derivatives due to the long time of exposure to the air.
The resulting digested peptide mixtures were spotted on an AnchorChip MALDI target together with the matrix solution. The dried spots were analyzed with a MALDI-TOF spectrometer in order to identify the protein portion containing the gold binding site.
For more details on "Materials and methods" see the three published papers reported at pg. 43.

4.3 Results and discussion

As already said in paragraph 3.3, a detailed discussion of all the results obtained in the three published papers reported at pg. 43 is not the aim of this chapter. Instead, we desire to focus our attention on the information obtained through the ESI-Orbitrap and MALDI-TOF experiments and we want to highlight their correlation with the results obtained with the other investigation techniques used in these three papers.

The antiproliferative activity of complexes **4**, **5**, **6a** and **6b** was investigated on four distinct human solid tumor cell lines resulting that three out of four tested gold(III) compounds are more active than cisplatin, namely **5**, **6a** and **6b**. DNA electrophoresis experiments demonstrated that the interactions of these gold(III) complexes with DNA are generally weak and, for this reason, the interactions of **5**, **6a** and **6b** with Cyt *c* was studied. These three compounds showed a remarkable reactivity with this model protein with formation of various kinds of adducts (figs. 4.5 and 4.6).

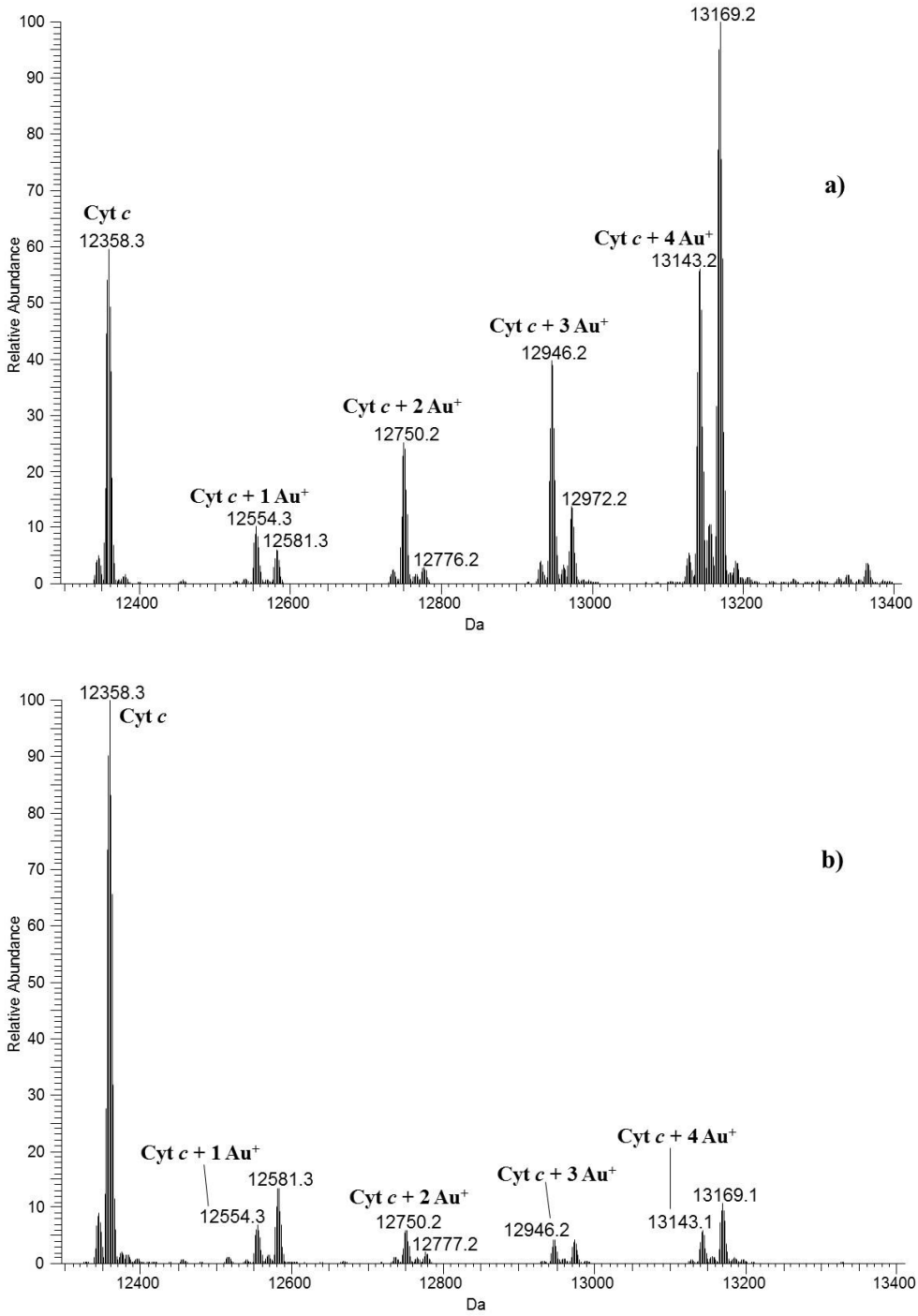

Fig. 4.5 Deconvoluted ESI-Orbitrap mass spectra of Cyt *c* treated with gold compounds (a) **6a** and (b) **6b** after 24 h incubation at 37 °C.

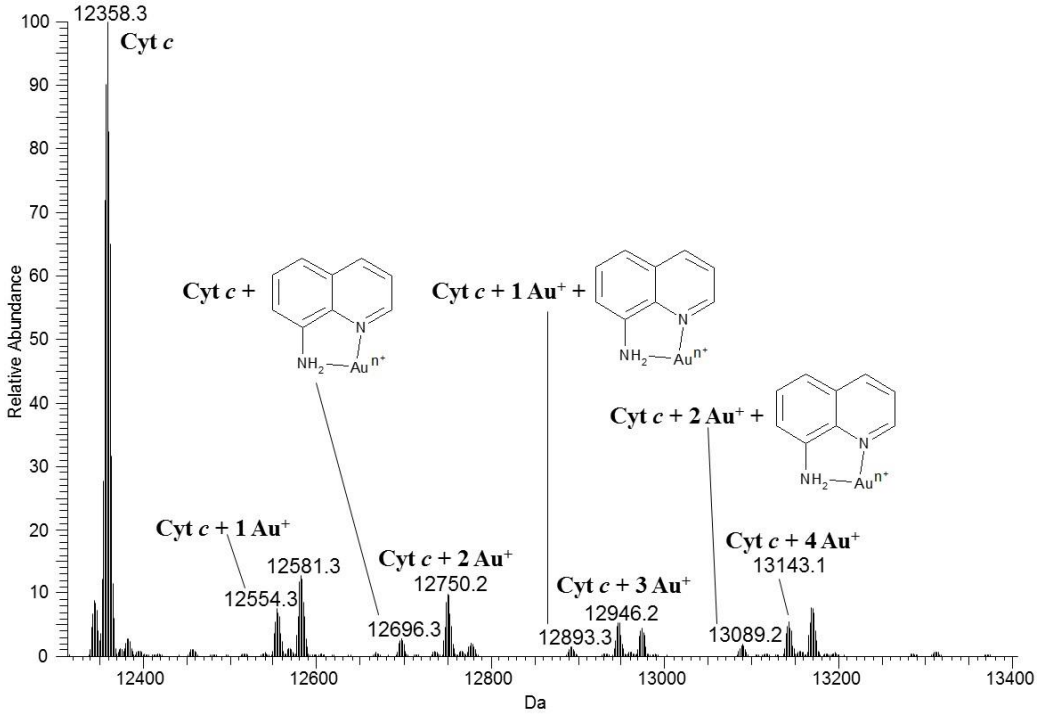

Fig. 4.6 Deconvoluted ESI-Orbitrap mass spectrum of Cyt *c* treated with gold compound **5** after 24 h incubation at 37 °C (n = 1 or 3).

The most reactive complex toward Cyt *c* was **6a**. Both **6a** and **6b** reacted with the protein just through coordination of the naked Au^+ cation with loss of the ligands. Multimetallated adducts were detected for all complexes (see peaks Au^+ (12554.3 Da), 2 Au^+ (12750.2 Da), 3 Au^+ (12946.2 Da) or 4 Au^+ (13143.1 Da)). Interestingly, at variance with complexes **6a** and **6b**, for complex **5** it was also possible to detect binding to Cyt *c* with ligand retention (8-aminoquinoline = $C_9H_8N_2$). Taking into account the peak at 12696.3 Da in fig. 4.6, and comparing its experimental multicharged isotopic profile (charge state = 7) in fig. 4.7 (a) with the theoretical simulation in fig. 4.7 (b), we can assess that in this case the binding seems to be occurring through simultaneous coordination of both Au^{3+} and Au^+ ions bound to aminoquinoline ligand: the concordance between the two isotopic profiles, as well as the low mass difference (- 3.2 ppm) calculated on the higher peaks of the isotopic profiles, strongly support this hypothesis.

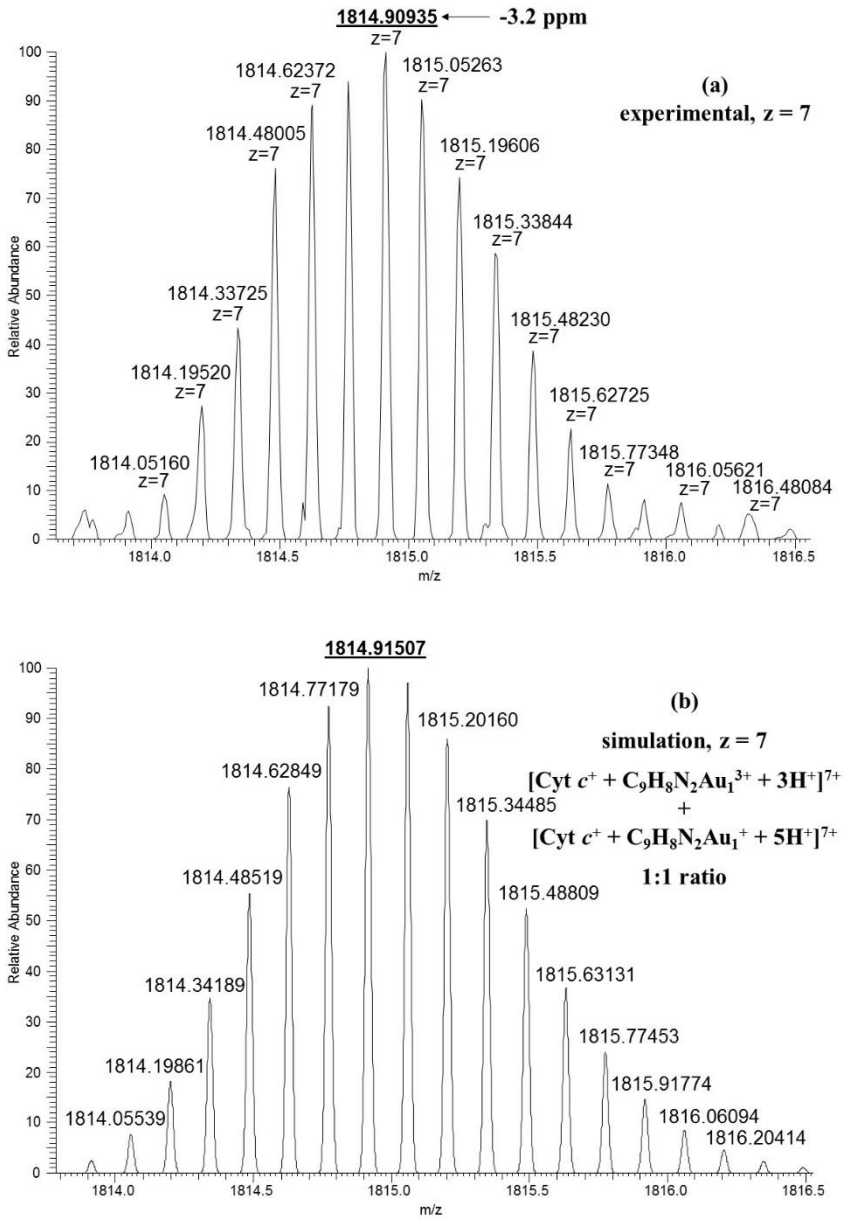

Fig. 4.7 Comparison between (a) the experimental multicharged isotopic profile (z = 7) of peak at 12696.3 Da in fig. 4.6 and (b) the theoretical simulation (z = 7) of Cyt *c* bound to a mixture of $[C_9H_8N_2Au_1]^{3+}$ and $[C_9H_8N_2Au_1]^{+}$ in a 1:1 ratio.

For compound **5** is thus conceivable a binding process that first implies the Au^{3+} coordination with 8-aminoquinoline bidentate ligand conservation, followed by Au^{3+} reduction to Au^{+} with loss of ligand.

All these results suggest that the cellular effects produced by these gold compounds may be predominantly mediated by interaction with relevant protein targets.

A comparative study involving Aubipy^{c} (**1**), its dimer Au$_2$bipy^{c} (**2**) and the novel complex Aubipy^{aa} (**3**) was carried out. The three compounds manifested rather similar chemical and biological properties and different grades of reaction with the model proteins Cyt *c*, RNase and Hewl. As demonstrated in a previous paper [19], Aubipy^{c} binds both Cyt *c* and Hewl; at variance, Aubipy^{aa} shows here the formation of an adduct only with lysozyme. Furthermore, Aubipy^{aa} seems to exhibit slightly lesser affinity with Hewl than Aubipy^{c}. Au$_2$bipy^{c}, unlike Aubipy^{c} and Aubipy^{aa}, besides binding Hewl, is able to form an adduct with the RNase A. Notably, regardless the different reactivity of the three compounds toward the model proteins, the nature of the metallo fragment is always the same, corresponding to the [Au(bipy^{dmb}-H)]$^{2+}$ moiety, *i.e.* the gold(III) center plus the N,N,C terdentate ligand, as proved by ESI–MS analysis (figs. 4.8, 4.9 and 4.10).

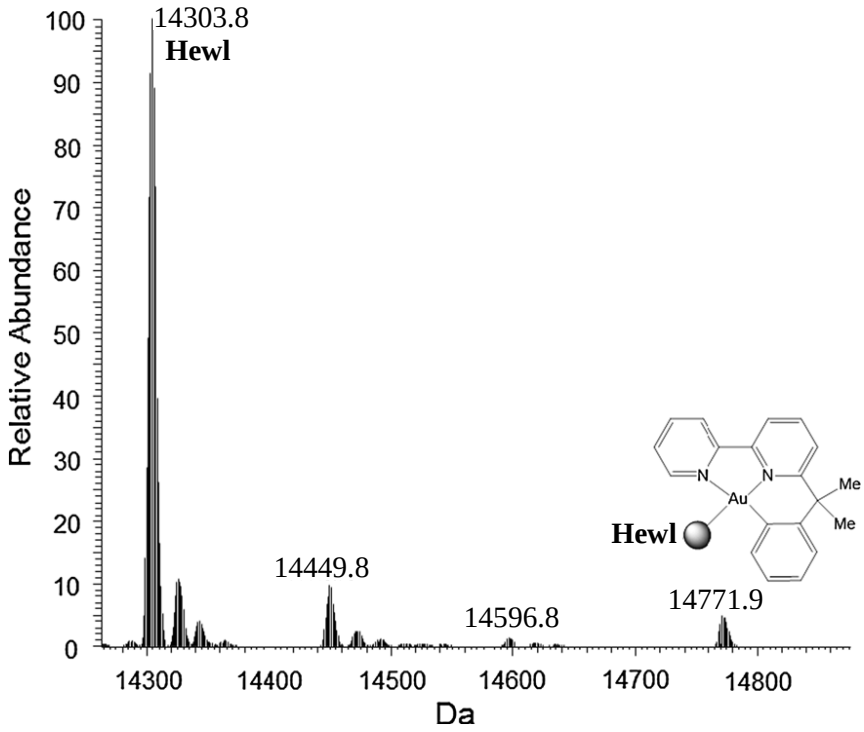

Fig. 4.8 Deconvoluted ESI-Orbitrap mass spectrum of the mixture Aubipy^{aa}-Hewl (gold compound:protein ratio 3:1, 48 h incubation at 37 °C in 20 mM AA buffer, pH 6.8).

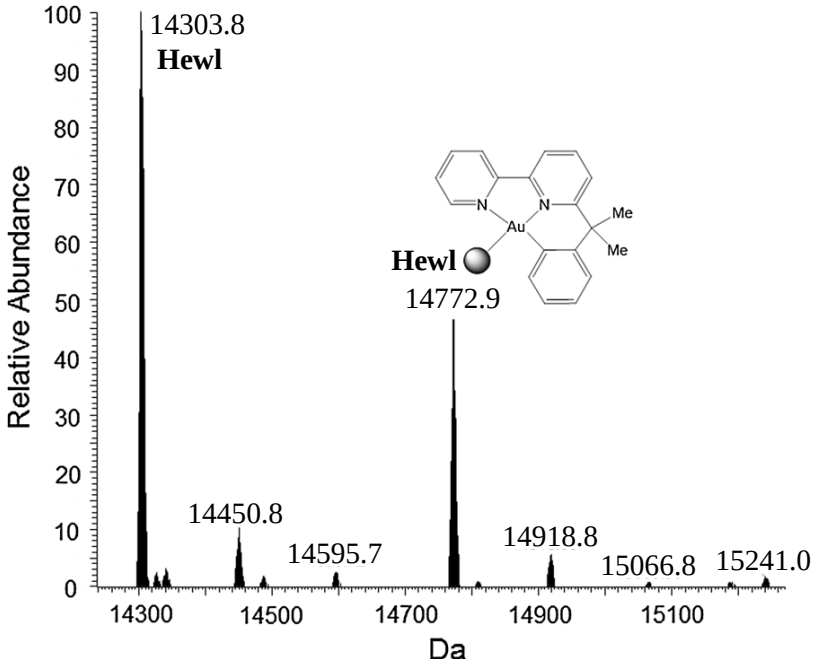

Fig. 4.9 Deconvoluted ESI-Orbitrap mass spectrum of the mixture Au_2bipy^c-HewI (gold compound:protein ratio 3:1, 48 h incubation at 37 °C in 20 mM AA buffer, pH 6.8).

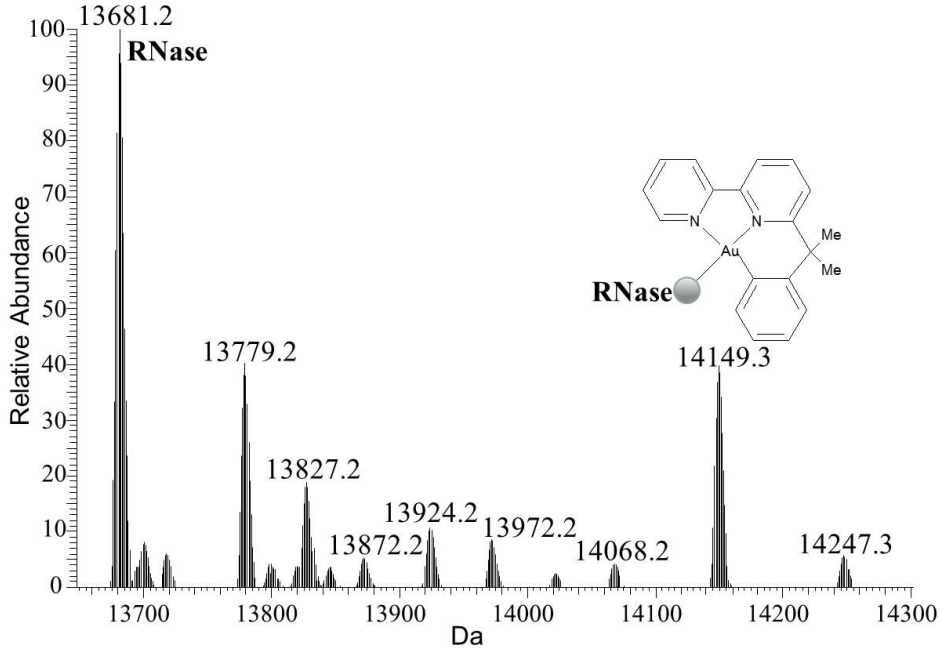

Fig. 4.10 Deconvoluted ESI-Orbitrap mass spectrum of the mixture Au_2bipy^c-RNase A (gold compound:protein ratio 3:1, 48 h of incubation at 37 °C in 20 mM AA buffer, pH 6.8).

Finally, we elucidated the nature of the gold binding site in the Aubipy^{c}-Atox1 adduct by tryptic digestion/MALDI-TOF analysis and metal competition experiments carried out with the ESI-Orbitrap mass spectrometer.

Under the solution conditions used to monitor metal binding to Atox1, *i.e.* within the strongly reducing environment created by the addition of DTT, the gold(III) center of Aubipy^{c} is reduced to gold(I), the terdentate ligand is released and the resulting gold(I) species binds Atox1. The main derivative that is formed corresponds to a single bare gold(I) ion bound to Atox1 [20]. Adduct formation is well witnessed by deconvoluted ESI-MS spectra showing a clear peak at 7465.6 Da, in agreement with previously published work [20]. Based on simple coordination chemistry considerations and HSAB concepts, it is straightforward to hypothesize that the binding of the soft gold(I) may occur at the same level of the soft copper(I). However, to better ascertain this point, tryptic digestion was carried out both on the Atox1/Atox1-M mixture alone (the protein starting material was a mixture of Atox1 and Atox1 without the N-terminal methionine) and on the same mixture incubated with Aubipy^{c}. Then, MALDI spectra were recorded from both tryptic digests. Notably, the most abundant tryptic fragment obtained from the first mixture was the 1–20 peptide of Atox1-M (fig. 4.11 (a)). Upon comparing this spectrum with the one obtained from tryptic digestion of the second mixture (*i.e.* Atox1/Atox1-M incubated with Aubipy^{c}) we noticed the appearance of a relatively intense peak at 2319.8 Da due to the binding of one Au^{+} to 1–20 peptide of the reduced Atox1-M (fig. 4.11 (b)). Further, the absence of a peak at 2317.9 Da implies that the oxidized form of peptide 1-20 is unable to coordinate the Au^{+} ion. This result is nicely consistent with the hypothesis that gold binding takes place at Cys12 and Cys15 in the CXXC motif, as already reported for copper(I) and cisplatin as well [44].

Subsequently, the metal binding properties of Atox1 toward a group of thiophilic metal species were explored by ESI-MS, a particular attention being paid to a few exogenous metals of medicinal or toxicological relevance such as antimony, arsenic, bismuth and mercury.

At first, a screening was carried out for each metal under the same experimental conditions used for Atox1-Aubipy^{c} system. As the result of this preliminary screening, adduct formation was demonstrated for bismuth and mercury, while the other species failed to form adducts, at least under the here adopted experimental conditions. Deconvoluted ESI-MS spectra, documenting adduct formation in the case of mercury and bismuth, are shown in fig. 4.12.

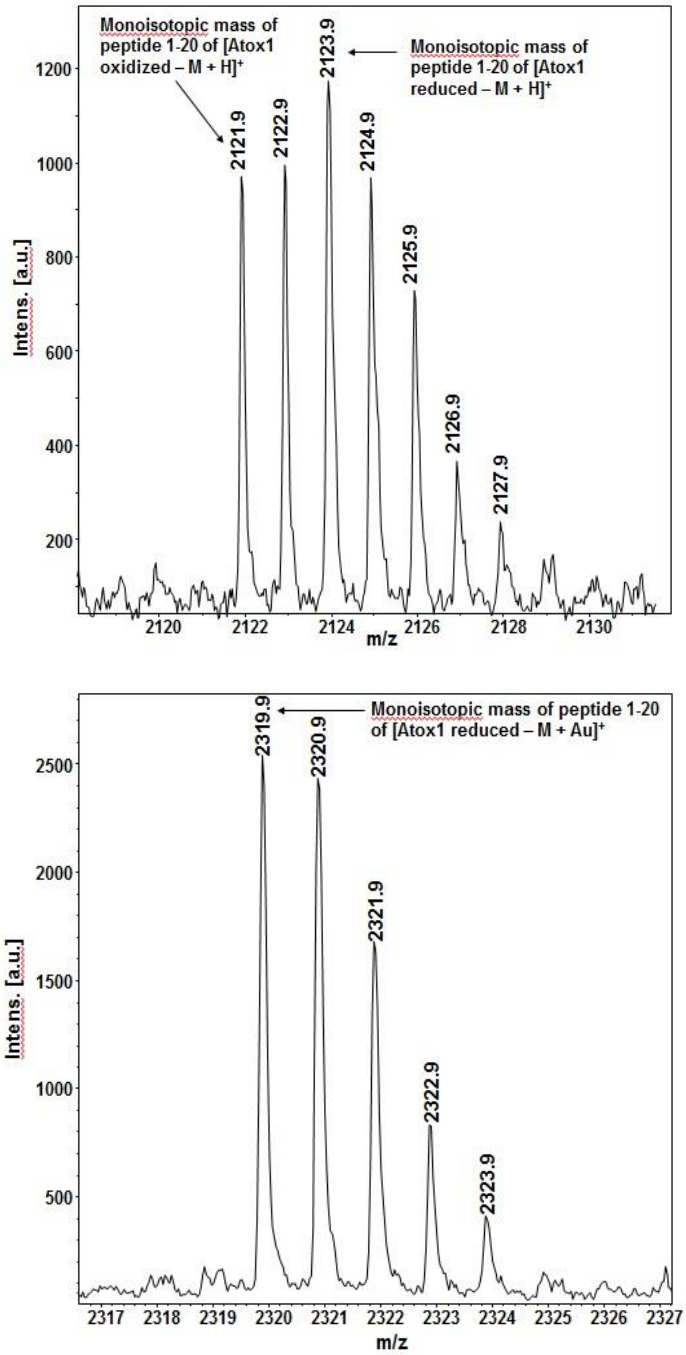

Fig. 4.11 MALDI-TOF spectra: (a) 1-20 fragment obtained through the tryptic digestion of Atox1-M. (b) [1-20 fragment + Au]$^{+}$ obtained through the tryptic digestion of Atox1-M + Aubipy^{c} (24 h of incubation at rt in 20 mM AA buffer, pH 6.8, 1:1 complex to protein ratio, DTT and N_2 inert atmosphere).

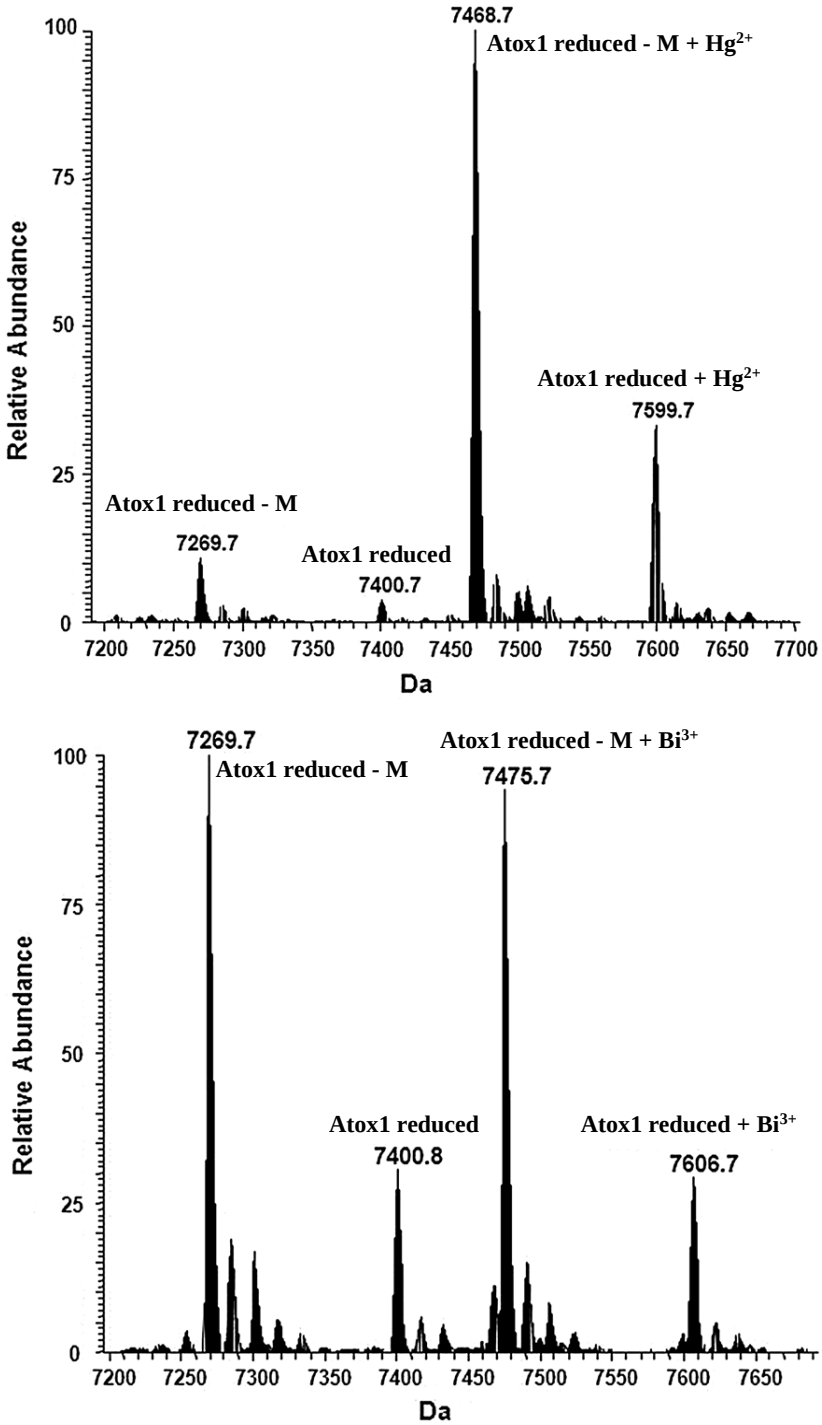

Fig. 4.12 Deconvoluted ESI-Orbitrap mass spectra of mixture Atox1/Atox1-M incubated with (a) $HgCl_2$ and (b) $Bi(NO_3)_3$ (incubation for 24 h at rt in 20 mM AA buffer, pH 6.8, 1:1 metal to protein ratio, DTT and N_2 inert atmosphere).

Notably, the peak of the adduct, in the case of mercury, is significantly higher than that of the native apoprotein, implying a large binding affinity of mercury for Atox1. For both species, *i.e.* mercury and bismuth ions, the formation of a monometallated derivative is evident, this suggesting the existence of a single metal binding site. In the case of bismuth, we could ascertain that the abundance of this derivative increases with increasing the metal to protein ratio, with no evidence of bismetallated species (see SI of the related published paper reported at pg. 43). The structure of a Hg-Atox1 derivative was previously reported [41] within a comparative crystallographic study that identified in the CXXC motif the Hg binding site; in contrast, formation of a tight adduct between Atox1 and the tripositive bismuth(III) ion is described here for the first time.
Having documented the strong affinity of the above metal species for Atox1, we moved to investigate possible competition among them in protein binding. In principle, the observation of a direct competition might support the hypothesis that these metal species share the same metal binding site; in addition, initial information may be inferred on the relative stabilities of the various metal-protein species. This goal could be accomplished straightforwardly through a single experiment where Atox1 was challenged simultaneously against bismuth, mercury and gold, presented at 1:1 metal to protein ratio, under the same experimental conditions reported above. The resulting sample was analyzed through ESI-MS and found to exhibit a single major peak at 7468.7 Da, corresponding to the Hg-Atox1 derivative (fig 4.13). Remarkably, no evidence was obtained for any Bi-Atox1 or Au-Atox1 derivatives. These facts strongly suggested that the three tested metal species, namely Hg, Bi and Aubipy^c, do compete for the same metal binding site or region, which realistically corresponds to the CXXC motif. Mercury turns out to be, by far, the strongest agonist for the Atox1 metal binding site, completely abolishing the binding of either bismuth or Aubipy^c to the same site.

The outcomes from MS experiments reported in this paragraph have highlighted the ability of this technique to offer valuable elucidations regarding the interaction between Au(III) complexes and proteins at molecular level, as declared in paragraph ″2.2 Aims of the research project″:

- the results supported the idea that proteins can act as primary target for quinoline-Au(III) derivatives **5**, **6a** and **6b**. The use of a high resolution mass analyzer provided useful information about the mechanism of binding of this class of compounds;
- it was confirmed that the presence of a C-Au bond in compounds **1**, **2** and **3** stabilizes the gold(III) center against reduction, in comparison with complexes **5**, **6a** and **6b**;

- only the presence of a potent reducing agent, like DTT, can reduce the Au(III) center of Aubipy^c to Au(I) with a complete ligand detachment;
- the binding of Aubipy^c to the peptide 1-20 of Atox1 (most probably on CXXC motif) was proved through tryptic digestion/MALDI-TOF experiments as well as metal competition/ESI-MS analyses.

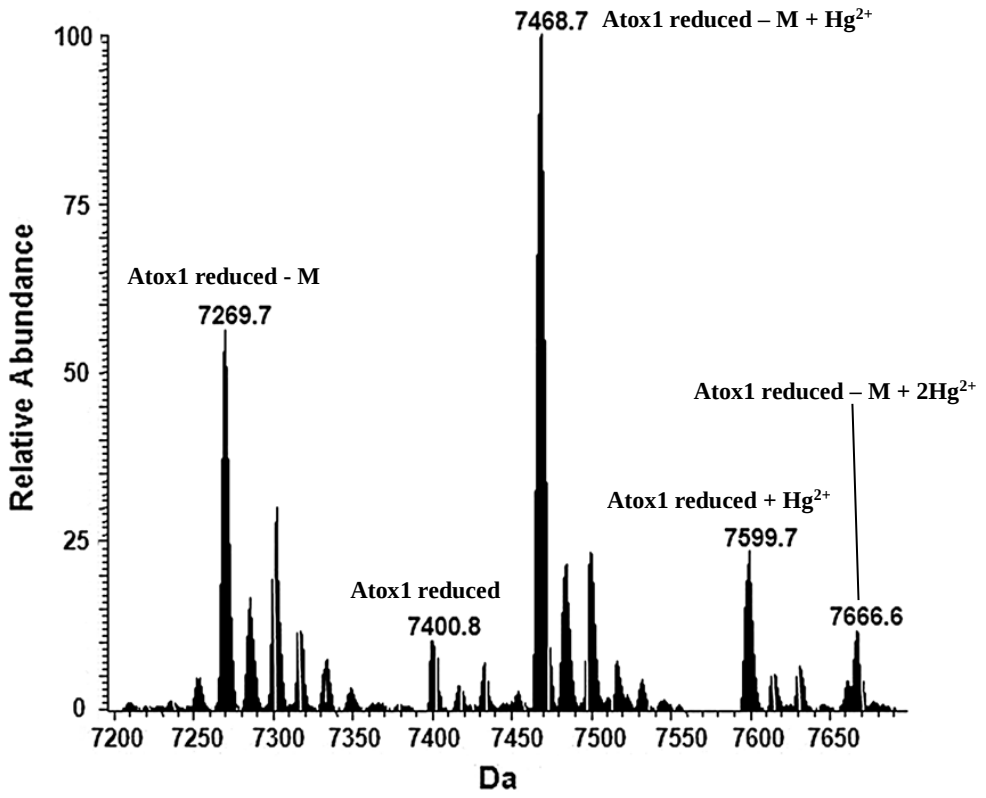

Fig. 4.13 Deconvoluted ESI-Orbitrap mass spectrum of competition experiment between Au, Hg, Bi incubated with Atox1/Atox1-M mixture (incubation for 24 h at rt in 20 mM AA buffer, pH 6.8, 1:1 metal to protein ratio, DTT and N_2 inert atmosphere).

4.4 References

[1] P. Ivo da Silva Maia, V. M. Deflon, U. Abram, *Future Med. Chem.*, **2014**, *6*, 1515-1536.

[2] B. Bertrand, A. Casini, *Dalton Trans*, **2014**, *43*, 4209-4219.

[3] N. Cutillas, G. S. Yellol, C. de Haro, C. Vicente, V. Rodríguez, J. Ruiz, *Coord. Chem. Rev.*, **2013**, *257*, 2784-2797.

[4] F. Cisnetti, A. Gautier, *Angew. Chem. Int. Ed*., **2013**, *52*, 11976-11978.
[5] S. J. Berners-Price, A. Filipovska, *Metallomics*, **2011**, *3*, 863-873.
[6] C.-M. Che, R. W.-Y. Sun, *Chem. Commun*., **2011**, *47*, 9554-9560.
[7] I. Ott, *Coord. Chem. Rev*., **2009**, *253*, 1670-1681.
[8] X. Wang, Z. Guo, *Dalton Trans*., **2008**, 1521-1532.
[9] T. Zou, C. T. Lum, S. S.-Y. Chui, C. M. Che, *Angew. Chem. Int. Ed*., **2013**, *52*, 2930-2933.
[10] S. D. Köster, H. Alborzinia, S. Can, I. Kitanovic, S.Wölfl, R. Rubbiani, I. Ott, P. Riesterer, A. Prokop, K. Merz, N. Metzler-Nolte, *Chem. Sci*., **2012**, *3*, 2062-2072.
[11] A. Casini, C. Hartinger, C. Gabbiani, E. Mini, P. J. Dyson, B. K. Keppler, L. Messori, *J. Inorg. Biochem*., **2008,** *102*, 564-575.
[12] L. Ronconi, L. Giovagnini, C. Marzano, R. Bettio, R. Graziani, G. Pilloni, D. Fregona, *Inorg. Chem*., **2005**, *44*, 1867-1881.
[13] A. Casini, L. Messori, *Curr. Top. Med. Chem*., **2011**, *11*, 2647-2660.
[14] G. Marcon, L. Messori, P. Orioli, *Expert. Rev. Anticancer. Ther*., 2002, 2, 337-346.
[15] G. Marcon, S. Carotti, M. Coronello, L. Messori, E. Mini, P. Orioli, T. Mazzei, M. A. Cinellu, G. Minghetti, *J. Med. Chem*., **2002**, *45*, 1672-1677.
[16] L. Messori, F. Abbate, G. Marcon, P. Orioli, M. Fontani, E. Mini, T. Mazzei, S. Carotti, T. O'Connell, P. Zanello, *J. Med. Chem*., **2000**, *43*, 3541-3548.
[17] T. Gamberi, L. Massai, F. Magherini, I. Landini, T. Fiaschi, F. Scaletti, C. Gabbiani, L. Bianchi, L. Bini, S. Nobili, G. Perrone, E. Mini, L. Messori, A. Modesti, *J. Proteomics*, **2014**, *103*, 103–120.
[18] A. Casini, G. Kelter, C. Gabbiani, M. A. Cinellu, G. Minghetti, D. Fregona, H. H. Fiebig, L. Messori, *J. Biol. Inorg. Chem*., **2009**, *14*, 1139–1149.
[19] C. Gabbiani, L. Massai, F. Scaletti, E. Michelucci, L. Maiore, M. A. Cinellu, L. Messori, *J. Biol. Inorg. Chem.*, **2012**, *17*, 1293–1302.
[20] C. Gabbiani, F. Scaletti, L. Massai, E. Michelucci, M. A. Cinellu, L. Messori, *Chem. Commun*., **2012**, *48*, 11623–11625.
[21] N. G. Faux, C. W. Ritchie, A. Gunn, A. Rembach, A. Tsatsanis, J. Bedo, J. Harrison, L. Lannfelt, K. Blennow, H. Zetterberg, M. Ingelsson, C. L. Masters, R. E. Tanzi, J. L. Cummings, C. M. Herd, A. I. Bush, *J. Alzheimers Dis*., **2010**, *20*, 509-516.
[22] S. K. Prashant, A. K. Dutta, *Curr. Bioact. Compd*., **2008**, *4*, 57-67.
[23] A. I. Bush, R. E. Tanzi, *Neurotherapeutics*, **2008**, *5*, 421-432.
[24] K. J. Barnham, E. Gautier, L. Colette, G. B. Kong, G. Krippner, *WO 2004/007461*, **2004**.
[25] H. R. Dholariya, K. S. Patel, J. C. Patel, A. K. Patel, K. D. Patel, *Med. Chem. Res.*, **2013**, *22*, 5848-5860.
[26] B. Choi, J. Young, G. Bong, J. H. Kim, J.-N. Seo, G. Wu, M. Sohn, T. N. Chung, S. W. Suh, *Neurobiol. Dis*., **2013**, *54*, 382-391.

[27] A. D. Schimmer, Y. Jitkova, M. Gronda, Z. Wang, J. Brandwein, C. Chen, V. Gupta, A. Schuh, K. Yee, J. Chen, S. Ackloo, T. Booth, S. Keays, M. D. Minden, *Clin. Lymphoma Myeloma Leuk.*, **2012**, *12*, 330-336.
[28] C. M. Darby, C. F. Nathan, *J. Antimicrob. Chemother.*, **2010**, *65*, 1424-1427.
[29] H. Jiang, J. E. Taggart, X. Zhang, D. M. Benbrook, S. E. Lind, W.-Q. Ding, *Cancer Lett.*, **2011**, *312*, 11-17.
[30] K. G. Daniel, D. Chen, S. Orlu, Q. C. Cui, F. R. Miller, Q. P. Dou, *Breast Cancer Res.*, **2005**, *7*, R897-R908.
[31] X. Mao, X. Li, R. Sprangers, X. Wang, A. Venugopal, T. Wood, Y. Zhang, D. A. Kuntz, E. Coe, S. Trudel, D. Rose, R. A. Batey, L. E. Kay, A. D. Schimmer, *Leukemia*, **2009**, *23*, 585-590.
[32] D. Chen, Q. C. Cui, H. Yang, R. A. Barrea, F. H. Sarkar, S. Sheng, B. Yan, G. P. Reddy, Q. P. Dou, *Cancer Res.*, **2007**, *67*, 1636-1644.
[33] S. M. Zhai, L. Yang, Q. C. Cui, Y. Sun, Q. P. Dou, B. Yan, *J. Biol. Inorg. Chem.*, **2010**, *15*, 259-269.
[34] H. Yu, Y. Zhou, S. E. Lind, W. Q. Ding, *Biochem. J.*, **2009**, *417*, 133-139.
[35] W. Q. Ding, B. Liu, J. L. Vaught, H. Yamauchi, S. E. Lind, *Cancer Res.*, **2005**, *65*, 3389-3395.
[36] H. Yu, J. R. Lou, W. Q. Ding, *Anticancer Res.*, **2010**, *30*, 2087-2092.
[37] T. Du, G. Filiz, A. Caragounis, P. J. Crouch, A. R. White, *J. Pharmacol. Exp. Ther.*, **2008**, *324*, 360-367.
[38] C. Martín Santos, S. Cabrera, C. Ríos-Luci, J. M. Padrón, I. López Solera, A. G. Quiroga, M. A. Medrano, M. C. Navarro-Ranninger, J. Alemán, *Dalton Trans.*, **2013**, *42*, 13343-13348.
[39] D. S. Goodsell, *Oncologist*, **2004**, *9*, 226-227.
[40] A. K. Boal, A. C. Rosenzweig, *Chem. Rev.*, **2009**, *109*, 4760–4779.
[41] R. Safaei, S. B. Howell, *Crit. Rev. Oncol. Hematol.*, **2005**, *53*,13–23.
[42] S. B. Howell, R. Safaei, C. A. Larson, M. J. Sailor, *Mol. Pharmacol.*, **2010**, *77*, 887–894.
[43] K. Katano, A. Kondo, R. Safaei, A. Holzer, G. Samimi, M. Mishima, Y. M. Kuo, M. Rochdi, S. B. Howell, *Cancer Res.*, **2002**, *62*, 6559–6565.
[44] A. K. Boal, A. C. Rosenzweig, *J. Am. Chem. Soc.*, **2009**, *131*, 14196–14197.
[45] F. Arnesano, L. Banci, I. Bertini, I. C. Felli, M. Losacco, G. Natile, *J. Am. Chem. Soc.*, **2011**, *133*, 18361–18369.
[46] M. E. Palm, C. F. Weise, C. Lundin, G. Wingsle, Y. Nygre, E. Bjo¨rn, P. Naredi, M. Wolf-Watz, P. Wittung-Stafshede, *PNAS*, **2011**, *108*, 6951–6956.
[47] M. E. Palm-Espling, P. Wittung-Stafshede, *Biochem. Pharm.*, **2012**, *83*, 874–881.

5. MASS SPECTROMETRY AND METALLOPROTEOMICS: A GENERAL PROTOCOL TO ASSESS THE STABILITY OF METALLODRUG-PROTEIN ADDUCTS IN BOTTOM-UP MS EXPERIMENTS

The results presented in this chapter have been published in the following paper:
- "Mass spectrometry and metallomics: a general protocol to assess stability of metallodrug-protein adducts in bottom-up MS experiments". E. Michelucci, G. Pieraccini, G. Moneti, C. Gabbiani, A. Pratesi, L. Messori, *Talanta*, **2017**, *167*, 30-38.

5.1 Introduction

As already explained in paragraph 1.2, ESI-MS represents a powerful tool to study, at the molecular level, the interactions between metal based drugs and proteins in such a way to rationally design novel and better anticancer metallodrugs through the so called "mechanism oriented" approach.
Regarding the specific topic of metallodrug-protein binding site location through MS, two main strategies can be generally exploited: the so-called top-down and bottom-up approaches.
In the top-down approach the whole metallodrug-protein adduct is directly fragmented in the mass spectrometer, avoiding any sample pretreatment and consequently reducing the possibility to lose the metallo fragments attached to the protein during those manipulations. However, its application generally requires the use of high resolving power instruments and is restricted to relatively small proteins, mainly because of the high complexity of the tandem mass spectra generated (see paragraph 1.2.3).
The classical bottom-up approach is preferably used for high molecular weight proteins, because it involves sample reduction, alkylation and enzymatic digestion prior to LC-ESI-MS/MS analysis (see paragraph 1.2.4). However, despite the general good stability of the coordination metallodrug-protein bond, each of these preparation/analytical steps might compromise the firmness of the metal adducts.
Halfway, there is the middle-down approach: it consists in a limited digestion process in order to generate a small number of peptide fragments of medium to large size (MW = 2000-20000 Da). The obtaining of the desired peptides requires the choose of a specific enzyme/digestion agent, in correlation to the protein sequence, or a study of the digestion times [1,2].
In figure 5.1, top-down, middle-down and bottom-up approaches are schematically represented.

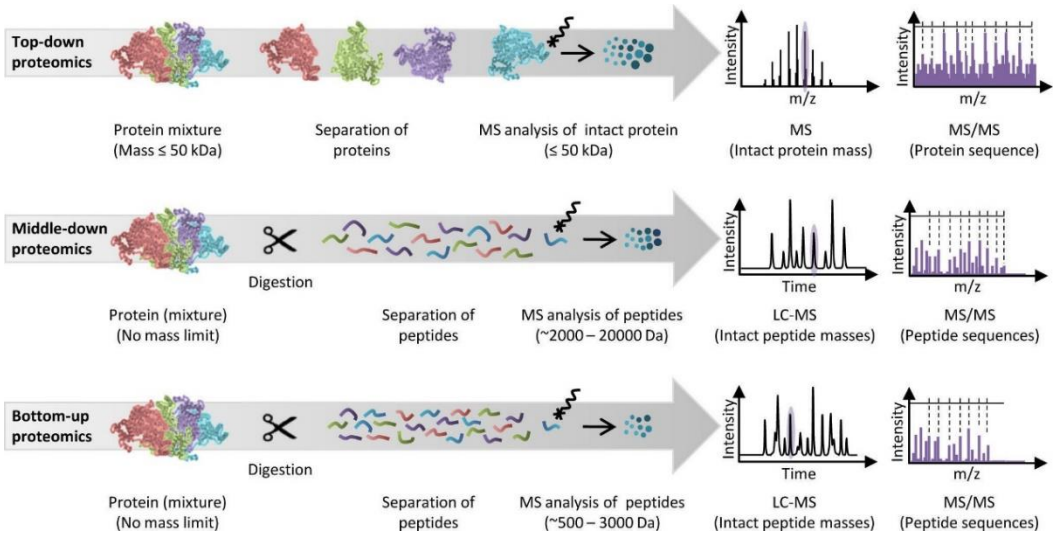

Fig. 5.1 Schematic representation of top-down, middle-down and bottom-up approaches.

As previously stated in paragraph 2.2, one of the aims of this PhD project is the development and introduction in our laboratories of an efficient and generally applicable MS method for metallodrugs binding site location on proteins, regardless of the MW and nature of the protein and the type of metal complex under investigation. It is our intention to start these MS studies by using, at least at the beginning, basic systems consisting of a single protein and one metallodrug, to extend then to simple mixtures of known proteins reacted with a metal complex. Finally, our ultimate goal is the analysis of more complex samples, such as metallodrug-treated cell populations and/or cell homogenates, a situation that reflects more closely the reality of metallic species in the cell world: the simultaneous identification of the unknown proteins and the metal binding site, as well as the possible quantitative evaluations on protein expression, would fully introduce our studies in the metalloproteomics field.
In this context, the bottom-up approach seemed to us the most suitable method for our aims, due to its wide range of applicability. Although this kind of approach has already been applied in studies of metal-protein binding side location, in our opinion the preparation/analytical conditions didn't receive yet an adequate attention, at least not in a systematic and exhaustive way, in order to ascertain their suitability to preserve metal-protein binding along the whole process.
For example, Moreno-Gordaliza *et al.* [3] studied in depth the effect of denaturing (urea), reducing (DTT) and alkylating (IAA) reagents in the presence of Tris buffer during routine procedure for in solution tryptic digestion of CDDP-insulin adducts. The same authors [4] tested the stability of the adducts formed between CDDP and five

model proteins along the whole in-gel digestion protocol. In turn, Moraleja *et al.* [5] focused their investigations on the comparison of two reducing agents, DTT and TBP, used in the FASP procedure [6] for CDDP-protein adducts.
In any case, the reagents typically used during the enzymatic digestion are not the only triggers of metal-protein coordination bond impairment. Karas *et al.* [7] reported the sensitivity of the coordination bond between Fe-heme and histidine in myoglobin to some mass spectrometer instrumental parameters (capillary temperature, capillary/skimmer voltage), while Li *et al*. [8] and Loo [9] described its sensitivity to pH, to the presence of organic co-solvents and to collision induced dissociation. Also, Will *et al.* [10] listed the requirements that must be fulfilled by CDDP-protein adducts for a subsequent MudPIT-MS/MS analysis (kinetic stability over the range $2.3 < pH < 8.5$, metallo fragment persistence on MS/MS fragments).
These arguments convinced us to design a general protocol to test, *a priori* and systematically, metallodrug-protein adduct stability under the conditions of the FASP/bottom-up mass spectrometry approach, starting from the digestion process, passing through the LC step and ending with ESI-MS/MS analysis in a LTQ-Orbitrap mass spectrometer.

5.2 Materials and MS method

We applied the protocol to two model systems, both containing Cyt *c* (see paragraph 4.2). For the first system, the well-known CDDP antitumor drug (see paragraph 1.1.3) was chosen while, for the second one, the less investigated RAPTA-C (see paragraph 1.1.4) was selected (fig. 5.2).

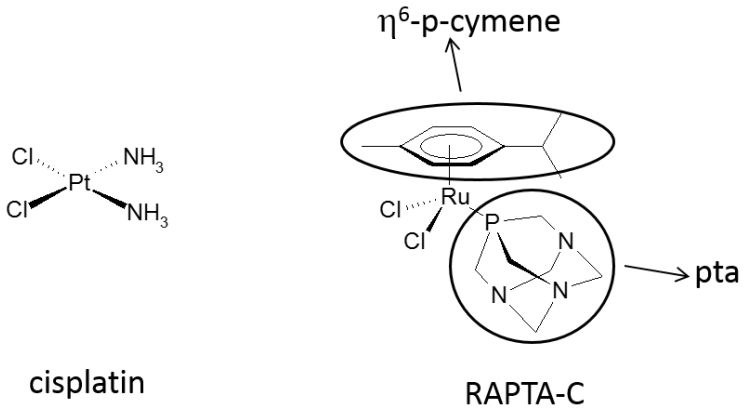

Fig. 5.2 Structures of the metal complexes used in this study.

The denaturation, reduction, alkylation and digestion steps were performed with FASP procedure, directly on a centrifugal filter device, in order to shorten the contact time between these reagents and the metallo fragment-protein adduct, thus limiting the possible side reactions causing metal loss.
Adduct stability to the different critical conditions was monitored by direct infusion in the ESI-mass spectrometer, using the Orbitrap high resolution analyzer for acquisition and the low resolution IT analyzer to perform CID experiments.
For more details on the experimental section see the published paper reported at pg. 61

5.3 Results and discussion

5.3.1 Critical issues for metallodrug-protein adduct stability in the FASP/bottom-up approach using nanoLC-nanoESI-LTQ-Orbitrap-MS/MS analysis: the "nine-point testing protocol"

The development of a reliable testing protocol was necessary on the basis that nothing can be said *a priori* about the stability of the adducts formed between metallodrugs and proteins: in fact, the nature of the metal, of its ligands and the protein micro-environment are variables that can affect, in a deep and unpredictable way, the resistance of the metal protein coordination bond during the bottom-up approach.
The method we intend to use for future studies of binding site location will imply the denaturation, reduction, alkylation, digestion FASP procedure and the nanoLC-nanoESI-MS/MS analysis, preceded by an on-line purification/concentration step. Within these steps we identified nine critical situations, either during the sample manipulations or instrumental analysis, as potential sources of metal-protein bond impairment. These are:
1) sample permanence in the Ambic buffer
2) denaturation with urea
3) reduction with DTT
4) alkylation with IAA
5) sample permanence in the loading mobile phase containing CH_3CN and TFA
6) sample permanence in the elution mobile phase containing CH_3CN and HCOOH
7) nanoESI process
8) transfer of the adducts along the optics of the MS instrument, in particular the ion transfer tube and tube lens in a LTQ-Orbitrap
9) collision induced dissociation in the ion trap.
In our opinion, these nine points (we called it the "nine-point testing protocol") constitute a useful and almost complete track (though this protocol is obviously open to additions and improvements, according to the chosen instrument and the applied sample preparation procedures) to be followed whenever one intends to study the

stability of metallo fragment-protein adducts throughout the whole bottom-up process. The protocol reveals its utility particularly in the case of less studied, or completely new, metal complexes.

5.3.2 Cyt c-CDDP and Cyt c-RAPTA-C adduct stability at denaturation, reduction, alkylation steps in Ambic aqueous solution (points 1–4)

Cyt *c*-CDDP and Cyt *c*-RAPTA-C solutions were subjected to purification on centrifugal filter device, in order to remove the excess of unreacted metal complex before adding urea, DTT and IAA. This step avoids undesired side reactions between the free metal complex and these three reagents. The solutions were subsequently denatured, reduced, alkylated directly on filter and then purified from urea, DTT, IAA by centrifugations and washings with 50 mM Ambic. Finally, the solutions were incubated overnight on filter at 37 °C to simulate tryptic digestion. The day after Ambic was washed away with H_2O and the samples, diluted to the desired concentration with H_2O, were analyzed by ESI-MS. Cyt *c*-CDDP adducts resulted stable toward Ambic, urea, DTT and IAA (data not shown; see the published paper reported at pg. 61). Instead, Cyt *c*-RAPTA-C adducts turned out to be unstable in the same conditions (fig. 5.3 a) and b)): indeed, after treatment with Ambic, urea, DTT and IAA, the mono-adducts, Cyt *c* + $[Ru(\eta^6\text{-}p\text{-cymene})]^{2+}$ at 12592.4 Da and Cyt *c* + $[Ru(\eta^6\text{-}p\text{-cymene})(pta)]^{2+}$ at 12750.4 Da, almost or completely disappeared while Cyt *c* at 12358.4 Da became the most intense peak in the spectrum. A deeper investigation was carried out on Cyt *c*-RAPTA-C adduct stability in Ambic using the same procedure described above but leaving out the denaturation, reduction and alkylation steps. Interestingly, the results showed adducts disappearance in 50 mM Ambic (fig. 5.3 c)), thus indicating that the use of this latter buffer poses a stability issue.

Gibson *et al.* already reported on the sensitivity of ubiquitin-CDDP adducts to Ambic [11] and our outcomes confirmed that an accurate evaluation of this crucial parameter must be always taken into account, especially in light of the different results obtained for Cyt *c*-CDDP and Cyt *c*-RAPTA-C: in fact, the same protein, incubated with different metal complexes, gives rise to adducts of diverse stability in 50 mM Ambic. Indeed, the different behavior of these Pt- and Ru-adducts in 50 mM Ambic is not easy to explain and we believe that this issue needs to be studied in depth with further experiments.

We must also underline that Cyt *c*-RAPTA-C adduct instability in Ambic does not rule out further instability to urea, DTT and IAA reagents but, at this level, we decided to investigate no longer this issue. In particular, for DTT, it has been already highlighted [4] how the disappearance of metal-protein adducts is probably related to the initial amount of the latter in the original sample, to their binding strength and their location in the protein.

Finally, it should be noted that Cyt *c* would not need reduction/alkylation since its unique two cysteines are covalently involved in heme *c* binding. Nevertheless, in this study we decided to perform these two steps in order to show the use of the "nine-point testing protocol" in its entirety.

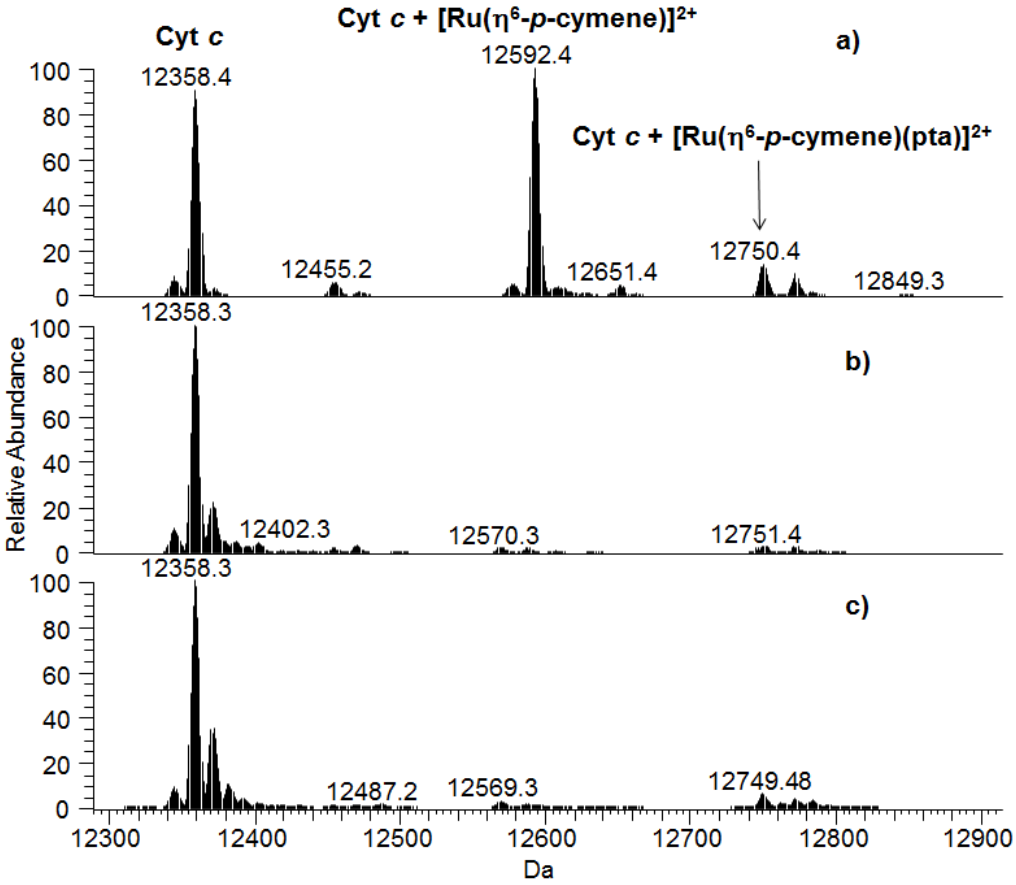

Fig. 5.3 ESI-Orbitrap deconvoluted mass spectra of Cyt *c*-RAPTA-C adduct solutions after a) 72 h incubation in H_2O, b) 72 h incubation in H_2O and following treatment, on filter, with Ambic, urea, DTT and IAA, c) 72 h incubation in H_2O and following treatment, on filter, with 50 mM Ambic.

5.3.3 Cyt c-CDDP and Cyt c-RAPTA-C adduct stability in loading and elution mobile phases (points 5–6)

We studied the stability of Cyt *c*-CDDP and Cyt *c*-RAPTA-C adducts to an organic co-solvent (CH_3CN) and acidity (0.1% TFA or 0.1% HCOOH) present in the loading and eluition mobile phases. To evaluate Cyt *c*-CDDP and Cyt *c*-RAPTA-C resistance to these conditions, we diluted adduct solutions in CH_3CN/H_2O 1/1 with 0.1% TFA or

0.1% HCOOH and we analyzed the resulting samples as such by ESI-MS after different incubation times at rt. The excess of metal compound was not removed from solutions before ESI-MS analyses: previously performed experiments (data not shown), as well as those reported in paragraph 5.3.4 (point 7 of the testing protocol), demonstrated the possibility to skip this purification step without the risk of incurring in the formation of nonspecific adducts. This purification step was also omitted during point 8 of the testing protocol (paragraph 5.3.5).
The results (spectra not shown here; see the published paper reported at pg. 61) clearly show the stability of Cyt *c*-CDDP and Cyt *c*-RAPTA-C adducts in the tested conditions.
Actually, it would be more appropriate to apply the stability tests described in this section to metallated peptides instead of protein adducts since, during the bottom-up approach, digested metallated peptides do come into contact with the mobile phases. However, it would be rather complicated and expensive, respectively, to foresee and synthesize all these peptides and therefore, in our opinion, this stability test performed on denatured protein adducts turns out to be a good compromise.

5.3.4 Cyt c-CDDP and Cyt c-RAPTA-C adduct stability in nanoESI source (point 7)
During the ESI process, metal-protein adduct dissociation may occur in the source: the mere transfer of the adduct from the solution to the gas phase, as well as the presence of an inert gas (nitrogen), can induce the detachment of the metal center [12]. In order to verify the stability of Cyt *c*-CDDP and Cyt *c*-RAPTA-C adducts during ESI process (absence of false negatives), aliquots were withdrawn from the two solutions at different incubation times, were diluted/denatured in CH_3CN/H_2O 1/1 with 0.1% HCOOH and then analyzed as such by ESI-MS. The nondestructive nature of the conventional ESI source was deduced by following the kinetic of adduct formation. The ESI-Orbitrap deconvoluted mass spectra of Cyt *c*-CDDP adduct solution at different incubation times are reported in fig. 5.4: the intensity of the adduct peaks grows congruently with time and, mutually, unreacted Cyt *c* peak intensity decreases.
Similar results were obtained for the system Cyt *c*-RAPTA-C (data not shown; see the published paper reported at pg. 61).
By the same experimental evidences, we also deduced the absence of nonspecific bond formation (false positives) between Cyt *c* and CDDP (or RAPTA-C) in conventional ESI source, even omitting the removal of the metal compound excess from the incubation solution.
A fortiori, the conservativeness of the nanoESI source, that will be used in our bottom-up approach, is ensured: nanospray is believed to be more gentle than conventional electrospray since lower voltages are applied and there is no presence of additional nitrogen (therefore there are fewer activating collisions in the nanospray source [9]). As already reported in the previous paragraph, it would be more appropriate to apply

this stability test to metallated peptides instead of protein adducts but, for the same reasons explained above, its application to denatured protein adducts is a good compromise.

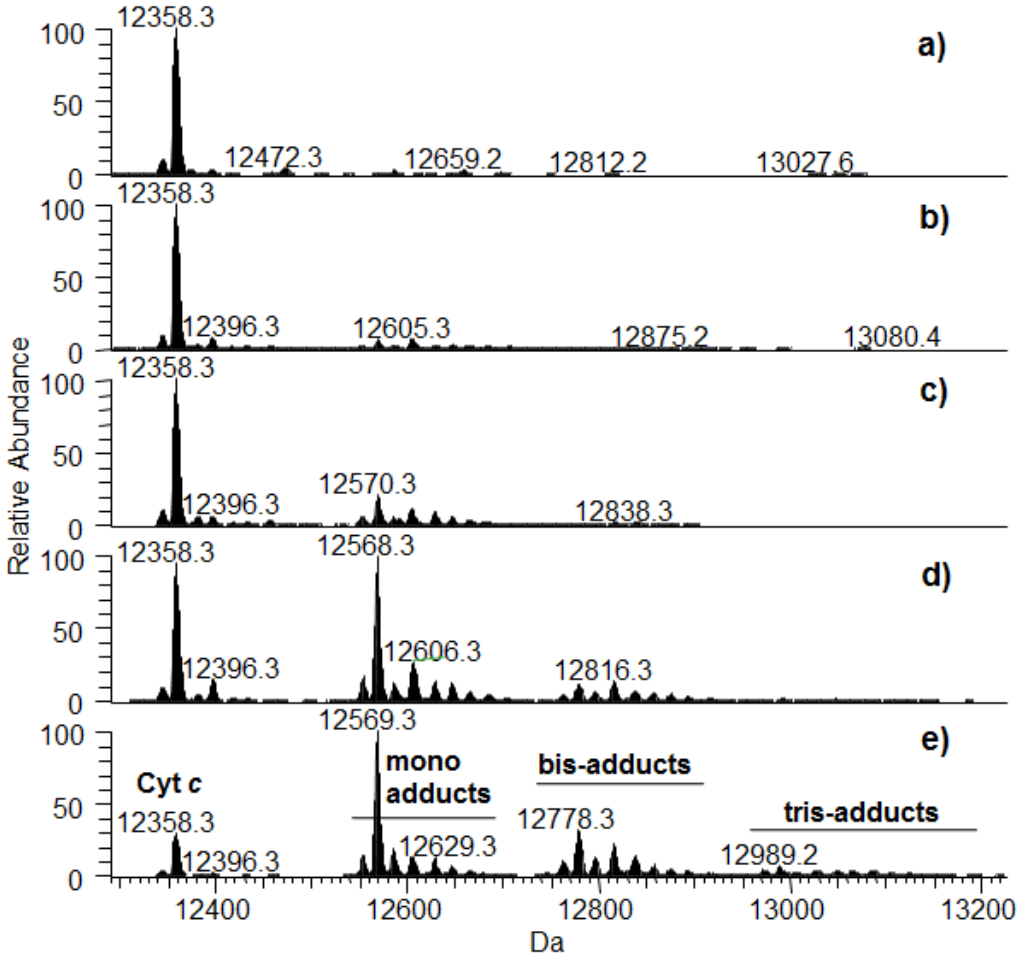

Fig. 5.4 ESI-Orbitrap deconvoluted mass spectra of Cyt *c*-CDDP adduct solution at different incubation times in 20 mM AA buffer pH 6.8: a) t = 0 h, b) t = 24 h, c) t = 48 h, d) t = 72 h, e) t = 144 h.

5.3.5 Cyt c-CDDP and Cyt c-RAPTA-C adduct stability to instrumental parameters (point 8)

We studied Cyt *c*-CDDP and Cyt *c*-RAPTA-C adduct stability to the variations imposed to capillary temperature/voltage applied to the ion transfer tube, and to tube lens voltage. The adduct solutions were diluted in CH_3CN/H_2O 1/1 with 0.1% HCOOH

and directly analyzed by ESI-MS. Cyt *c*-CDDP and Cyt *c*-RAPTA-C adducts showed their complete stability to the variations imposed in the mass spectrometer (spectra not shown here; see the published paper reported at pg. 61).
For the same reasons already explained in the previous two paragraphs, also these stability tests were performed on denatured protein adducts instead of metallated peptides.

5.3.6 Metallo fragment-peptide adduct stability at CID (point 9)
Experiments were carried out to evaluate the stability at CID of metallo fragment-peptide adducts generated during the enzymatic digestion of metallo fragment-protein adducts. This test aims to investigate the resistance to CID not only of Pt-peptide (or Ru-peptide) bond but also of Pt-ligand (or Ru-ligand) one. In fact, the energy provided during MS/MS experiments for peptide chain sequencing could generate, in addition, breakage of metal-peptide and metal-ligand bonds. In particular, the study of this last type of fragmentation provides important information to be used in the design of targeted MS/MS experiments [14] and in the subsequent reworking of bottom-up results through search engines [15], like Sequest and Mascot, or by manual interpretation [6].
From an experimental point of view, the above-mentioned stabilities were evaluated by using a simplified system consisting of CDDP, or RAPTA-C, incubated with model peptides. The choice of the model peptides was done by taking into account the high affinity of Pt(II) and Ru(II) complexes for S- and N-donors contained in amino acid side chains [16-18]. For our experiment, in order to explain how to deal with point 9) of the testing protocol, we selected the model tetrapeptides MRFA, containing Met, and EHSG, containing His, leaving out, in the first instance, other possible S-, N- and O-donors. Obviously, for a general applicability of such test, the nature of the model peptides will have to be modulated, from time to time, depending on the specific nature of the metal complex under examination.
In each of the four incubation mixtures (CDDP-MRFA, CDDP-EHSG, RAPTA-C-MRFA, RAPTA-C-EHSG), a specific Pt-peptide, or Ru-peptide, adduct ion was selected for CID experiments. Figs. 5.5 and 5.6 show the CID spectra of the four selected peptides, namely $[MRFA+Pt^{2+}-H^+]^+$ at 717.22 *m/z*, $[EHSG+Pt(NH_3)(DMSO)^{2+}-H^+]^+$ at 717.16 *m/z*, $[MRFA+Ru(\eta^6\text{-}p\text{-cymene})^{2+}-H^+]^+$ at 758.27 *m/z* and $[EHSG+Ru(\eta^6\text{-}p\text{-cymene})(pta)^{2+}-H^+]^+$ at 820.25 *m/z*. In each spectrum 30% relative collision energy was used, the same that will be imposed for bottom-up experiments, and the appropriate isolation width was selected in order to include the entire and characteristic isotopic pattern typical of Pt and Ru compounds. CID spectra of figs. 5.5 and 5.6 show the stability of metal-amino acid bonds, namely Pt-Met, Pt-His, Ru-Met and Ru-His, at the energy tested while a partial loss of Pt ligands (NH_3 and DMSO, fig. 5.5 b)) and Ru ligands (pta and η^6-*p*-cymene, fig. 5.6) is observed.

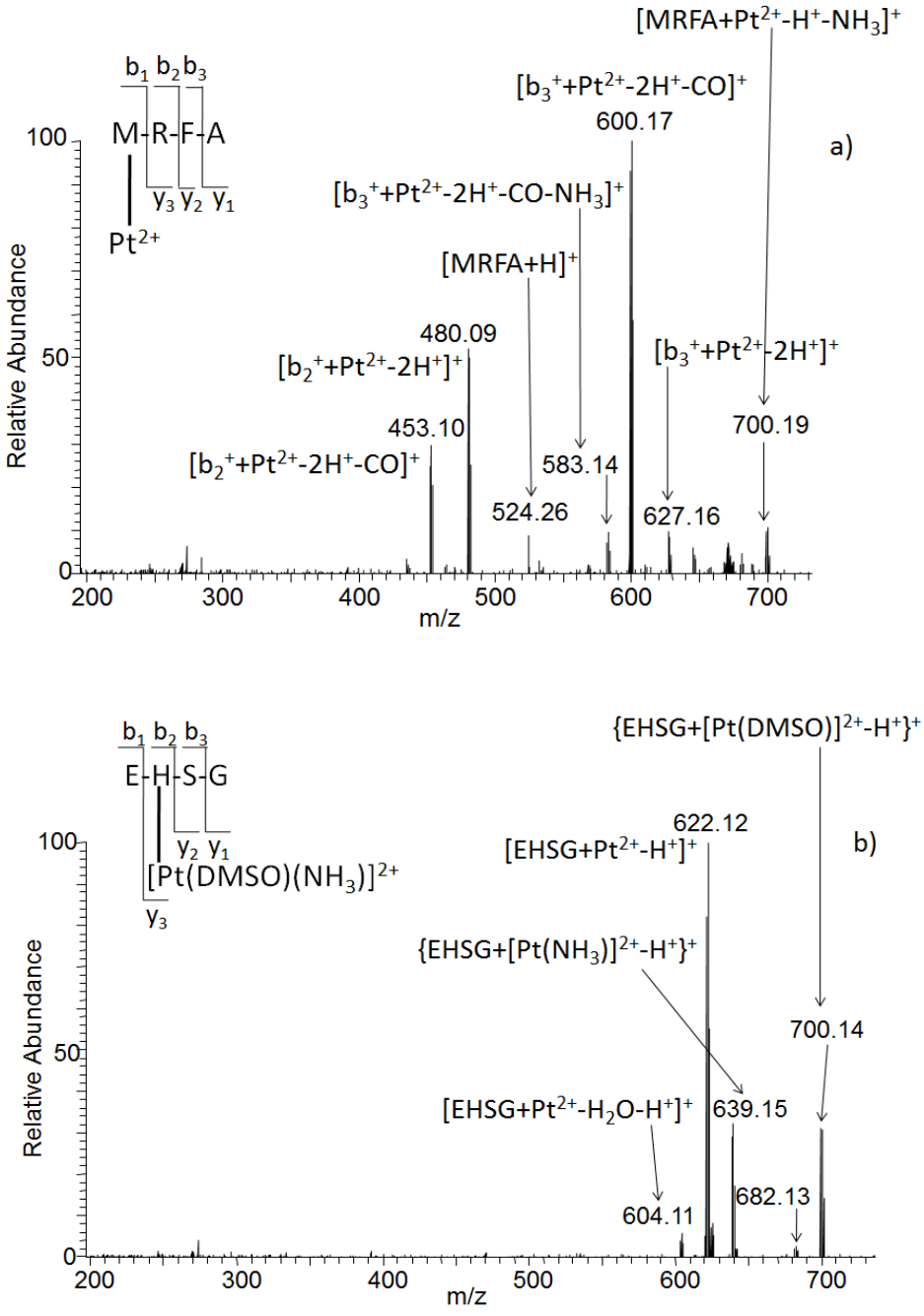

Fig. 5.5 ESI-CID mass spectra (fragmentation in IT, acquisition in Orbitrap) of a) $[MRFA+Pt^{2+}-H^+]^+$ and b) $[EHSG+Pt(NH_3)(DMSO)^{2+}-H^+]^+$. The formation of peptide-CDDP (as well as Cyt *c*-CDDP) adducts containing DMSO as ligand is due to the initial solubilization of CDDP in that solvent.

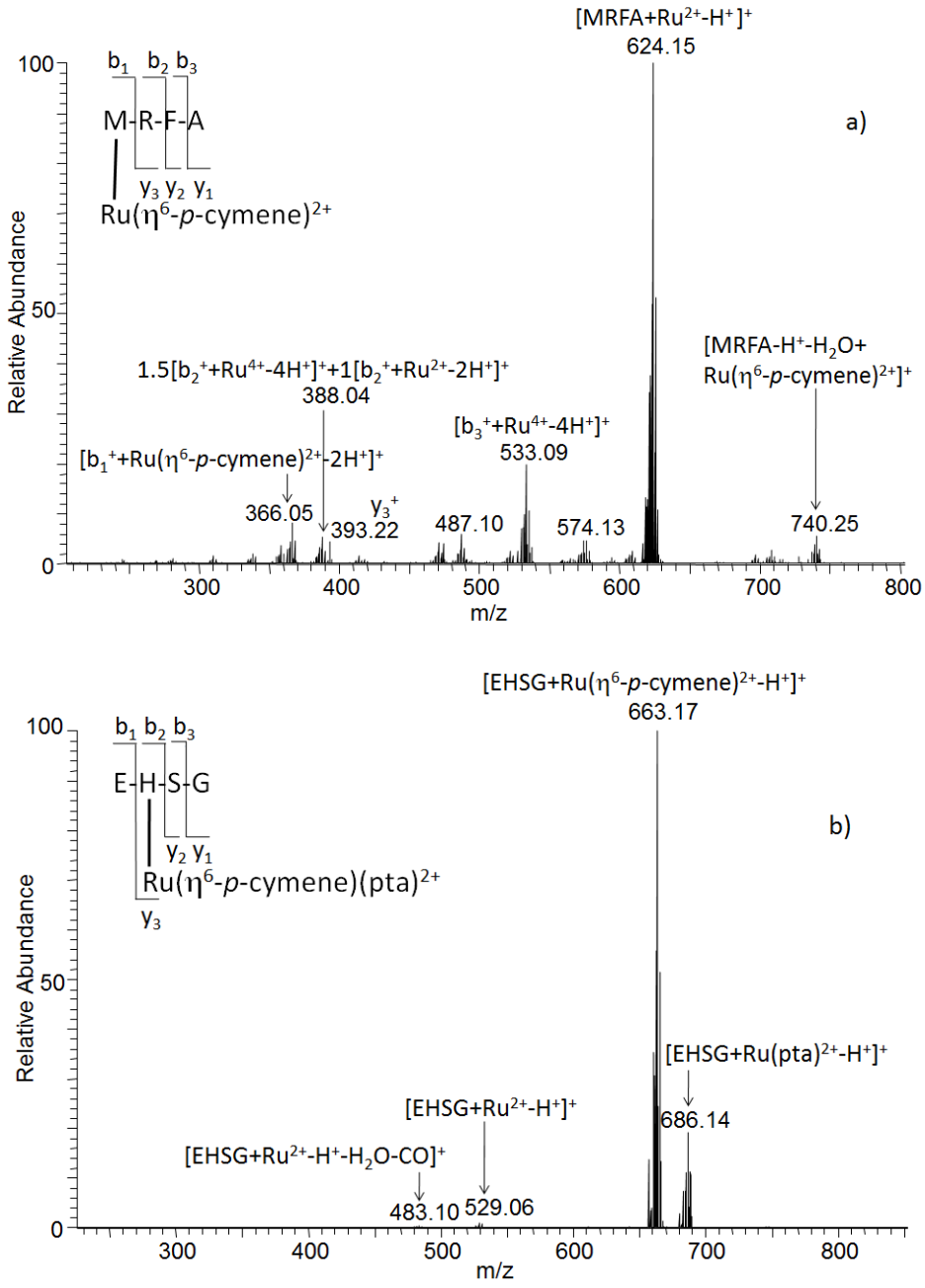

Fig. 5.6 ESI-CID mass spectra (fragmentation in IT, acquisition in Orbitrap) of a) [MRFA+Ru(η^6-*p*-cymene)$^{2+}$-H$^+$]$^+$ and b) [EHSG+Ru(η^6-*p*-cymene)(pta)$^{2+}$-H$^+$]$^+$.

The information on Pt metallo fragment stability at CID will turn out useful in the bottom-up experiments of chapter 6 (see paragraph 6.2.5).
It is also interesting to notice the presence of fragments containing Ru^{4+} (attributions verified through simulations not reported here; see the published paper reported at pg. 61) in the CID spectrum of $[MRFA+Ru(\eta^6\text{-}p\text{-cymene})^{2+}\text{-}H^+]^+$ probably due to some rearrangements and/or redox processes during fragmentation in IT.

5.4 Conclusions

In this work we have designed a general and systematic protocol to test, *a priori*, the stability of metallodrug-protein adducts under the typical conditions of the FASP/bottom-up mass spectrometry approach. This study may turn helpful to scientists working in the field of metalloproteomics and investigating metallodrug-protein interactions. The protocol here developed constitutes a useful and almost complete track to be followed but it is obviously open to additions and improvements, according to the chosen MS instrument and the applied sample preparation procedures. The protocol was specifically applied to two representative model systems, Cyt *c*-CDDP and Cyt *c*-RAPTA-C. Cyt *c*-CDDP adducts were stable in all tested conditions, while Cyt *c*-RAPTA-C adducts manifested a remarkable instability in the 50 mM ammonium bicarbonate buffer. This latter finding demonstrates the advisability to perform a test-protocol like this when starting any bottom-up MS investigation on protein-metallodrug systems, especially with novel, or scarcely studied, metal complexes. In fact, the nature of the metal, of its ligands and of the protein microenvironment are variables that may undoubtedly affect the stability of the metal-protein coordination bond during the bottom-up approach, and are not easy to predict.

5.5 References

[1] C. Wu, J. C. Tran, L. Zamdborg, K. R. Durbin, M. Li, D. R. Ahlf, B. P. Early, P. M. Thomas, J. V. Sweedler, N. L. Kelleher, *Nat. Methods*, **2012**, *9*, 822-826
[2] A. Cristobal, F. Marino, H. Post, H. W. P. van den Toorn, S. Mohammed, A. J. R. Heck, *Anal. Chem.*, **2017**, *89*, 3318−3325.
[3] E. Moreno-Gordaliza, B. Cañas, M.A. Palacios, M.M. Gómez-Gómez, *Analyst*, **2010**, *135*, 1288–1298.
[4] E. Moreno-Gordaliza, B. Cañas, M.A. Palacios, M.M. Gómez-Gómez, *Talanta*, **2012**, *88*, 599–608.
[5] I. Moraleja, E. Moreno-Gordaliza, M.L. Mena, M.M. Gómez-Gómez, *Talanta*, **2014**, *120*, 433-442.

[6] I. Moraleja, E. Moreno-Gordaliza, D. Esteban-Fernández, M.L. Mena, M.W. Linscheid, M.M. Gómez-Gómez, *Anal. Bioanal. Chem.*, **2015**, *9*, 2393–2403.
[7] M. Karas, U. Bahr, T. Dülcks, *Fresenius J. Anal. Chem.*, **2000**, *366*, 669–676.
[8] Y. T. Li, Y.L. Hsieh, J.D. Henion, *J. Am. Soc. Mass Spectrom.*, **1993**, *4*, 631–637.
[9] J. A. Loo, *Int. J. Mass Spectrom.*, **2000**, *200*, 175–186.
[10] J. Will, W.S. Sheldrick, D. Wolters, *J. Biol, Inorg. Chem.*, **2008**, *13*, 421–434.
[11] D. Gibson, C.E. Costello, *Eur. Mass Spectrom.*, **1999**, *5*, 501–510.
[12] A. Schmidt, M. Karas, *J. Am. Soc. Mass Spectrom.*, **2001**, *12*, 1092–1098.
[13] V. Gabelica, C. Vreuls, P. Filée, V. Duval, B. Joris, E. De Pauw, *Rapid Commun. Mass Spectrom.*, **2002**, *16*, 1723–1728.
[14] A. Ariza, D. Garzon, D.R. Abánades, V. de los Ríos, G. Vistoli, M. J. Torres, M. Carini, G. Aldini, D. Pérez-Sala, *J. Proteom.*, **2012**, *77*, 504–520.
[15] J. Will, D. A. Wolters, W. S. Sheldrick, *ChemMedChem*, **2008**, *3*, 1696–1707.
[16] C. Gabbiani, A. Casini, G. Mastrobuoni, N. Kirshenbaum, O. Moshel, G. Pieraccini, G. Moneti, L. Messori, D. Gibson, *J. Biol. Inorg. Chem.*, **2008**, *13*, 755-764.
[17] H. Li, Y. Zhao, H. I. A. Phillips, Y. Qi, T. Lin, P. J. Sadler, P. B. O'Connor, *Anal. Chem.*, **2011**, *83*, 5369-5376.
[18] R. H. Wills, A. Habtemariam, A. F. Lopez-Clavijo, M. P. Barrow, P. J. Sadler, P. B. O'Connor, *J. Am. Soc. Mass Spectrom.*, **2014**, *25*, 662-672.

6. CISPLATIN BINDING SITE LOCATION ON CYTOCHROME *C* AND HUMAN SERUM ALBUMIN: FASP/BOTTOM-UP MASS SPECTROMETRY APPROACH

6.1 Introduction

As reported in chapter 2, one of the aims of this PhD thesis was the development and introduction in our laboratories of an efficient and generally applicable method for metallodrugs binding site location on proteins, regardless of the MW and nature of the protein and the type of metal complex under investigation. The preliminary stability tests performed in chapter 5 demonstrated the resistance of CDDP-Cyt *c* adducts to all the preparative/analytical steps of the selected FASP/bottom-up nanoLC-nanoESI-MS/MS approach. Consequently, we decided to perform our first systematic study of binding site location on this model system.

This system has already been intensively investigated in the literature in order to elucidate Pt position on Cyt *c*, but the reported results are not completely concordant with each other. Zhao *et al*. found Met65 as primary binding site of CDDP on Cyt *c* through bottom-up infusion-ESI-LTQ-Orbitrap-MS/MS and MS^3 analyses on the digested peptide mixture [1], while Zhang *et al*., with the same kind of experiment performed on a FT-ICR mass spectrometer, discovered three more binding sites, namely Met80, His18 and His33 [2]. In turn, Gordaliza *et al*. identified Glu61, Glu62, Thr63, Met65 and Met80 as binding sites by a nanoLC-ESI-LTQ-MS/MS gel-based bottom-up approach [3]. Finally, Ferraro *et al*. studied the system with an XRD experiment and they found Glu61 and Met65 as Pt binding sites [4]. The partial concordance of these results can be certainly attributed to the different preparative/analytical conditions used for sample analysis and this issue makes the study of CDDP-Cyt *c* binding site location a topic that still deserves to be investigated.

Within this frame, the results of our study will benefit, on one hand, from the comparison with the ones already present in the literature, in order to ascertain their reliability and, on the other hand, they could generate new knowledge on this still controversial topic.

In parallel, we decided to apply the FASP/bottom-up nanoLC-nanoESI-MS/MS approach to the investigation of CDDP binding sites on HSA, in order to test the method on a more complex system than the CDDP-Cyt *c* model, thus opening the way to studies involving proteins that are actual targets for metallodrugs.

HSA (fig. 6.1) is the most abundant plasma protein (about 52%). It consists of a single chain with 585 amino acids (MW 66-67 kDa) organized in three domains (I, II and III), each of which contains two subdomains (IA, IB, etc.). It is basically a helical protein

(67% of α-helix content) and its amino acid sequence contains 17 disulfide bridges and one thiol group (Cys34) which is a potential binding site toward many type of compounds, including metallodrugs [5].

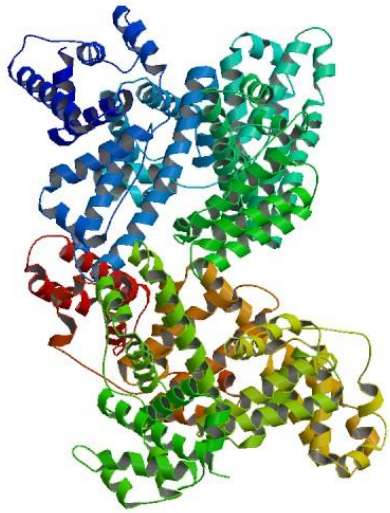

Fig. 6.1 Crystal structures of HSA (PDB 4K2C).

HSA, together with other serum proteins, like transferrin, may perform a transport function for platinum based-drugs and influence the overall drug distribution and excretion, as well as its efficacy, activity and toxicity. Controversial opinions still exist on the consequences of cisplatin binding to HSA. Some authors postulate that human serum albumin forms a ‘‘reservoir’’ for the biologically active Pt species, while others consider Pt binding to serum albumin as a form of drug inactivation. For example, it was suggested that an excessive cisplatin affinity for HSA may prevent its effective tissue delivery, thus hampering the antitumor actions [6]. On the other hand, it was shown that hypoalbuminemic patients respond poorly to cisplatin treatment [7]. Additionally, albumin binding may prevent some of the side effects of cisplatin treatment, especially its nephrotoxicity [8]. Therefore, an understanding of the molecular mechanism of albumin-cisplatin interactions may have an impact on the optimization of strategies for cisplatin treatment.

The CDDP-HSA system has already been studied in the literature; attention has been paid to Pt binding site location and, as already reported for the system CDDP-Cyt *c*, also in this case the results are not completely concordant with each other. Gordaliza *et al*. identified His288, Cys289, Met298, Met329 and His338 as binding sites by a nanoLC-ESI-LTQ-MS/MS gel-based bottom-up approach [3]. Will *et al*. found Cys34, Tyr148, Tyr150, Met329, Asp375, Glu376 and Met548 through bottom-up

multidimensional nanoLC-nanoESI-LTQ-MS/MS analyses [9], while Moraleja *et al*., by bottom-up FASP-OFFGEL/IEF-nanoLC-nanoESI-LTQ-Orbitrap-MS/MS experiments, found His9, Asp13, His67, His105, His128, His247, Met298 and Met329 as binding sites [10]. In turn, Hu *et al*. found His67, Cys124, His128, His247 and Met298 through LC-ESI-Q-TOF-MS/MS bottom-up approach [11]. Finally, Ivanov *et al*., by NMR experiments, found Met87, Met298 and Met446 as CDDP binding sites on HSA [6], while Ferraro *et al.* found His67, His105, His247, His288, Met298, Met329, His535 and Met548 through XRD analysis [12].
Again, as in the case of CDDP-Cyt *c* adducts, we will exploit the results already present in the literature for the CDDP-HSA adducts in order to verify the reliability of the binding sites we will find for this last system. On the other hand, our findings could confirm the current knowledge or bring new information to be used for a better comprehension of the nature of the binding sites of CDDP on HSA.
Finally, for the automated search of the binding sites of Pt on proteins, we decided to use Mascot search engine, already employed in our laboratories for "classical" proteomics experiments. To the best of our knowledge, it is the first time that this interface is exploited for metalloproteomics purposes with the aim to locate metal binding sites.

6.2 Experimental

6.2.1 Solvents, reagents and materials

Water (412091) and acetonitrile (412042), both UHPLC-MS grade, were purchased from Carlo Erba (BP 616, F-27106, Val de Reuil Cedex, France). Ammonium acetate (A1542), ammonium bicarbonate (09830), DTT (43815), IAA (57670), HCOOH (56302) and TFA (40967) were purchased from Sigma-Aldrich (St. Louis, MO, USA) and urea from Serva (Heidelberg, Germany). Sequencing grade modified trypsin (V5111) was purchased by Promega (Madison, WI, USA). Microcon centrifugal filter devices with nominal cutoff of 3 kDa (42404) or 10 kDa (42407) were purchased from Millipore (Bedford, MA 01730, USA). CDDP (P-4394), HSA (A-3782) and horse heart Cyt *c* (C7752) were purchased from Sigma-Aldrich.

6.2.2 Cyt c-CDDP and HSA-CDDP adduct formation and purification

Nine mg of CDDP (final concentration 300 μM) were dissolved in 100 ml of 20 mM AA buffer at pH 6.8. To 1 ml of this solution, 1.2 mg of Cyt *c* or 6.6 mg of HSA (protein concentration 100 μM; protein to metal ratio 1 to 3) were added, respectively. The two solutions were incubated for 144 h at 37 °C (the adduct formation was monitored by direct infusion in the ESI-Orbitrap for Cyt *c* and in ESI-IT for HSA,

using the conditions and instrumental settings already reported by Michelucci *et al.* [13]). After this time, an aliquot containing 50 μg of protein/protein adducts was withdrawn from each solution and purified on the proper centrifugal filter device (3 kDa for Cyt *c* and 10 kDa for HSA): dilution on filter with 200 μl of 50 mM Ambic, spinning for 45 min at 13,000 rpm, washing with 200 μl 50 mM Ambic and again spinning for 45 min at 13,000 rpm. The same procedure of purification was performed for the solutions of Cyt *c* and HSA in AA not incubated with CDDP.

6.2.3 FASP procedure: denaturation, reduction, alkylation and digestion steps

The four purified samples were denatured on centrifugal filter device (200 μl of 8 M urea in 50 mM Ambic were added and the filter was spun for 45 min at 13,000 rpm; this procedure was repeated once and then 200 more μl of 8 M urea in 50 mM Ambic were added). For the reduction step, 3.3 μl of a freshly prepared 0.5 μg/μl DTT aqueous solution (30:1 protein-to-DTT ratio, w/w) were added directly on each centrifugal filter device and the samples were incubated for 30 min at room temperature (rt). For the alkylation step, 3.3 μl of a freshly prepared 2.5 μg/μl IAA aqueous solution (6:1 protein-to-IAA ratio, w/w) were added directly on each centrifugal filter device and the samples were incubated for 20 min at rt in the dark. The four samples were then purified from urea, DTT and IAA (the samples were spun for 30 min at 13,000 rpm, twice washed with 100 μl of 50 mM Ambic and spun for 30 min at 13,000 rpm). The samples were then diluted with 100 μl of 50 mM Ambic and finally overnight digested at 37 °C on filter with trypsin (30:1 protein-to-trypsin ratio, w/w). The morning after a new reservoir was placed under each filter and the samples were spun for 25 min at 13,000 rpm. The filters were washed with 30 μl of 50 mM Ambic and spun for 25 min at 13,000 rpm. These last two steps were repeated twice. The four peptide mixtures recovered in the reservoir were subjected to nanoLC-nanoESI-MS/MS analysis.

6.2.4 NanoLC-nanoESI-MS/MS analysis

The four peptide mixtures were submitted to nanoLC-nanoESI-MS/MS analysis on an Ultimate 3000 HPLC (Dionex-Thermo Fisher, San Donato Milanese, Milano, Italy) coupled to a LTQ Orbitrap mass spectrometer (Thermo Fisher, Bremen, Germany). For each sample, 5 μl were injected. Peptides were concentrated on a precolumn cartridge PepMap100 C18 (300 μm i.d. × 5 mm, 5μm, 100 Å, LC Packings Dionex) and then eluted on a homemade nano column packed with Aeris Peptide XB-C18 phase (75 μm i.d. × 15 cm, 3.6 μm, 100 Å, Phenomenex, Torrance, CA, USA) at 300 nl/min. The loading mobile phases were: 0.1% TFA in H_2O (phase A) and 0.1% TFA in CH_3CN (phase B). The elution mobile phases composition was: H_2O 0.1% formic acid/CH_3CN 97/3 (phase A) and CH_3CN 0.1% formic acid/ H_2O 97/3 (phase B). The elution program was: 0 min, 4% B; 10 min, 40% B; 30 min, 65% B; 35 min, 65% B; 36 min,

90% B; 40 min, 90% B; 41 min, 4% B; 60 min, 4% B. Mass spectra were acquired in positive ion mode, setting the spray voltage at 1.8 kV, the capillary voltage and temperature at 45 V and 200 °C, respectively, and the tube lens at 130 V. Data were acquired in data-dependent mode with dynamic exclusion enabled (repeat count 2, repeat duration 15 s, exclusion duration 30 s); survey MS scans were recorded in the Orbitrap analyzer in the mass range 300-2000 *m/z* at a 15,000 nominal resolution at *m/z* = 400; then up to three most intense ions in each full MS scan were fragmented (isolation width 3 *m/z*, 30% relative collision energy) and analyzed in the IT analyzer. Monocharged ions did not trigger MS/MS experiments. Xcalibur 2.0 software (Thermo) was used for data acquisition.

6.2.5 Mascot automated search and subsequent manual check

The acquired data were searched with Mascot Daemon 2.4.0 search engine (Matrix Science Ltd., London, UK) against a customized database consisting of, respectively, the horse heart Cyt *c* (Uniprot P00004) or the HSA (Uniprot P02768) sequence. For Mascot search on peptide mixture coming from Cyt *c* digestion, the following variable modifications were introduced: N-terminal acetylation, heme$^+$ group on C and oxidation of M. For the peptide mixture coming from Cyt *c* incubated with CDDP, in addition to those above mentioned, other variable modifications were introduced on the potentially coordinating residues C, D, E, H, K, M, T, W and Y: $[Pt]^{2+}$, $[(NH_3)Pt]^{2+}$, $[(NH_3)_2Pt]^{2+}$ and $[(NH_3)_2PtCl]^+$. For the peptide mixture coming from HSA digestion the introduced variable modifications were: carbamidomethylation and cysteinylation on C, oxidation on M, phosphorylation on S, T, Y, and N-glycosylation on R and K. Finally, for the peptide mixture coming from the digestion of HSA incubated with CDDP, the introduced variable modifications were: carbamidomethylation and cysteinylation on C, oxidation on M, N-glycosylation on K, and $[Pt]^{2+}$, $[(NH_3)Pt]^{2+}$, $[(NH_3)_2Pt]^{2+}$, $[(NH_3)_2PtCl]^+$ on the potentially coordinating residues C, D, E, H, K, M, S, T, W and Y. The monoisotopic mass values were used for the calculation of the mass gains related to the variable modifications. In order to consider the net loss of two protons from the bi-charged modifications and of one proton from mono-charged modifications, two mass units or one mass unit were subtracted, respectively, from the monoisotopic mass of the modification itself. The Mascot searches were performed considering: (i) trypsin as enzyme, (ii) up to two missed cleavage sites, (iii) 10 ppm of tolerance for the monoisotopic precursor ion and 0.5 mass unit for monoisotopic fragment ions, (iv) only bi-, tri- and tetra-charged precursor peptides. Following the Mascot automated search, precursor peptide and MS/MS spectra were visually assessed to positively confirm the presence of platinum in Mascot assignments on the basis of the characteristic isotopic pattern of platinated peptides. Peptide sequences whose MS or MS/MS spectra did not respect this criterion were removed from the final list of the correct assignments.

6.2.6 HSA-CDDP adduct stability at denaturation, reduction, alkylation, digestion in Ambic and in loading/elution mobile phases: sample preparation for ICP-AES analyses

One ml of HSA-CDDP adduct solution (protein concentration 100 μM, CDDP concentration 300 μM) was purified from unbound Pt excess and AA with a procedure analogue to that already described in paragraph 6.2.2, but using water in the three washing steps. The filter was then spun upside down at 3500 rpm for 3 min and the volume recovered was diluted to 1 ml with H_2O. Twenty-five μl of this solution were diluted with H_2O to the final volume of 500 μl (final protein concentration 5 μM) and directly analyzed by ICP-AES. Moreover, three aliquots (50 μl each) were withdrawn from the purified solution and were subjected to the stability tests to a) urea, DTT, IAA, Ambic, b) loading mobile phase and c) elution mobile phase, according to the protocol reported in the published paper by Michelucci *et al.* (see pg. 61). At the end of the stability tests, the three samples were opportunely purified and diluted with H_2O to the final volume of 1 ml (protein concentration of 5 μM). Different volumes of the three samples (840 μl for sample a) and 800 μl for samples b) and c)) were analyzed by ICP-AES.

6.2.7 ICP-AES analyses

The determination of protein bound platinum was performed by a Varian 720-ES Inductively Coupled Plasma Atomic Emission Spectrometer equipped with a CETAC U5000 AT+ ultrasonic nebulizer, in order to increase the method sensitivity. The four samples prepared in paragraph 6.2.6. were put in PE vials and digested in a thermos-reactor at 90 °C for 24 h with 2 ml of aqua regia (HCl and HNO_3, both suprapure grade, at 3:1 ratio). After digestion, the samples were diluted to a final volume of 6 ml with ultrapure water (≤ 18 MΩ), were spiked with 1 ppm of Ge, used as the internal standard, and analyzed. Calibration standards were prepared by gravimetric serial dilution from commercial standard solution of Pt at 1000 mg/L. The wavelength used for Pt determination was 214.424 nm whereas for Ge the line at 209.426 nm was used. The operating conditions were optimized to obtain maximum signal intensity and, between each sample, a rinse solution of aqua regia was use in order to avoid any "memory effect".

6.3 Results and discussion

6.3.1 Adduct formation, FASP procedure and nanoLC-nanoESI-MS/MS analyses

The adduct formation in CDDP-Cyt *c* solution was monitored by ESI-Orbitrap infusions (see fig. 6.2).

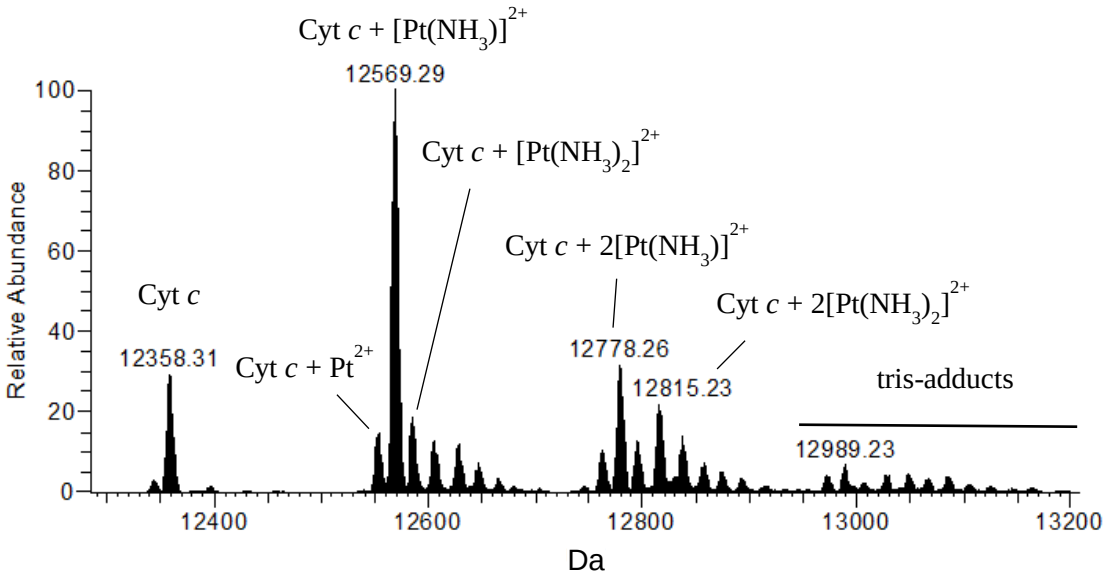

Fig. 6.2 ESI-Orbitrap deconvoluted mass spectrum of Cyt *c*-CDDP solution after 144 h incubation at 37 °C in 20 mM AA, pH 6.8 (1:3 Cyt *c*:CDDP ratio).

To explain the structure of the adducts reported in fig. 6.2, we supposed that the protein acts as a multidentate ligand, as previously reported by Gibson and Costello for the CDDP-ubiquitin system [14]. The Pt–N bonds are kinetically inert and thermodynamically stable, whereas Pt–Cl bonds are semilabile and Pt–O bonds are labile. Pt–S bonds are inert and have a strong *trans* effect, *i.e.* they labilize the bonds that are *trans* to the sulfur atom. The course of the reaction between CDDP and Cyt *c* probably involves the initial aquation of one chloride ligand to yield [*cis*-$Pt(NH_3)_2Cl(H_2O)]^+$ which reacts with the side chain of an amino acid (probably M) to form a monodentate covalent adduct *cis*-$Pt(NH_3)_2Cl(Cyt\ c)_m$ (m = monodentate). The second chloride ligand is then substituted by an aqua ligand to give the more reactive monodentate *cis*-$Pt(NH_3)_2(H_2O)(Cyt\ c)_m$. Excluding the loss of a ligand during the ionization process [15], we believe that aqua ligand on the bound platinum is substituted by a nucleophile on the protein to form the bidentate adduct *cis*-$Pt(NH_3)_2(Cyt\ c)_b$ (b = bidentate). Although platinum(II)–ammine bonds are inert, the thioether group of methionine is known to *trans*-labilize the ammine ligand from cisplatin. *Trans*-labilization of the ammine ligand could lead to the substitution of the inert ammine ligand by the reactive water ligand that, in turn, can react with another amino acid side chain to form a tridentate adduct, $Pt(NH_3)(Cyt\ c)_t$ (t = tridentate) with

MW = 12569.3 Da. Theoretically, even tetradentate adducts are possible and, in our specific case, they are formed only in small quantity.
The adduct formation in CDDP-HSA solution was monitored by ESI-IT infusions (see fig. 6.3).

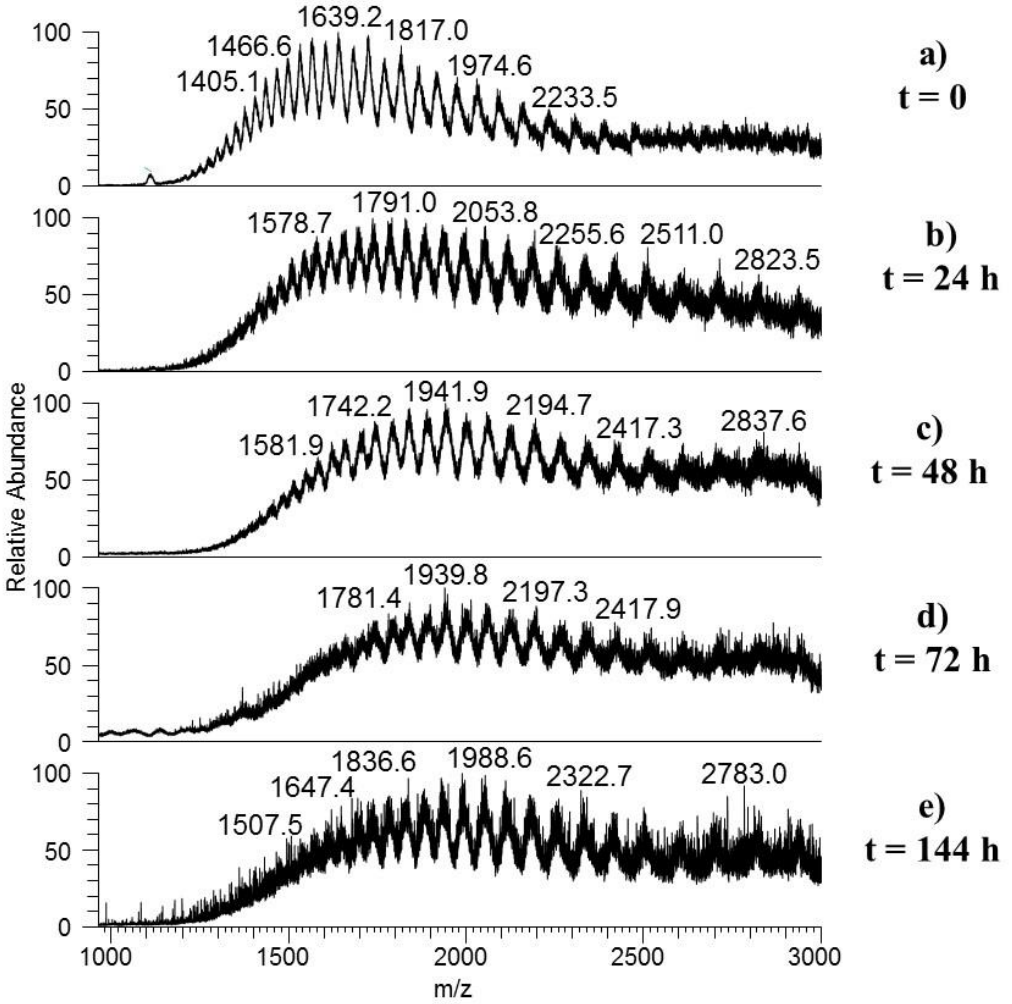

Fig. 6.3 ESI-IT multicharged mass spectrum of HSA-CDDP solution a) before CDDP addition and after b) 24 h, c) 48 h, d) 72 h, e) 144 h incubation at 37 °C in 20 mM AA, pH 6.8 (1:3 HSA:CDDP ratio).

As already explained in paragraph 2.1, our Orbitrap high resolution mass analyzer is able to properly detect molecules with a maximum MW of 20-30 kDa. Since HSA MW is about 66-67 kDa, we were forced to use the low resolution analyzer IT to follow its platinated adduct formation. This formation is well documented by comparing the ESI-IT multicharged spectra of HSA solution before (fig. 6.3 a) and after (fig. 6.3 b-e)

CDDP addition: the generation of new signals, that decreases peak resolution, and the shift of the multicharged profile to higher masses are a clear witness of the binding of metallo fragments to HSA.
In order to obtain a more direct prove of platinated adduct formation, the HSA-CDDP solution was, first of all, carefully washed on centrifugal filter device to remove the unbound Pt excess and then was subjected to ICP-AES analysis. A Pt to protein molar ratio 2.9:1 was determined.
Before starting with the bottom-up MS approach on HSA-CDDP adducts, we decided to investigate on their stability during this procedure. As already reported for the system Cyt *c*-CDDP in paragraph 5.3.4, HSA-CDDP adduct stability in nanoESI source can be deduced by following the kinetic of adduct formation shown in fig. 6.3: the multicharged profile shifts to higher masses congruently with the increasing of the incubation time, thus indicating the non-involvement of the nanoESI process in adduct formation/destruction. For the stability tests to urea, DTT, IAA, Ambic and loading/elution mobile phases, we followed the protocol cited in the paper reported at pg. 61 and we verified the presence of Pt on HSA by ICP-AES analyses. In particular, after denaturation, reduction, alkylation and Ambic treatment, a Pt to protein molar ratio 2.3:1 was determined, while, after permanence in loading and elution mobile phases, 2.7:1 and 2.5:1 Pt to protein molar ratios were, respectively, found. HSA-CDDP adduct stability to instrumental parameters was verified according to the testing protocol reported in chapter 5: the analysis of the acquired spectra (not reported here) seemed to confirm the stability to the variations imposed to capillary temperature/voltage applied to the ion transfer tube and to tube lens voltage; however, these data were not as informative as those reported for the system Cyt *c*-CDDP, due to the low resolution of the ion trap analyzer. Finally, regarding the stability of the metallo fragment-peptide adducts at CID, the results obtained for the Cyt *c*-CDDP system (see paragraph 5.3.6) can be extended to the HSA-CDDP one: in fact, the metal compound and the amino acids involved in the binding are the same.
Before starting with the denaturation step, Cyt *c*, CDDP-Cyt *c*, HSA and CDDP-HSA solutions were put on centrifugal filter device and washed with 50 mM Ambic. The washing with ammonium bicarbonate fulfills a dual function: it sets the right pH value for the tryptic digestion step and removes the unbound CDDP excess from CDDP-Cyt *c* and CDDP-HSA solutions. The removal of Pt excess from these solutions is particularly important in order to avoid undesired side reactions between the free metal complex and the reagents used during the subsequent denaturation, reduction, alkylation and digestion steps. The FASP procedure was chosen, as already explained in chapter 5, to limit the contact time between the denaturing/reducing/alkylating agents and the metallo fragment-protein adducts, thus avoiding possible side reactions causing metal loss. Moreover, it should be noted that Cyt *c* would not need reduction-alkylation steps since its unique two cysteines are covalently involved in heme *c*

binding. Nevertheless, in this model study, we decided to perform these two steps in order to practice with the procedure in its entirety.
The instrumental analysis consisted of an initial on-line purification/concentration step, in order to eliminate Ambic from the peptide mixtures before injection into the nano column, followed by a nanoLC-nanoESI-MS/MS analysis. The sample quantities we had to deal with did not necessarily required the use of nanoflows. However, we decided, for these first attempts, to already set the instrument in a configuration proper to analyze future samples, potentially available in small quantity or lower concentration.

6.3.2 How to "deceive" the Mascot search engine designed for "classical" proteomics and force it to work in metalloproteomics

The files generated by nanoLC-nanoESI-MS/MS analyses were used for an automated Mascot search.
Mascot, together with Sequest (Proteome Discoverer, Thermo) and Andromeda (MaxQuant, Max Planck Institut für Biochemie), is one of the most famous search engine used in "classical" proteomics experiments. These softwares are not specifically designed for metalloproteomics purposes and their application is effectively limited to bottom-up analysis of small peptides containing common elements such as C, H, N, O, S and P.
On the other hand, there is an increasing interest in the study of the interaction of proteins with heavy elements of biological and medicinal relevance. These include Cr, Mo, W, Fe, Ru, Os, Pd, Pt, Cd, Hg, Pb, Se and Gd, all of which feature lightest isotope(s) of low abundance(s). Due to this fact, ions containing these isotopes may not be easily detected and may present complicated isotopic patterns.
The employment of the aforementioned search engines for metalloproteomics purposes is however possible, but a number of tricks must be used:

- the most abundant isotope of the metal element is manually defined to be the 'lightest isotope' (*e.g.*, ^{190}Pt, ^{192}Pt, ^{194}Pt, $^{\mathbf{195}}\mathbf{Pt}$, ^{196}Pt, ^{198}Pt);
- the software assumes that protons are the only source of positive charges in spectra generated by electrospray ionizations, so users need to manually subtract proton(s) from ions containing fixed positive charge(s) from other elements (*e.g.*, by entering "Pt - 2H" instead of Pt^{2+}, where Pt means Pt^{0});
- the software does not generate theoretical isotope patterns and does not consider experimental isotope patterns. No comparison between the theoretical and experimental isotope patterns is possible. The user must generate theoretical isotope patterns manually and compare those with experimental patterns that are claimed to contain metal ion(s) by the software based on searches for monoisotopic species only. The researcher also uses his/her

judgement to eliminate false positives or negatives. This visual analysis is always tedious and very time-consuming.

Sequest has already been used for metalloproteomics purposes with the intent to locate metal binding sites [9,16,17]. Instead Mascot, the software we currently utilize in our laboratories for "classical" proteomics experiments, to the best of our knowledge, has never been used for binding site location of a metallo fragment on a protein. For this reason, we decided to test the applicability of Mascot in this specific metalloproteomics application.

6.3.3 Binding site location in the CDDP-Cyt c model system through Mascot automated search followed by manual check

First of all, we introduced in Mascot interface a customized database consisting only of the horse heart Cyt *c* sequence, thus deleting any possible statistic evaluation on the results.

Among the variable modifications listed in paragraph 6.2.5, it is worth to linger over the platinated ones, *i.e.* $[Pt]^{2+}$, $[(NH_3)Pt]^{2+}$, $[(NH_3)_2Pt]^{2+}$ and $[(NH_3)_2PtCl]^{+}$, the possible CDDP metallo fragments that can bind to proteins [9] (see fig. 6.2). Due to the high affinity of Pt(II) for the S-donors present in the amino acid side chains, it is reasonable to introduce C and M among the possible binding sites. However, N-donors, as H, K and W, and O-donors, as D, E, S, T and Y cannot be excluded *a priori*. It means a total of four platinated modifications on nine possible nucleophilic binding sites (S can be excluded since it is not present in horse heart Cyt *c* sequence). This elevated number of variable modifications turned out to be unmanageable by Mascot within just one search file, thus forcing us to create nine different search files, one for each of the possible binding sites. In this way, obviously, the presence of mixed bis- and tris-adducts (adducts where the two/three Pt centers are bound to two/three amino acids of different nature) is not revealed. However, we have to say that the presence of bis- and tris-adducts in the starting material (see fig. 6.2) is quite irrelevant in comparison to the most intense mono-adduct peak.

The results coming from Mascot automated search are simply based on the mass tolerance imposed in Mascot interface for the precursor peptide and its fragments. So, as anticipate in paragraph 6.3.2, all the platinated precursor peptides/fragments claimed by Mascot must be checked by manually generating the relative theoretical isotope pattern and comparing it with the corresponding experimental isotopic patterns of the precursor ion in the HR full scan or its fragments in the MS/MS spectra. To understand how the manual check works, let's consider, as exemplificative case, one of the Mascot results coming from the automated assignment: the binding of $[(NH_3)Pt]^{2+}$ on Met65 contained in the peptide 56-72. Fig. 6.4 shows the comparison between the experimental isotopic pattern of peptide 56-72 + $[(NH_3)Pt]^{2+}$ (a) and its theoretical simulation (b): the correspondence is excellent, both in terms of mass values

(monoisotopic mass error = 4.5 ppm) and isotopic profile shape (characteristic of the presence of one Pt atom). In the figure, it is also highlighted the monoisotopic mass value that Mascot uses to perform the assignment.

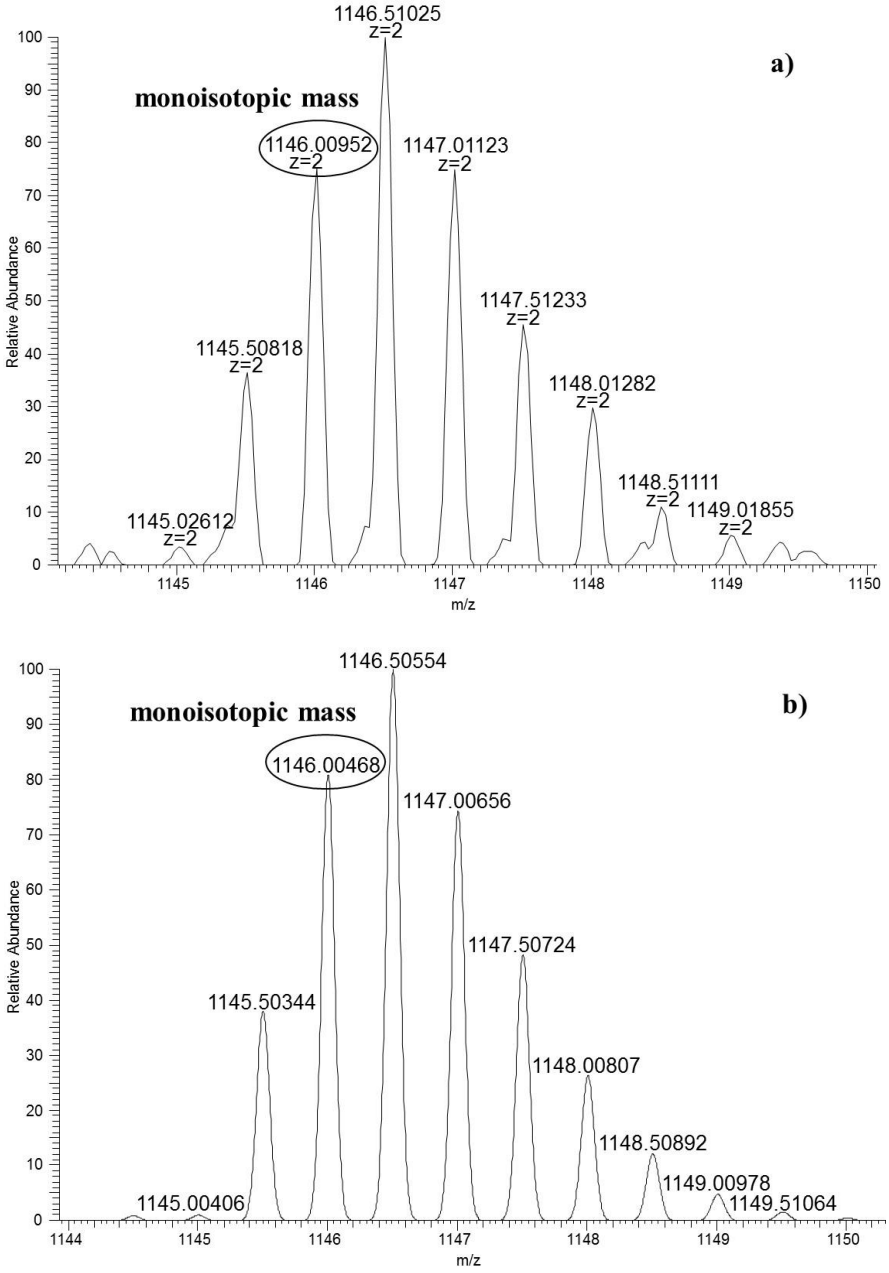

Fig. 6.4 Comparison between a) the experimental isotopic pattern of peptide 56-72 + $[(NH_3)Pt]^{2+}$ (acquisition in Orbitrap) and b) its theoretical simulation.

A similar procedure was applied to verify the reliability of the attributions of all the twenty-one b and y fragment ions identified by Mascot and coming from the CID of peptide 56-72 + $[(NH_3)Pt]^{2+}$ on Met65. Only for explanatory purpose, we report in fig. 6.5 the comparison between the experimental isotopic pattern of the claimed b_{13}^{*++} fragment ion of peptide 56-72 with $[(NH_3)Pt]^{2+}$ on Met65 (a) and its theoretical simulation (b). Mascot assignment is, in this case, a false positive. Despite that the error on the mass value used for the assignment (black circles in fig. 6.5) is within the tolerance imposed in Mascot interface, the isotopic profiles and the charge states are completely in disagreement. In fact, the species on the left doesn't contain Pt and is mono-charged, while that on the right contains one Pt and is doubly-charged.

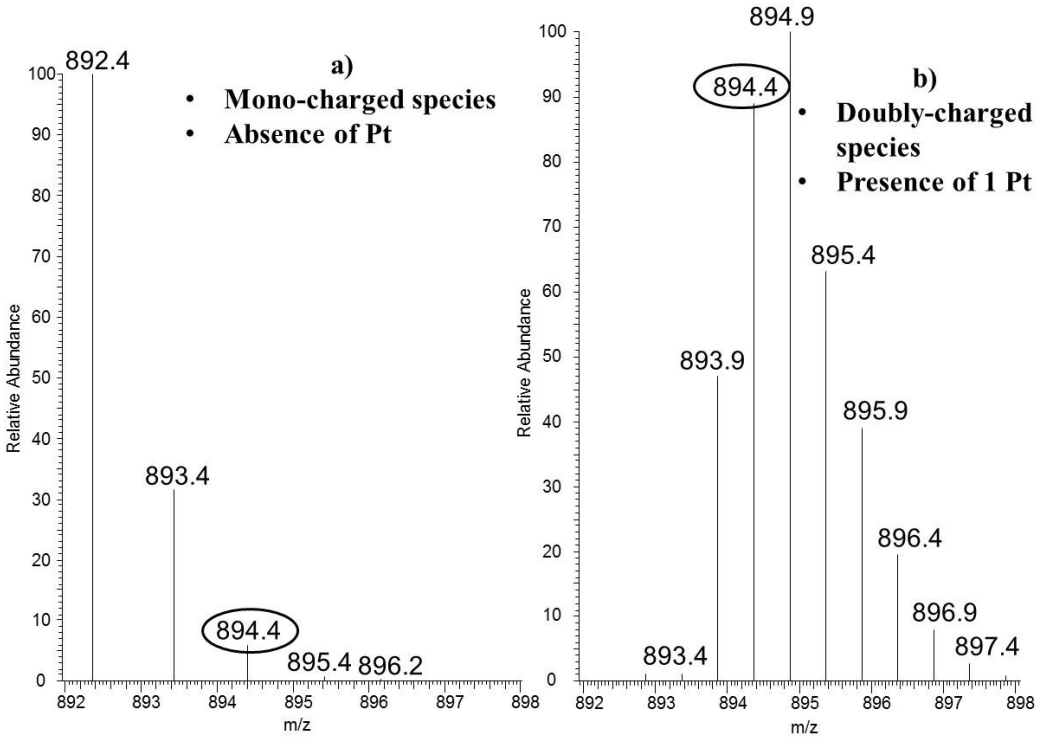

Fig. 6.5 Comparison between a) the experimental isotopic pattern of the claimed b_{13}^{*++} fragment ion of peptide 56-72 + $[(NH_3)Pt]^{2+}$ on Met65 (acquisition in IT) and b) its theoretical simulation.

Using the manual check, the reliability of the assignment for the remaining twenty fragment ions was tested and the number of correct attributions was thus reduced from twenty-one to eleven (fig. 6.6).

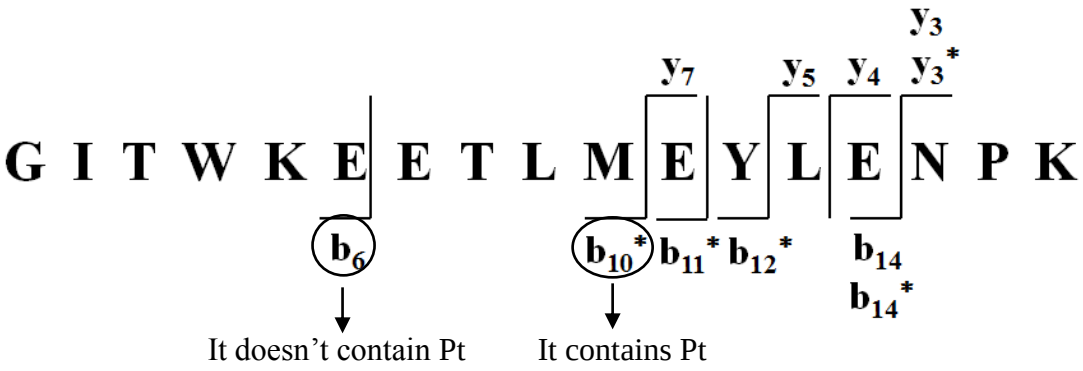

Fig. 6.6 Peptide 56-72 + $[(NH_3)Pt]^{2+}$ on Met65: the eleven correct Mascot b and y attributions after manual check.

Among these attributions, only b_6 and b_{10}^* resulted to be very informative fragments: in fact, b_6 doesn't contain Pt, while b_{10}^* does. It means that $[(NH_3)Pt]^{2+}$ modification must be within the ETLM portion of peptide 56-72 and, therefore, the metallo fragment can be placed on the S-donor Met65. However, Met65 is not the only one possible binding site in the ETLM portion: the E62 and T63 O-donors must be taken into account as additional potential binding sites.

This ambiguous binding site attribution can be explain by considering that:

1) a relative small number of b and y fragments was generated in CID spectra, probably due to the fact that Cyt *c*, in principle, can act as mono-, bi-, tri- and tetradentate ligand on CDDP (the simultaneous involvement of more than one binding site is possible), thus preventing an extensive fragmentation process;
2) it is difficult to suppose a chromatographic separation for two peptides having the same sequence but being mono-platinated on two different amino acid residues, for example, the peptide 56-72 platinated on M65 or on E62 or on T63. As a consequence, in CID spectrum, the coexistence of fragments coming from all these peptides is possible.

The above explained work methodology was applied to all the platinated peptides found by Mascot automated search relatively to the nine possible binding sites (M, C, D, E, H, K, T, W, Y; data not reported here): this manual check is a very time-consuming process, but it is indispensable in order to guarantee the reliability of the proposed binding sites.

After manual check, the final list of CDDP binding sites on Cyt *c* encompassed: T58, W59, K60, E61, E62, T63, M65, E66, Y67 and M80. From these results, it is possible to notice that only two different specific portions of the protein seem to be involved in the binding, namely peptide W59-Y67 and M80. Moreover, not all the possible donors present in the tryptic peptides 56-72 and 80-86 resulted involved in the binding (see

E69, K72 and K86). Finally, not all the tested binding sites resulted to be binding sites (see C, H, D). All these findings revealed that our bottom-up approach was able to highlight the binding selectivity of CDDP on Cyt *c*, despite the elevate number of possible nucleophilic donors in the protein (four S-donors, twenty-three N-donors, twenty-six O-donors).
In table 6.1 we compare our results with those present in the literature and already reported in paragraph 6.1.

		EXPERIMENT				
		I	**II**	**III**	**IV**	**V**
BINDING SITE	**H18**				X	
	H33				X	
	T58	X				
	W59	X				
	K60	X				
	E61	X		X		X
	E62	X		X		
	T63	X		X		
	M65	X	X	X	X	X
	E66	X				
	Y67	X				
	M80	X		X	X	

Table 6.1 Summary of CDDP-Cyt *c* binding sites, according to the literature and our experiment. I = our experiment; II = [1]; III = [3]; IV = [2]; V = [4]. In light blue = bottom-up MS experiments. In light green = XRD experiment. The references cited here are discussed in detail in paragraph 6.1.

Discrepancies among the results of table 6.1 can be, at least in part, ascribed to different preparative/analytical conditions. In this frame, however, considering also the issue of the ambiguous binding site attribution, our results are in good agreement with the literature and Met65 can be confirmed again as the primary binding site of CDDP on Cyt *c*.

Finally, we decided to investigate the 3D structure of the horse heart Cyt *c* present in the RSCB Protein Data Bank (ID 1AKK), in order to ascertain the real accessibility of the ten proposed binding sites. T58, K60, E61, E62, M65 and E66 resulted fully accessible, T63 only partially accessible while W59, Y67 and M80 not accessible. These results, added with those of table 6.1, together with the issue of the ambiguous binding site attribution and the fact that M80 is covalently involved in the binding with heme group, convinced us that probably it is more appropriate to exclude W59, Y67 and M80 from the list of CDDP binding sites on Cyt *c*.

6.3.4 Binding site location in the CDDP-HSA system through Mascot automated search followed by manual check

The binding site search for the CDDP-HSA system was performed in an analogue way to that already explained for the CDDP-Cyt *c* system in the previous paragraph, with only three variations:

1) serine was introduced among the possible binding sites of CDDP, since this amino acid is present in HSA sequence;
2) for the automated search on digested HSA, some non-platinated variable modifications were introduced in Mascot interface, in accordance with what declared by the manufacturer of the protein (possible presence of cysteinylation on C, phosphorylation on S, T, Y and N-glycosylation on R and K);
3) based on the results obtained for the digested HSA in the automated Mascot search followed by manual check, we introduced cysteinylation on C and N-glycosylation on K among the other non-platinated variable modifications for the CDDP-HSA system.

For the CDDP-HSA system, the same difficulties in manual re-processing of data and the same ambiguities in the attribution of binding sites were found, as for the CDDP-Cyt *c* system.

In table 6.2 we compare our results for the CDDP-HSA system with those present in the literature and already reported in paragraph 6.1.

		EXPERIMENT						
		I	**II**	**III**	**IV**	**V**	**VI**	**VII**
BINDING SITE	**D1**	X						
	H3	X						
	K4	X						
	S5	X						
	E6	X						
	H9	X					X	
	D13						X	
	C34			X				
	H67				X		X	X
	M87		X					
	H105						X	X
	C124				X			
	H128				X		X	
	Y148			X				
	Y150			X				
	H247				X		X	X
	H288					X		X
	C289					X		
	M298		X		X	X	X	X
	M329			X		X	X	X
	H338					X		
	D375			X				
	E376			X				
	M446		X					
	H535							X
	M548			X				X

Table 6.2 Summary of CDDP-HSA binding sites, according to the literature and our experiment. I = our experiment; II = [6]; III = [9]; IV = [11]; V = [3]; VI = [10]; VII = [12]. In light blue = bottom-up MS experiments. In apricot = NMR experiment. In light green = XRD experiment. The references cited here are discussed in detail in paragraph 6.1.

Having a look to columns from experiment II to experiment VII, it is possible to notice a certain degree of heterogeneity among the results presented in the literature: the identified binding sites in the different experiments are in poor agreement with each other, except probably for M298 and M329, thus indicating that the study of the location of Pt on HSA is not a trivial issue. Surprisingly, our results turned out to be even more out of trend: they suggested a binding in the N-terminal region of HSA (D1, H3, K4, S5, E6, H9), while the other results seem to show a more homogeneous binding all over the entire protein. Moreover, it has to be notice that, while the majority of the experiments indicates M and H as the most probable binding sites, our results, instead, propose a preponderance of O- and N-donors, but no methionine.
The possible cause of the general discrepancies present in table 6.2 could be searched, first of all, in the different preparative/analytical conditions used in experiments I-VII. Moreover, the complexity and wide heterogeneity of the HSA, which makes difficult a safe identification of the variable modifications present in the starting material, can complicate automated search on metallated adducts. Regarding our specific results, we are confident we can exclude the detachment of Pt center from HSA during the bottom-up MS approach (see discussion in paragraph 6.3.1) and, instead, we tentatively explained them by considering the inability of Mascot to find platinated cross-linked peptides, almost surely present in the HSA-CDDP system due to the high number of nucleophiles in human serum albumin. However, platinated cross-linked peptide search was taken into account only by Moraleja *et al.* in experiment VI [10], and it was manually accomplished.
Despite the poor concordance of our findings with those present in the literature, we decided that it might be worth to take a look at the 3D structure of the HSA in the RSCB Protein Data Bank (ID: 4K2C), just to verify the real accessibility of the six binding sites we found. K4, E6 and H9 resulted fully accessible while S5 only partially accessible. D1 and H3 were not evaluated because, due to their high mobility, they are not included in the various HSA structures present in the RSCB Protein Data Bank.

6.4 Conclusions and future perspectives

Our first attempt to apply the FASP/bottom-up MS approach for cisplatin binding site location on Cyt *c* gave results in good agreement with those already present in the literature. The binding seems to involve two specific portions of the protein: M80 and peptide 58-67, in particular the amino acids T58, W59, K60, E61, E62, T63, M65, E66 and Y67. After a check on the 3D structure of the horse heart Cyt *c*, in order to ascertain real accessibility of the found binding sites, and considering the fact that M80 is covalently involved in the binding with heme group, the list of the potential binding sites was reduced to T58, K60, E61, E62, T63, M65 and E66. The FASP/bottom-up

approach demonstrated its capability to highlight the selective binding of CDDP to Cyt *c*, even though a certain degree of indeterminacy in the location of vicinal binding site persists, due to the intrinsic limitations of this technique (lack of an extensive fragmentation process and absence of chromatographic separation among the same peptide platinated on different positions). Our approach does not require, at least for single-protein samples, a pre-fractioning of platinated adducts/peptides, despite their poor ionization in ESI-MS [3,9,10]. Moreover, the methodology was developed in order to analyze low quantities of proteins (nanoLC-nanoESI analysis), thus offering the possibility to apply it to the survey of real biological samples. We believe that this approach can be extended, in a systematic way, to other simple, model systems endowed of the needed stability but, in our opinion, a comparison with the results coming from other analytical techniques (XRD, NMR) is always advisable. However, we have also to take into account that any possible discrepancies in the results, obtained with different techniques, may be attributed to the very different sample preparation/analytical conditions.
Possible future experiments on the CDDP-Cyt *c* system could include:

- the use of higher collision energy, hoping to obtain a more extended degree of fragmentation for platinated peptides. On the other hand, too high collision energies may lead to breakage of the Pt-peptide and Pt-ligand bonds;
- targeted MS^3 experiments on specific platinated fragments of proper intensity, as well as different methods of peptide fragmentation (for example ETD) or peptide separation (IMS), in order to solve ambiguous attributions of binding site location;
- to try different incubation times and different CDDP/Cyt *c* ratios, with the aim to evaluate their correlation with the nature and the number of CDDP binding sites.

The application of the FASP/bottom-up MS approach to the more complex system CDDP-HSA produced results which do not find a match with those reported in the literature. The possible causes of this discrepancy could be searched in the wide heterogeneity of the HSA starting material, which complicates Mascot automated search, as well as in the inability of the search engine to find platinated cross-linked peptides, almost surely present in the HSA-CDDP system due to the high number of nucleophiles in human serum albumin. This last issue, in particular, would require an additional manual search in addition to the manual check already performed on the claimed platinated peptides. In our opinion, for the CDDP-HSA system, a more detailed investigation is advisable before attempting to extend the method, in a systematic way, to other proteins of large size or mixtures of proteins from biological samples. Possible future studies might include middle-down approaches on CDDP-

HSA adducts, as well as surveys on the incubation of CDDP with the three domains of HSA.

Finally, regarding the very time-consuming manual check on the platinated peptides claimed by the search engine, two new tools were developed in the last year to help the researchers. The first, Polycut [18], is a computer program created at Melbourne University and it should be ready in a few months for free downloading. It was written to assist mass spectrometry-based bioinorganic studies via top-down and bottom-up approaches. It does automatic assignment of MS^n signals by considering the entire experimental and simulated isotopic patterns of a metallated ion rather than reading only the mono-isotopic *m/z* values. The second, SNAP [19], is an algorithm pre-programmed into the Data Analysis software by Bruker Daltonics. Similarly to Polycut, it allows the identification of metal-containing peptides in proteomic LC-MS and MS/MS data sets by considering their characteristic isotopic patterns. The re-processing of our raw files with these two programs/algorithms would be very interesting, in order to verify the reliability of Mascot automated search followed by manual check in comparison with a fully automated search.

6.5 References

[1] T. Zhao, F. L. King, *J. Am. Soc. Mass Spectrom.*, **2009**, *20*, 1141-1147.
[2] N. Zhang, Y. Du, M. Cui, J. Xing, Z. Liu, S. Liu, *Anal. Chem.*, **2012**, *84*, 6206-6212.
[3] E. Moreno-Gordaliza, B. Cañas, M. A. Palacios, M. M. Gómez-Gómez, *Talanta*, **2012**, *88*, 599-608.
[4] G. Ferraro, L. Messori, A. Merlino, *Chem. Commun*., **2015**, *51*, 2559-2561.
[5] B. P. Esposito, R. Najjar, *Coord. Chem. Rev*., **2002**, *232*, 137-149.
[6] W. Bal, M. Sokołowska, E. Kurowska, P. Faller, *Biochim. Biophys. Acta*, **2013**, *1830*, 5444-5455.
[7] W. C. Cole, W. Wolf, *Chem.-Biol. Interact*., **1980**, *30*, 223-235.
[8] A. I. Ivanov, J. Christodoulou, J. A. Parkinson, K. J. Barnham, A. Tucker, J. Woodrow, P. J. Sadler, *J. Biol. Inorg. Chem*., **1998**, *273*, 14721–14730.
[9] J. Will, D. A. Wolters, W. S. Sheldrick, *ChemMedChem*, **2008**, *3*, 1696-1707.
[10] I. Moraleja, E. Moreno-Gordaliza, D. Esteban-Fernández, M. L. Mena, M. W. Linscheid, M. M. Gómez-Gómez, *Anal. Bioanal. Chem.*, **2015**, *407*, 2393–2403.
[11] W. Hu, Q. Luo, K. Wu, X. Li, F. Wang, Y. Chen, X. Ma, J. Wang, J. Liu, S. Xionga, P. J. Sadler, *Chem. Commun*., **2011**, *47*, 6006–6008.
[12] G. Ferraro, L. Massai, L. Messori, A. Merlino, *Chem. Commun*., **2015**, *51*, 9436-9439.

[13] E. Michelucci, G. Pieraccini, G. Moneti, C. Gabbiani, A. Pratesi, L. Messori, *Talanta*, **2017**, *167*, 30-38.
[14] D. Gibson, C. E. Costello, *Eur. Mass Spectrom.*, **1999**, *5*, 501–510.
[15] G. K. Poon, G. M. F. Bisset, P. Mistry, *J. Am. Soc. Mass Spectrom.*, **1993**, *4*, 588-595.
[16] J. Will, A. Kyas, W. S. Sheldrick, D. Wolters, *J. Biol. Inorg. Chem.*, **2007**, *12*, 883–894.
[17] J. Will, W. S. Sheldrick, D. Wolters, *J. Biol. Inorg. Chem.*, **2008**, *13*, 421–434.
[18] http://www.biorxiv.org/content/early/2016/11/26/089706.full.pdf+html
[19] C. A. Wootton, Y. P. Y. Lam, M. Willetts, M. A. van Agthoven, M. P. Barrow, P. J. Sadler, P. B. O'Connor, *Analyst*, **2017**, *142*, 2029-2037.

7. GENERAL CONCLUSIONS AND FUTURE PERSPECTIVES

In this PhD thesis, mass spectrometry-based approaches were used to characterize, at molecular level, the adducts formed between some metallodrugs (or novel, promising metal compounds) and several proteins. The obtained results can be profitably exploited for a more rational design of novel anticancer metallodrugs through a "mechanism oriented" approach.

This aim was pursued through two main search directions:
i) the study on the chemical nature and the binding stoichiometry of the adducts formed between small size proteins and: a) new analogues of cisplatin and oxaliplatin anticancer drugs (chapter 3); b) novel Au(III) complexes (chapter 4);
ii) the development and introduction in our laboratories of an efficient and generally applicable method for metallodrugs binding site location on proteins, regardless of the MW and nature of the protein and the type of metal complex under investigation, in order to get closer to the study of real, interesting biological systems (chapters 5 and 6).

In the first phase of the thesis, the chemical and biological profiles of the novel complexes *cis*$PtBr_2$ and PtI_2(DACH) were studied in comparison to those of their precursors, respectively cisplatin and oxaliplatin. In particular, ESI-MS experiments showed the similarity of behavior between *cis*$PtBr_2$ and CDDP in their binding to the model protein HEWL: Pt coordination involves the preferential detachment of halide ligands and the full retention of ammonia ligands. Instead, regarding the incubation of PtI_2(DACH) with HEWL and RNase A, no metallodrug–protein adduct was detected in ESI-MS, this indicating that PtI_2(DACH), in contrast to oxaliplatin, is not able to bind these model proteins. However, the two compounds showed a significant affinity for standard DNA oligonucleotides. Regardless of the differences and analogies of behavior highlighted by ESI-MS experiments, oxaliplatin and PtI_2(DACH) induced roughly comparable cytotoxicity in three representative CRC cell lines. This implies that the replacement of oxalate with two iodide does not impair the cellular effects of oxaliplatin, that may be thus attributed mainly to the $[Pt(DACH)]^{2+}$ chemical moiety.
In the second phase, we studied the chemical and biological profiles of Au(III) complexes bearing chelating nitrogen/carbon donors or quinoline derivatives as N-/O-donors. The ESI-MS results highlighted that the presence of a C-Au bond stabilizes the gold(III) center against reduction, in comparison with quinoline derivatives. Moreover, the use of a high resolution mass analyzer provided useful information about the mechanism of binding of these compounds to model proteins. Finally, MALDI-TOF

experiments pointed out the binding of the complex Aubipy^{c} on the CXXC motif present in peptide 1-20 of the Atox1 protein.
The valuable information, obtained in chapters 3 and 4 thanks to the use of the Orbitrap high resolution mass analyzer, are strictly circumscribed to proteins of small size. The studies here described could be extended to proteins of larger size by exploiting state-of-the-art instruments, able to routinely deal with biomolecules of higher MW. For examples, the use of Q-TOF or Q-Orbitrap mass analyzers might introduce us to the study of bigger and more relevant biological systems.

In the third phase, we have designed a general and systematic protocol to test, *a priori*, the stability of metallodrug-protein adducts under the typical conditions of the FASP/bottom-up mass spectrometry approach, being this latter the methodology we chose for the binding site location studies described in phase four. This protocol may turn helpful to scientists working in the field of metalloproteomics and investigating metallodrug-protein interactions. The protocol developed constitutes a useful and almost complete track to be followed but it is obviously open to additions and improvements, according to the chosen MS instrument and the applied sample preparation procedures. The protocol was specifically applied to two representative model systems, the more investigated Cyt *c*-CDDP adducts and the less studied Cyt *c*-RAPTA-C ones. The results we obtained showed that Cyt *c*-CDDP adducts were stable in all tested conditions, while Cyt *c*-RAPTA-C adducts manifested a remarkable instability in the 50 mM ammonium bicarbonate buffer (the buffer used during the tryptic digestion step). This latter finding demonstrates the advisability to perform a test-protocol like this when starting any bottom-up MS investigation on protein-metallodrug systems, especially with novel, or scarcely studied, metal complexes. In fact, the nature of the metal, of its ligands and of the protein microenvironment are variables that may undoubtedly affect the stability of the metal-protein coordination bond during the bottom-up approach, and are not easy to predict.

Finally, in the fourth phase of the thesis, we applied, for the first time in our laboratories, the FASP/bottom-up MS approach for cisplatin binding site location on the model protein Cyt *c* and the actual target protein HSA.
For the CDDP-Cyt *c* system we obtained results in good agreement with those already present in the literature and, after a check on the 3D structure of the horse heart Cyt *c*, the proposed binding sites were T58, K60, E61, E62, T63, M65 and E66. The FASP/bottom-up approach demonstrated its capability to highlight the selective binding of CDDP to Cyt *c*, even though a certain degree of indeterminacy in the location of vicinal binding site persists, due to the intrinsic limitations of this technique, as the lack of an extensive fragmentation process and the absence of chromatographic separation among the same peptide platinated on different positions.

The issue of the ambiguous attributions could be overcome by using a higher collision energy during CID in IT, targeted MS^3 experiments on specific platinated fragments of proper intensity and different methods of peptide fragmentation (for example ETD) or peptide separation (IMS). Our approach does not require, at least for single-protein samples, a pre-fractioning of platinated adducts/peptides, despite their poor ionization in ESI-MS. Moreover, the methodology was developed in order to analyze low quantities of proteins (nanoLC-nanoESI analysis), thus offering the possibility to apply it to the survey of real biological samples. We believe that this approach can be extended, in a systematic way, to other simple model systems endowed of the needed stability but, in our opinion, a comparison with the results coming from other analytical techniques (XRD, NMR) is always advisable. However, we have also to take into account that any possible discrepancies in the results, obtained with different techniques, may be attributed to the very different sample preparation/analytical conditions.

The application of the FASP/bottom-up MS approach to the more complex system CDDP-HSA produced results which do not find a match with those reported in the literature, already poorly concordant with each other. The possible causes of this discrepancy could be searched in the wide heterogeneity of the HSA starting material, which complicates Mascot automated search, as well as in the inability of the search engine to find platinated cross-linked peptides, almost surely present in the HSA-CDDP system due to the high number of nucleophiles in human serum albumin. This last issue, in particular, would require an additional manual search in addition to the manual check already performed on the claimed platinated peptides. In our opinion, a more detailed investigation on the CDDP-HSA system is advisable before attempting to extend the methodology, in a systematic way, to other proteins of large size or mixtures of proteins from biological samples. Possible future studies might include middle-down approaches on CDDP-HSA adducts, as well as surveys on the incubation of CDDP with the three domains of HSA.

Regarding the very time-consuming manual check on the platinated peptides claimed by the search engine, two new tools were developed in the last year to help the researchers: the computer program Polycut and the algorithm SNAP. They both do automatic assignment of MS^n signals by considering the entire experimental and simulated isotopic patterns of a metallated ion rather than reading only the mono-isotopic *m/z* values. The re-processing of our raw files with Polycut or SNAP would be very interesting, in order to verify the reliability of Mascot automated search followed by manual check in comparison with a fully automated search.

Concluding, ESI-HRMS confirmed to be a valuable ally for the molecular characterization of the adducts formed between metallodrugs and relatively small, model proteins. Instead, metalloproteomics studies involving proteins of larger size,

might be better faced out with new generation hybrid HR mass spectrometers. In parallel, this must be accompanied by the development of software tools more specifically designed for the analysis of these complex data.

ACKNOWLEDGMENTS

I would like to thank Prof. Luigi Messori, my tutor, who gave me the opportunity to work on this project. Thanks for supervising me, for giving me useful advice and ideas and the freedom to work independently.

A special thanks goes to Prof. Gloriano Moneti, my boss at CISM, who gave me the time to work towards my PhD in the best way possible.

Thanks to Dr. Giuseppe Pieraccini, who was a constant inspiration and go-to person for scientific discussions.

Thanks to Dr. Damiano Cirri, Prof.ssa Chiara Gabbiani, Dr. Tiziano Marzo, Dr.ssa Lara Massai and Dr. Alessandro Pratesi for their collaboration and all the useful work discussions.

Thanks to Dr.ssa Francesca Boscaro and Dr. Riccardo Romoli, my day-to-day labmates.

Thanks to Dr. Vito Calderone for helping me with the Chimera program and the RCSB Protein Data Bank.

Finally, I would like to thank my family, my mum and dad, who are always there for me.

And the last thanks goes to “Il Cate e La Puzzola”, who shared with me all the troubles and all the joys of these past three years.